STATE MODELS FOR SIMULATION OF AN INERTIAL GUIDANCE AND CONTROL SYSTEM

Thesis for the Degree of M. S.

MICHIGAN STATE UNIVERSITY

RODNEY DAN WIERENGA

1964

THESIS

This is to certify that the

thesis entitled

STATE MODELS FOR SIMULATION
OF AN INERTIAL GUIDANCE
AND CONTROL SYSTEM

presented by

Rodney Dan Wierenga

has been accepted towards fulfillment
of the requirements for

M.S. degree in Electrical Engineering

Herman E. Koenig
Major professor

Date March 17, 1964

O-169

STATE MODELS FOR SIMULATION OF AN INERTIAL GUIDANCE AND CONTROL SYSTEM

Rodney Dan Wierenga

AN ABSTRACT

Submitted to
Michigan State University
in partial fulfillment of the requirements
for the degree of

MASTER OF SCIENCE

Department of Electrical Engineering

1964

ABSTRACT

STATE MODELS FOR SIMULATION OF AN INERTIAL GUIDANCE AND CONTROL SYSTEM

by Rodney Dan Wierenga

In this thesis, state models of a satellite launching vehicle with an inertial guidance and control system are developed for purposes of simulated preliminary design studies. The rigid body dynamics of a typical large space carrier vehicle are derived in detail from basic concepts, and the necessary data for simulation of the selected vehicle is given. A fundamental type of guidance and control system is described and the state models for the individual components, such as the gyros and the accelerometers, are derived. A technique of optimizing the guidance and control system is given along with an example problem. Simulation of the complete system is briefly described and the state models for a suggested simulation are listed.

STATE MODELS FOR SIMULATION OF AN INERTIAL GUIDANCE AND CONTROL SYSTEM

Rodney Dan Wierenga

A THESIS

Submitted to
Michigan State University
in partial fulfillment of the requirements
for the degree of

MASTER OF SCIENCE

Department of Electrical Engineering

1964

ACKNOWLEDGEMENTS

The existence of this thesis would not have been possible without the assistance of several persons. I wish to express graditude to my advisor, Dr. H. E. Koenig of the MSU Electrical Engineering Dept., for suggesting the topic of this thesis and for his many helpful suggestions during its preparation. I wish to thank Mr. W. Haan and Mr. Q. Ward of LSI for their advice on the vehicle and gyro dynamics, respectively. I would also like to thank Miss M. Ransom for typing the manuscript and the LSI Publications Department for its publication. Finally, a special vote of thanks to my wife Betty for her patience and understanding throughout the preparation of this thesis.

TABLE OF CONTENTS

TABLE OF CONTENTS (cont)

TABLE OF CONTENTS (cont)

Table

LIST OF TABLES

LIST OF ILLUSTRATIONS

LIST OF ILLUSTRATIONS (cont)

LIST OF ILLUSTRATIONS (cont)

LIST OF ILLUSTRATIONS (cont)

LIST OF APPENDICES

1. INTRODUCTION

In recent times, much effort has been put forth in the design and understanding of guidance control systems for extra-terrestrial as well as terrestrial vehicles. Included in these categories are sub-marine, marine, land, airborne, and space vehicles. The tasks of guidance and control of these vehicles is divided between man and a host of electromechanical systems. One important class of systems which is used to accomplish guidance and control when accuracy and self-contained features are desired is known as "inertial systems."

In essence, inertial systems use sensors that provide measurements with respect to inertial space. Rate gyros are used to provide measures of angular rate while integrating rate and doubly integrating rate gyros are used to establish coordinate systems with respect to which angular position and linear acceleration measurements can be made, where the linear accelerations are measured by accelerometers.

Guidance consists of determining the position and velocity of a vehicle with respect to a known reference and the generation of the necessary commands to cause the vehicle to follow a desired path or to accomplish a desired end. Control consists of the act of controlling the attitude of the vehicle in response to commands generated by the guidance system.

Three orthogonally mounted accelerometers can be used to completely define the motions of the vehicle. It is desired to express these accelerations in a coordinate frame known as the "computational frame." One method of accomplishing this is to mount the three accelerometers on a gyro-stabilized platform and then by applying torques to the gyros, rotate the platform so that the sensitive axes of the accelerometers always remain aligned with the computational frame axes. On the other hand, this could be accomplished also by performing a coordinate transformation of the accelerometer outputs using an on-board computer to obtain the accelerations in the computational frame. If the gyros are torqued to cause the accelerometer coordinate frame to rotate with respect to inertial space, corrections must be made for coriolis and centrifugal effects. In addition, with both types of systems, corrections must be made for gravitational effects since an accelerometer does not indicate accelerations due to gravitation. After corrections, the first integral of the acceleration is velocity and the second integral is distance in the computational coordinate system. If desired, gravitational corrections can be made in the computed velocity or even in the computed distance rather than in the acceleration itself.

In the design of a guidance and control system, the first consideration is the mission which is to be performed and how to guide and control the vehicle to accomplish this mission. Things that must be weighed in the design of the system are stability and response, size and weight, cost, and accuracy.

In the study of the stability and response, it is an absolute necessity to study in detail the complete system considering all known influential effects. Included must be the vehicle, the gyros and/or the gyro-stabilized platform, the accelerometers, the on-board computer, the engines, and the technique or techniques of applying moments to the vehicle. It is most desirable to study the complete system, including the many non-linearities, using state models for each of its components. The system can then easily be analyzed by simulation, for example, using digital and/or analog computers.

To verify analytical results or to include non-linearities that might be difficult to define, actual system hardware can be utilized with a simulation. Components that might be used are rate gyros

however,

operates i

of the hard

The

concern of

and the bas

fundamenta

ing for expa

intended to

can be made

rate gyros, servos, or a stable platform. Steps must be taken, however, if hardware is included, to make sure that the system operates in real time so that the time dependent characteristics of the hardware are properly taken into account.

The stability and response of the system are the prime concern of this thesis. It is assumed that the mission, the vehicle and the basic guidance and control systems are specified. The fundamental characteristics of each component are derived allowing for expansion to more detailed descriptions if desired. It is intended to furnish enough detail so that preliminary design studies can be made.

2.1 BA

For

an earth sa

it is desire

circular or

in the guida

vous with a

example, c

be the stati

vous with a

tion, when a

reaching orl

The

C-5 type" of

It is 350 feet

powered by t

five engines

7,500,000 lb;

type with a co

2. SYSTEM DESCRIPTION

2.1 BASIC SYSTEM

For purposes of illustrating inertial guidance and control, an earth satellite launching system is chosen. With this system it is desired to launch a 200,000 lb payload into a 300 nautical mile circular orbit around the earth. Although not specifically included in the guidance scheme, it is assumed that the payload is to rendezvous with a satellite which is already in orbit. The payload, for example, could be a supply vehicle for a space station, or it could be the station itself being placed into orbit and required to rendezvous with a previously launched supply vehicle. This type of operation, when a vehicle launched from the earth is to rendezvous upon reaching orbit, is known as an "ascent rendezvous."

The space carrier chosen to launch the payload is a "Saturn C-5 type" of vehicle (one which is similar to the actual Saturn C-5). It is 350 feet long including the payload (see Figure C-1) and is powered by three stages of rocket engines. The first stage uses five engines of the F-1 type with a combined sea level thrust of 7,500,000 lb; the second stage also uses five engines, of the J-2 type with a combined sea level thrust of 1,000,000 lbs; and the third stage

thrust of 2

engines on

trol about a

pitch are c

two axes wh

To c

accomplish

have a guida

2.1 the guid

third stage uses a single engine of the J-2 variety with a sea level thrust of 200,000 lbs. On the first and second stages, 4 of the 5 engines on each stage are gimballed and are used for attitude control about all three of the vehicle axes. On the third stage yaw and pitch are controlled by the single engine which is gimballed about two axes while roll is controlled by reaction jets.

To cause the flight of the vehicle to be directed so as to accomplish injection into the desired orbit, it is necessary to have a guidance system and a control system. As shown in Figure 2.1 the guidance and control systems operate on inputs from the

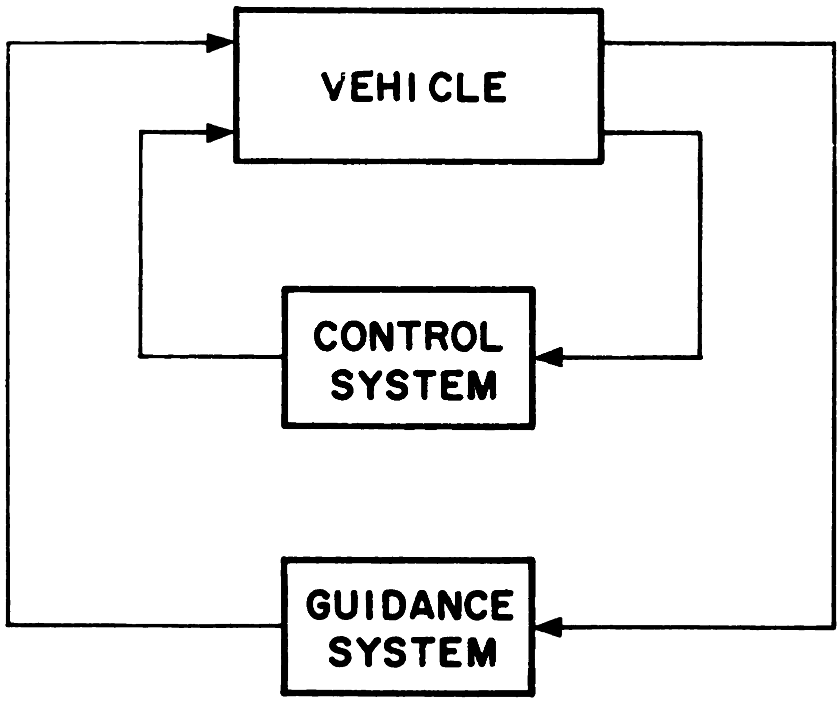

FIGURE 2.1

SYSTEM BLOCK DIAGRAM

vehicle and

it to perfor

The

to stabilize

with most s

center-of-p

g.). Thus,

causes a fo

in a directio

this results

effective c.

equipped wi

is necessary

tive aerodyn

AER

vehicle and, in turn, provide commands back to the vehicle to cause it to perform as required.

The control system has two functions. The first function is to stabilize the vehicle. This is necessary because this vehicle, as with most space carriers, is aerodynamically unstable since the center-of-pressure (c. p.) is foreward of the center-of-gravity (c. g.). Thus, as shown in Figure 2. 2, a flow incidence angle (η) causes a force F, acting at the c. p., around the c. g., which acts in a direction to increase η. With an increase in η, F is increased; this results in an unstable vehicle. It would be stable only if the effective c. p. were behind the c. g. as would be the case if it were equipped with large aero-dynamic fins. With a control system it is necessary to add enough negative feedback to overcome the positive aerodynamic feedback.

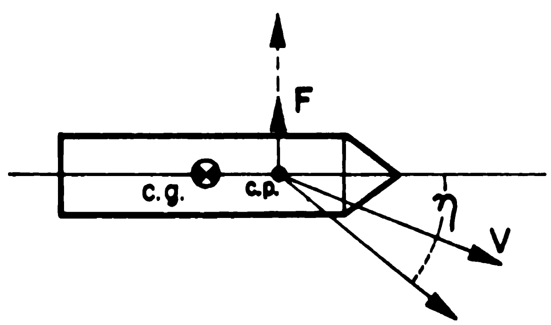

FIGURE 2. 2

AERODYNAMICALLY UNSTABLE VEHICLE

The
attitude cor
tions of the

The
informatior
system.

Bec
vehicle, it
tem to com
and control
parameters
these parar

As s
control are
by vehicle e
by rate gyr
form, and a
on the stabl
guidance an
sensed infor

The second function of the control system is to provide for attitude command to the vehicle so that commanded angular positions of the vehicle can be achieved.

The guidance system, based on computations, programmed information, and time, provides attitude commands to the control system.

Because of an extremely large range of parameters of the vehicle, it is necessary for both stability and response of the system to compensate for these changes with changes in the guidance and control systems. This can be done as a function of the vehicle parameters themselves, or possibly as a function of just one of these parameters, or even possibly just as a function of time.

As shown in Figure 2. 3, the functions of guidance and control are accomplished by sensors, a computation section, and by vehicle engine controls. The vehicle angular rates are sensed by rate gyros, the attitude angles are provided by the stable platform, and accelerations are measured by accelerometers mounted on the stable element of the stable platform. The computer and the guidance and control equations section of the system process the sensed information and give commands to the vehicle through the


ENGINE SERVOS
δ's
VEHICLE

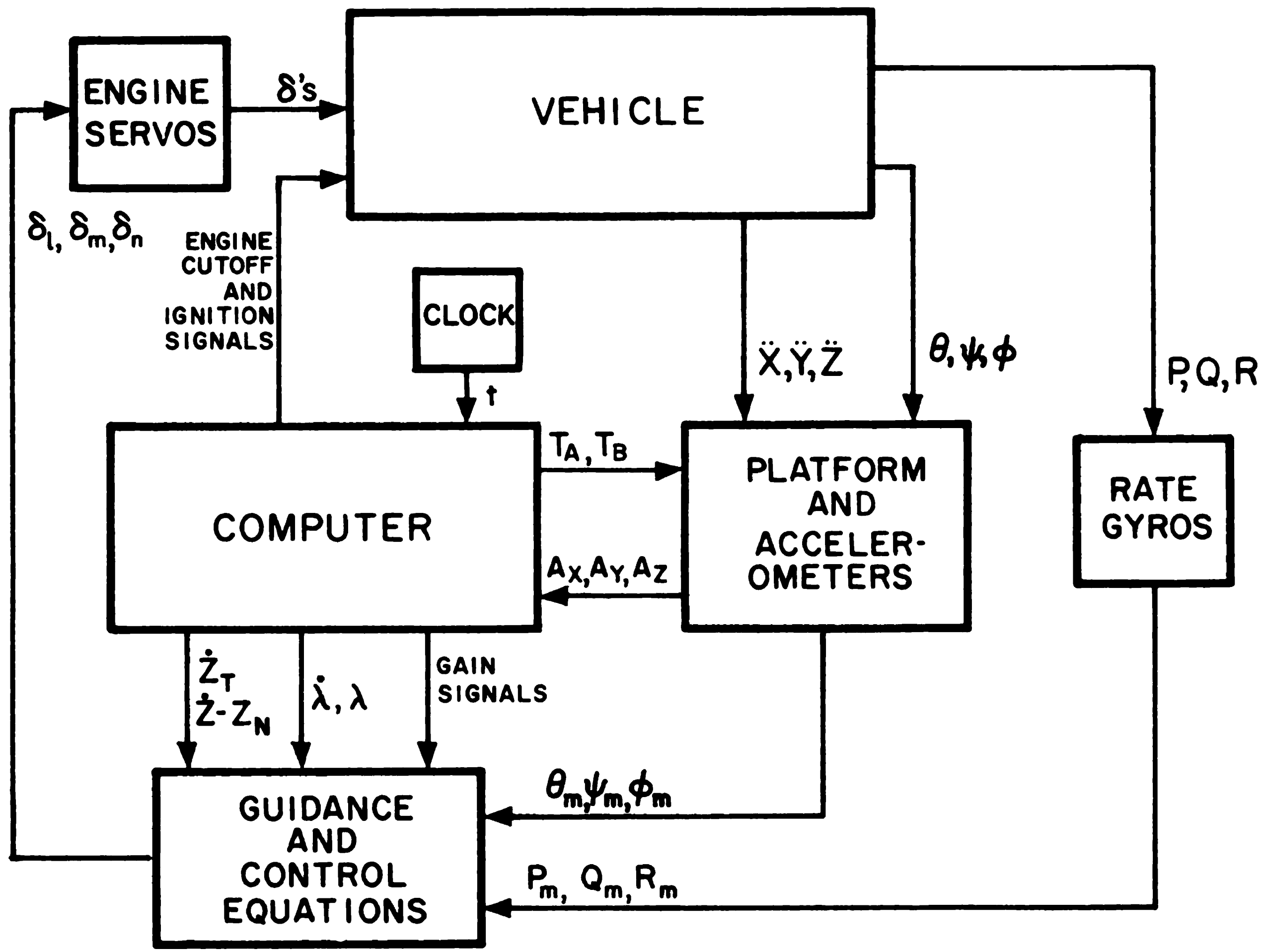

FIGURE 2.3

EXPANDED SYSTEM BLOCK DIAGRAM

third stage

both by rot

tion and cu

2.2 FL

It i

around the

is desired

with the p

defined by

rendezvou

pressures

be non-ro

A

system is

ter of the

third stage reaction jets and through the gimballed rocket engines both by rotation of the engines for attitude commands and by ignition and cutoff signals for linear acceleration control.

2.2 FLIGHT PLAN

It is desired to place the satellite into a specified orbit around the earth. Thus, in the process of launching the vehicle it is desired to guide the trajectory of the vehicle so that it coincides with the plane defined by the desired orbit. This plane, which is defined by the orbit of the satellite with which it is desired to rendezvous, is slowly precessing due to earth's oblateness, solar pressures, etc., but for purposes of the launch it is assumed to be non-rotating with respect to inertial space.

As shown in Figure 2.4, a right hand rectangular coordinate system is attached to this plane where the center, T, is at the center of the earth, the X_T axis is perpendicular to the trajectory

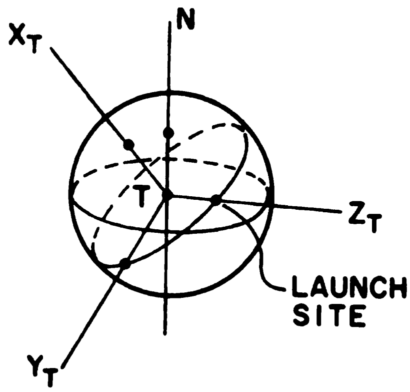

FIGURE 2.4

TRAJECTORY PLANE COORDINATE SYSTEM

plane, and

passing thr

(at V) in thi

by the rang

As s

into two pha

is an atmos

phere, it is

a minimum

ing will not

example, b

bending, sl

ing the pos

plane, and the Y_T and Z_T axes are in the plane with the Z_T axis passing through the launch site. The angular location of the vehicle (at V) in this coordinate system is defined, as shown in Figure 2.5, by the range angle σ and the cross-range angle λ.

As shown in Figure 2.6, the flight of the vehicle is divided into two phases. Because the vehicle is "moment limited", there is an atmospheric phase and a vacuum phase. While in the atmosphere, it is necessary to limit the angular motions of the vehicle to a minimum so that aerodynamic moments caused by the maneuvering will not damage the vehicle structurally. The vehicle could, for example, break at one of the junctions between stages, or, the bending, sloshing, or compliance modes could be excited increasing the possibility of damage.

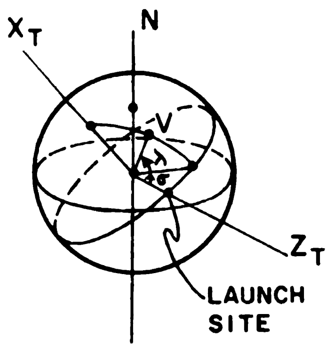

FIGURE 2.5

RANGE AND CROSS-RANGE ANGLES

The

mosphere

shown in F

are the ver

Pri

platform, a

vehicle, on

vertical, bu

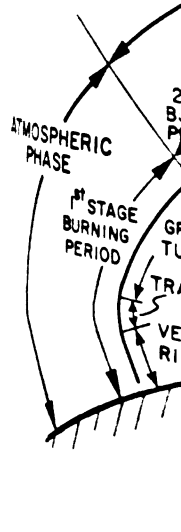

The vehicle is considered to be within the appreciable atmosphere for the duration of the first stage burning period. As shown in Figure 2. 6 this period is divided into three parts. These are the vertical rise, the transition turn, and the gravity turn.

Prior to liftoff the accelerometers, mounted on the stable platform, are oriented with respect to the trajectory plane. The vehicle, on the other hand, is oriented with its longitudinal axis vertical, but is not, in general, at the proper roll angle. (It is

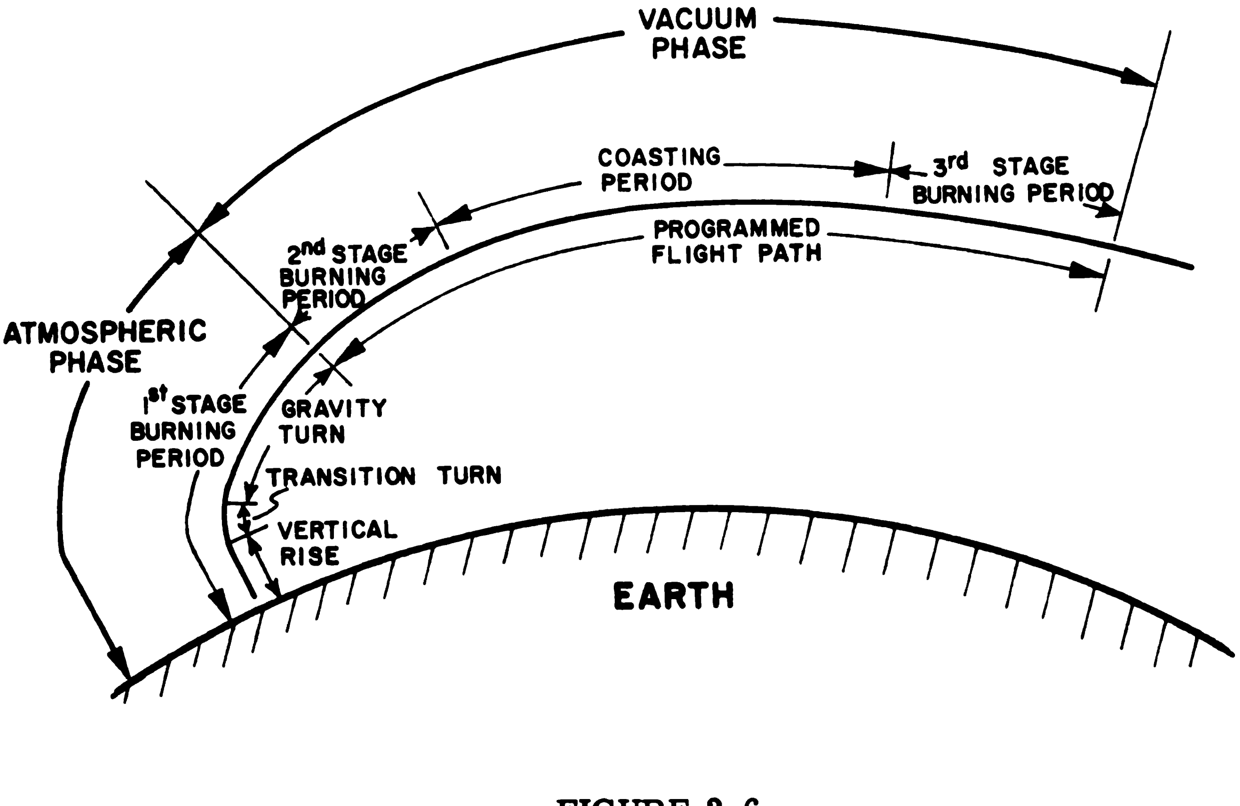

FIGURE 2. 6

LAUNCH SEQUENCE

assumed to be within 20 degrees, however.) During the vertical rise period the vehicle is rolled at a maximum rate of 1 deg/sec until the vehicle axes are aligned in the desired directions. The vertical rise is a timed period which, for this vehicle, is chosen to end 20 secons after liftoff.

The next period is the transition turn. During this period the so called "kick angle" is developed. The vehicle is slowly rotated at a maximum rate of 1deg/sec to give an angle of attack which causes a change in the direction of flight toward the downrange direction in the trajectory plane. The kick angle chosen for this system is 6 degrees.

After the vehicle reaches 6 degrees, the gravity turn period begins. While in the gravity turn, the vehicle attitude is controlled so that it flies with zero angle of attack. Thus, the vehicle is controlled to fly in the direction of the relative wind and, as a result, aerodynamic moments are held to a minimum. This is done by controlling the vehicle so that accelerations normal to the vehicle longitudinal axis are driven to zero. The name "gravity turn" is used because gravity is the only acceleration acting normal to the vehicle.

The atmospheric phase is terminated by shutting down the engines when an acceleration of 5.4 g's is reached. Upon completion of the shut-down, first stage separation is initiated.

At separation of the first stage, large moments can be applied to the upper stages and thus it is desired to ignite the second stage for purposes of control not more than a few seconds after separation. On the actual hardware, small retro-rockets are used to "back" the first stage away in addition to ullage rockets on the upper stages to move them away and to hold the liquid fuel on the bottom of the tanks. For purposes of this system, however, it is assumed that the second stage ignites immediately upon first stage shut-down and separation.

The vacuum phase of the vehicle trajectory is guided by controlling the flight path of the vehicle as a function of range traveled and by holding the cross-range distance to zero. While the atmospheric phase was an open-loop operation; this phase is closed loop. The second stage burns until a velocity determined by the desired nominal trajectory is reached. The engines are then cut off and the stage is separated--again by using small retro-rockets. The vehicle coasts until an altitude determined by the nominal trajectory is reached.

The third stage engine is ignited and thrusts until circular orbital velocity is reached at the desired altitude. Here again, on the actual hardware, ullage rockets are used to cause the fuel to fill the bottom of the tanks. It is assumed that the vehicle is close to the desired attitude at third stage ignition. In practice, when the orbital velocity is nearly achieved, the third stage main engine is shut down and a vernier engine is used to supply the final additional velocity. For this system, however, it is assumed that the unpredictable shut down is perfect and immediate at the instant orbital velocity is reached. This velocity is

$$V_{ORB} = (\mu/Z)^{1/2} \tag{2.1}$$

which at the equator is

$$V_{ORB} = \left(\frac{1.4077 \times 10^{16}}{20,925,732 + 300\,(6076.11)} \right)^{1/2} \tag{2.2}$$

$$V_{ORB} = 24875.9 \text{ fps} \tag{2.3}$$

T

express t

with resp

dices A a

of forces

gravitatio

3.1 C

Th

to define

dinate sys

frame), a

and a vehi

3.1.1 I-

Th

based are

define a co

ordinate sy

3. VEHICLE STATE MODEL

The state model of the vehicle is a set of equations which express the translational and rotational dynamics of the vehicle with respect to a defined coordinate system as derived in Appendices A and B. The driving functions for these expressions consist of forces and moments that act on the vehicle plus the forces due to gravitational attraction.

3.1 COORDINATE SYSTEMS

There are four (4) coordinate systems that are necessary to define the dynamics of the vehicle. These are an inertial coordinate system (I-frame), an earth fixed coordinate system (E-frame), an earth-vehicle geocentric coordinate system (V-frame), and a vehicle body fixed coordinate system (B-frame).

3.1.1 I-Frame

The foundations upon which the dynamics of the vehicle are based are Newton's Laws. It follows then, that it is necessary to define a coordinate system in which these laws are valid. This coordinate system is known as an inertial coordinate system. For convenience, it is defined as an orthogonal right hand triad of axes whose center, designated I, is fixed with respect to inertial space. This coordinate system is referred to as the I-frame.

In Newtonian mechanics, inertial space is defined by a coordinate system which is non-rotating and non-accelerating with respect to the "fixed stars." The so-called "fixed stars" are the distant stars, and are assumed to be stationary in inertial space. With respect to this coordinate system, according to Newton's first law, a body, in the absence of external forces, will either be at rest or moving in a straight line at a constant velocity. By expansion of this concept, an inertial frame can also be defined as one which is either stationary or moving at a constant velocity in a straight line with respect to inertial space since motion in this frame will also be consistant with the first law.

With relativistic considerations, an inertial reference frame must be non-rotating and non-accelerating in a space free from gravitation, or, in a gravitational field, an inertial reference frame is a local non-rotating coordinate system whose center is accelerating as though in free fall in the gravitational field. It is assumed that the resultant curvature of space due to the effect of a gravitational field on the inertial coordinate system can be

neglecte
apparent
insignifi
trial veh
ly adequa
tivistic r

3.1.2 E

Tl
as shown
with its c
the polar
fixed to th
ing the Gr

neglected. Also, the effects on time, length, and mass that become apparent as the speed of light is approached are assumed to be insignificant. Thus, it is assumed that for purposes of the terrestrial vehicle under consideration, Newtonian mechanics are entirely adequate. For a brief but comprehensive consideration of relativistic rocket mechanics see [1, Chapter 11].

3.1.2 E-Frame

The E-frame, designating an earth fixed coordinate system as shown in Figure 3.1, is a right-hand orthogonal set of axes with its center fixed at the center of the earth. The z axis is along the polar axis of the earth, positive north; the x and y axes are fixed to the earth in the equatorial plane with the x axis intersecting the Greenwich meridian.

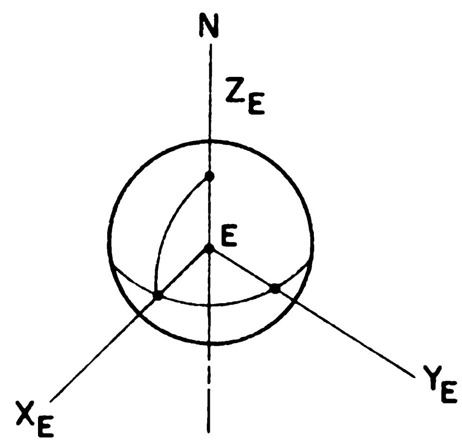

FIGURE 3.1

E-FRAME

3.1.3 V-Frame

The V-frame is a right hand rectangular earth-vehicle geocentric coordinate system with center at the center of gravity of the vehicle as shown in Figure 3.2. The z axis is along the earth radius line between the center of the earth and the vehicle c.g.. The z axis is positive away from the center of the earth. The mutually perpendicular x and y axes form a plane which is tangent to a spherical earth where the x axis is initially (at the instant of launch) aligned in the desired direction of flight. The coordinate system is defined so that there are no rotations around the z axis after launch.

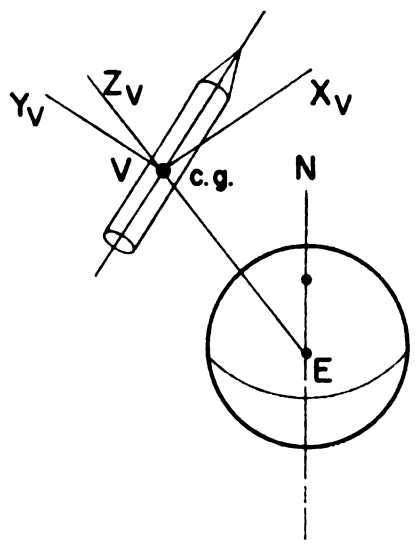

FIGURE 3.2

V-FRAME

3.1.4 B-Frame

The B-frame is a right-hand orthogonal coordinate system with axes coincident with the principle axes of the vehicle, as shown in Figure 3.3, with center at the c.g. of the vehicle. The x axis is along the longitudinal axis where the vehicle center line is assumed to be a principle axis of the vehicle. The y and z axes are fixed in directions defined by the planes of the fins and the engines. The y and z axes are assigned arbitrarily to a given pair of fins and engines, and then, for purposes of identification of the vehicle components, remain fixed in the chosen directions.

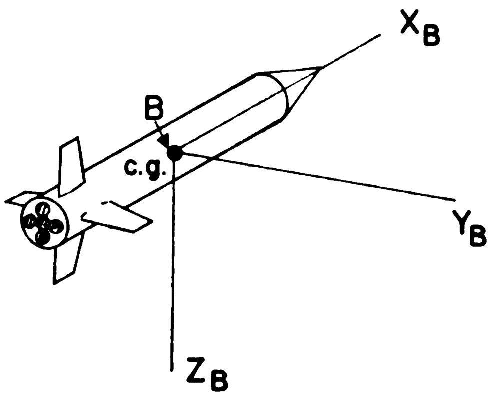

FIGURE 3.3

B-FRAME

3.2 RELATIONSHIPS BETWEEN COORDINATE SYSTEMS

To relate inertial characteristics of the vehicle to inertial space, and to relate motions of the vehicle to the earth, it is necessary to determine the relationships between the above defined coordinate systems.

3.2.1 Earth Rate

The earth rotates about its celestial pole (not the earth's polar axis) with respect to the "fixed stars" at a rate known as the earth's siderial rate. One siderial day, or the time for one rotation of the earth with respect to the "fixed stars", is approximately 23 hours, 56 minutes, 4.09 seconds of mean solar time, as opposed to the approximate average time of 24 hours of mean solar time for one rotation with respect to the sun. Based on [2, p. 19] the siderial rate of the earth is

$$\omega_{IE} = \frac{2\pi}{86,164.09892 + 0.00164T} \text{ rad/sec} \tag{3.1}$$

where T is the number of Julian Centuries of 36,525 days from noon January 1, 1900. For the year 1963

$$\omega_{IE} = 0.729211505 \times 10^{-4} \text{ rad/sec} \tag{3.2}$$

$$\omega_{IE} = 0.417807416 \times 10^{-2} \text{ deg/sec} \tag{3.3}$$

Also, as given in [2, p. 20], the seasonal variation of the period of this rotation in milliseconds slow is

$$T = 21 \sin\left[\frac{2\pi}{365}(d - 17)\right] + 10 \sin\left[\frac{4\pi}{365}(d - 93)\right] \tag{3.4}$$

where d is the day of the year. The maximum variation is

$$T_{MAX} \quad = \quad 29.14 \text{ msec slow} \tag{3.5}$$

The slowing down of the earth expressed in Equation 3.1 and even the maximum seasonal variation (Equation 3.5) are, for purposes of the system under consideration, insignificant.

The E-frame z axis lies along the polar axis (geometric pole) of the earth. The majority of the angular motion of this axis with respect to the celestial pole is accounted for by two different types of periodic motion [see 2, p. 20; 3, pp. 2-3]. The first is a precession of the earth's polar axis about an axis normal to the plane defined by the path of the earth around the sun (ecliptic plane) at a rate of 50.26 seconds of arc per year. This is known as the "Precession of the Equinoxes" and is caused by the combined gravitational moment on the earth because of its non-spherical distribution of mass due to the sun and due to the moon. The second type periodic motion is similar to the nutational oscillation of a gyroscope where the motion of the earth's polar axis describes a circle about the celestial pole with a half amplitude of 0.13 seconds of arc and a period of 428 days. For purposes of the system under consideration, these motions of the earth's polar axis are ignored and it is assumed that the siderial rate given by Equations 3.2 and 3.3 are around the E-frame z axis. The direction of rotation is in the positive Z_E direction.

The components of the earth's rotational rate appearing in the V-frame prior to launch as observed from inertial space can be obtained from Figure 3. 4, remembering that the Z_V component

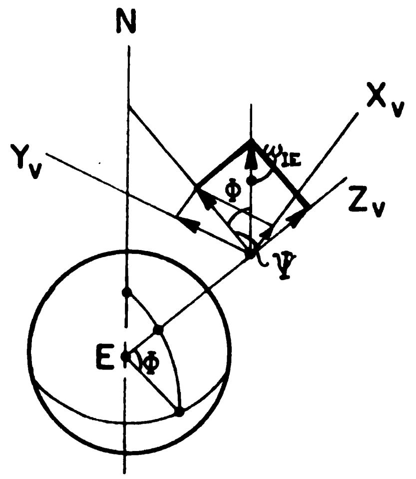

FIGURE 3. 4

INITIAL V-FRAME RATES DUE TO EARTH RATE

is zero, as

$$(\bar{\omega}_{IV})_0 = \omega_{IE} \begin{bmatrix} \cos\Phi_0 \cos\Psi_0 \\ \cos\Phi_0 \sin\Psi_0 \\ 0 \end{bmatrix} \tag{3.6}$$

3.2.2 B- to V-frame Transformation

Figure 3. 5 illustrates the coordinate transformation between the V-frame and the B-frame through the Euler angles that are defined by the platform gimbal order (y, z, x). This gimbal order is chosen to eliminate gimbal lock with a vertical launch and to provide appropriate angles for the control system.

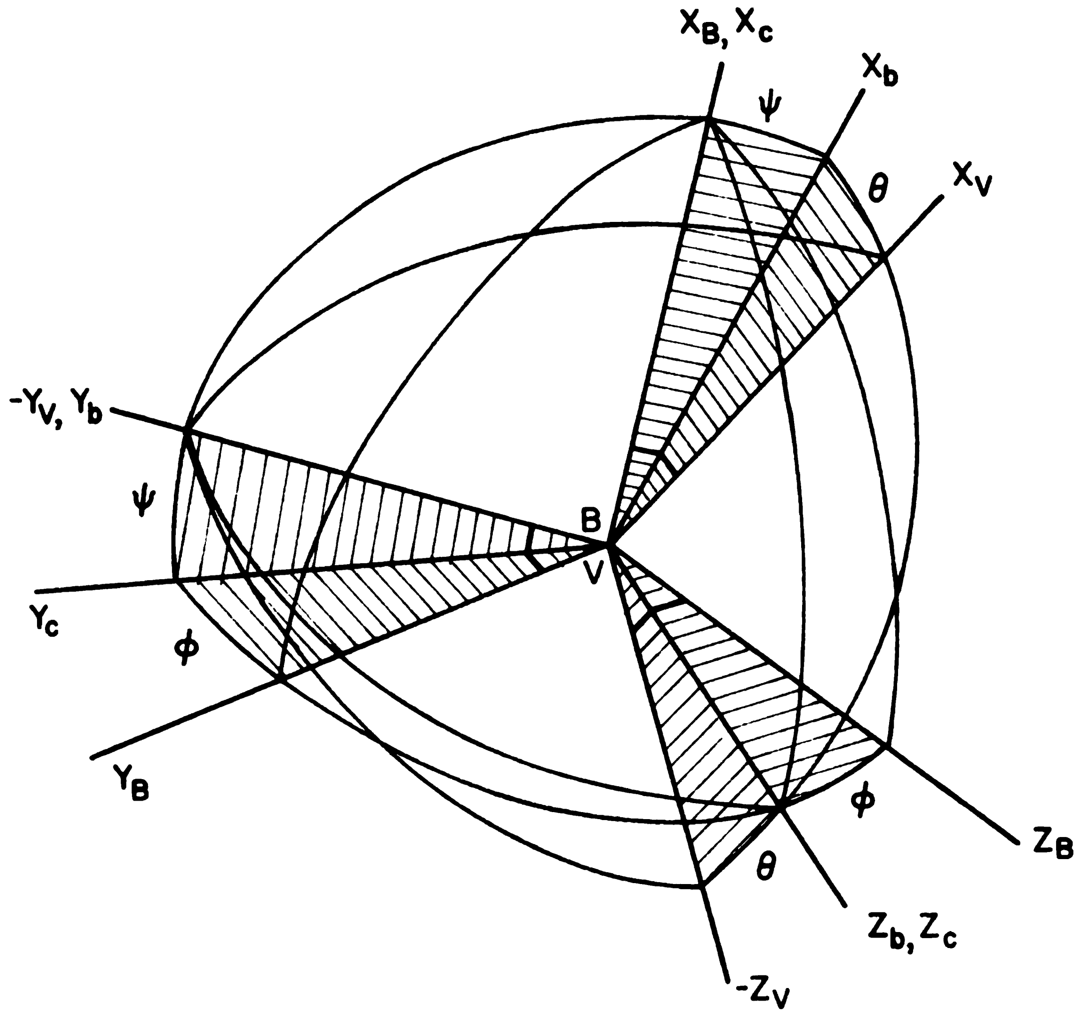

FIGURE 3. 5

B- TO V-FRAME COORDINATE TRANSFORMATION

The transformation from the V-frame to the B-frame is

$$\begin{bmatrix} X_B \\ Y_B \\ Z_B \end{bmatrix} = [\phi] \; [\psi] \; [\theta] \begin{bmatrix} X_V \\ Y_V \\ Z_V \end{bmatrix} \tag{3.7}$$

which

$$\begin{bmatrix} X_B \\ Y_B \\ Z_B \end{bmatrix}$$

and u

$$\begin{bmatrix} X_B \\ Y_B \\ Z_B \end{bmatrix} =$$

This i

B-fra

consi

serve

This r

V-fra

of the

ω_x is

which upon expansion with direction cosines is

$$\begin{bmatrix} X_B \\ Y_B \\ Z_B \end{bmatrix} = \begin{bmatrix} 1 & 0 & 0 \\ 0 & \cos\phi & \sin\phi \\ 0 & -\sin\phi & \cos\phi \end{bmatrix} \begin{bmatrix} \cos\psi & \sin\psi & 0 \\ -\sin\psi & \cos\psi & 0 \\ 0 & 0 & 1 \end{bmatrix} \begin{bmatrix} \cos\theta & 0 & \sin\theta \\ 0 & -1 & 0 \\ \sin\theta & 0 & -\cos\theta \end{bmatrix} \begin{bmatrix} X_V \\ Y_V \\ Z_V \end{bmatrix} \quad (3.8)$$

and upon multiplication becomes

$$\begin{bmatrix} X_B \\ Y_B \\ Z_B \end{bmatrix} = \begin{bmatrix} \cos\psi\cos\theta & -\sin\psi & \cos\psi\sin\theta \\ \sin\phi\sin\theta - \cos\phi\sin\psi\cos\theta & -\cos\phi\cos\psi & -\sin\phi\cos\theta - \cos\phi\sin\psi\sin\theta \\ \cos\phi\sin\theta + \sin\phi\sin\psi\cos\theta & \sin\phi\cos\psi & -\cos\phi\cos\theta + \sin\phi\sin\psi\sin\theta \end{bmatrix} \begin{bmatrix} X_V \\ Y_V \\ Z_V \end{bmatrix} \quad (3.9)$$

This is the direction cosine transformation from the V-frame to the B-frame. To simplify notation the transformation is shown as

$$\begin{bmatrix} X_B \\ Y_B \\ Z_B \end{bmatrix} = \begin{bmatrix} l_1 & l_2 & l_3 \\ m_1 & m_2 & m_3 \\ n_1 & n_2 & n_3 \end{bmatrix} \begin{bmatrix} X_V \\ Y_V \\ Z_V \end{bmatrix} \quad (3.10)$$

The angular rate of the B-frame with respect to the I-frame, consisting of components measured around the B-frame axes as observed from the I-frame is,

$$\omega_{IB} = P\, i_B + Q\, j_B + R\, k_B \quad (3.11)$$

This rate, in terms of the Euler angles relating the B-frame to the V-frame (refer to Figure 3.5) and, from Equation A-40, in terms of the y component of the V-frame with respect to the I-frame (as ω_X is very small and ω_Z is zero) is

$$\bar{\omega}_{IB} = \bar{\omega}_{IV} + \bar{\omega}_{VB}$$
$$\bar{\omega}_{IB} = (\dot{\theta} - \omega_Y)\, j_b + \dot{\psi} k_c + \dot{\phi} i_B \tag{3.12}$$

Now since

$$j_b = (\sin\psi)\, i_c + (\cos\psi)\, j_c \tag{3.13}$$

Equation 3.12 becomes

$$\bar{\omega}_{IB} = \left[(\dot{\theta} - \omega_Y) \sin\psi \right] i_c + \left[(\dot{\theta} - \omega_Y) \cos\psi \right] j_c + \dot{\psi} k_c + \dot{\phi} i_B \tag{3.14}$$

The direction cosine transformation between the c-frame and the B-frame is

$$\begin{bmatrix} i_c \\ j_c \\ k_c \end{bmatrix} = \begin{bmatrix} 1 & 0 & 0 \\ 0 & \cos\phi & -\sin\phi \\ 0 & \sin\phi & \cos\phi \end{bmatrix} \begin{bmatrix} i_B \\ j_B \\ k_B \end{bmatrix} \tag{3.15}$$

which upon combination with Equations 3.11 and 3.14 yields

$$\bar{\omega}_{IB} = \begin{bmatrix} P \\ Q \\ R \end{bmatrix} = \begin{bmatrix} 1 & \sin\psi & 0 \\ 0 & \cos\psi \cos\phi & \sin\phi \\ 0 & -\cos\psi \sin\phi & \cos\phi \end{bmatrix} \begin{bmatrix} \dot{\phi} \\ \dot{\theta} - \omega_Y \\ \dot{\psi} \end{bmatrix} \tag{3.16}$$

Solution for the Euler rates yields

$$\begin{bmatrix} \dot{\phi} \\ \dot{\theta} - \omega_Y \\ \dot{\psi} \end{bmatrix} = \begin{bmatrix} 1 & -\cos\phi \tan\psi & \sin\phi \tan\psi \\ 0 & \dfrac{\cos\phi}{\cos\psi} & -\dfrac{\sin\phi}{\cos\psi} \\ 0 & \sin\phi & \cos\phi \end{bmatrix} \begin{bmatrix} P \\ Q \\ R \end{bmatrix} \tag{3.17}$$

Equations 3.17 can be solved for ϕ, θ, and ψ, and used in Equations 3.9 for the direction cosine transformation from the V-frame to the B-frame.

3.3 EXTERNAL FORCES AND MOMENTS

The forces and moments that act on the vehicle are produced by the vehicle aerodynamics, the propulsion system, and the attitude control system. The aerodynamic inputs are forces and moments that act along and around the three body, or B-frame, axes and are functions of the vehicle size and shape, the vehicle speed, the density of the atmosphere, the flow incidence angles, etc.. The propulsion system primarily produces a force which acts along the X_B axis. Due to misalignment of the engine, or engines, however, forces can also be applied along the Y_B and Z_B axes. Likewise, due to misalignment, and/or due to unequal thrust from the engines of the multiple engine stages, moments can be produced about all three of the X_B, Y_B, Z_B axes. The attitude control inputs for all three stages (except for third stage roll) are produced by gimballing the engines. With gimballed engines, moments are applied about the X_B, Y_B, Z_B axes by a small rotation of the thrust vector. In doing so, forces are also applied along the Y_B and Z_B axes while a small reduction of the propulsion system input along the X_B axis is introduced. Roll of the third stage, since there is a single axially mounted engine, cannot be controlled by the single thrust vector. Therefore, on the third stage only, reaction jets are used for roll control.

3.3.1 Vehicle Aerodynamics

The aerodynamic inputs to the vehicle consist of forces along the three B-frame axes and moments, or torques, around these three axes. To separate the major effects on these forces and moments due to the vehicle speed relative to the air mass, vehicle size, and air density, non-dimensional coefficients are used as

$$C_F = \frac{F_a}{qA} \tag{3.18}$$

$$C_M = \frac{M_a}{qAd} \tag{3.19}$$

where C_F and C_M are the non-dimensional force and moment coefficients, respectively, and A and d are the maximum vehicle cross-sectional area and diameter, respectively. The major effects of the vehicle speed and the air density are accounted for in the free stream dynamic pressure term (free stream pressure due to motion of the vehicle through the atmosphere) where the dynamic pressure is defined as

$$q = \frac{1}{2} \rho V_a^{\;2} \tag{3.20}$$

The air density, ρ , that is usually used is one which is referred to as belonging to a "standard atmosphere." The air density is assumed to be only a function of altitude. The air density based on the 1959 ARDC Model Atmosphere [4] is given in Figure 3. 6. A good approximation to this curve is an exponential as shown in Figure 3. 6 with

$$\begin{aligned} \rho &= 0.003\, e^{-h/22,500} \\ h &= Z - Z_0 \end{aligned} \tag{3.21}$$

In the study of such things as vehicle heating and loading, trajectory analyses, and control system gain, it may be desirable to consider variations of air density from that given by the standard atmos-

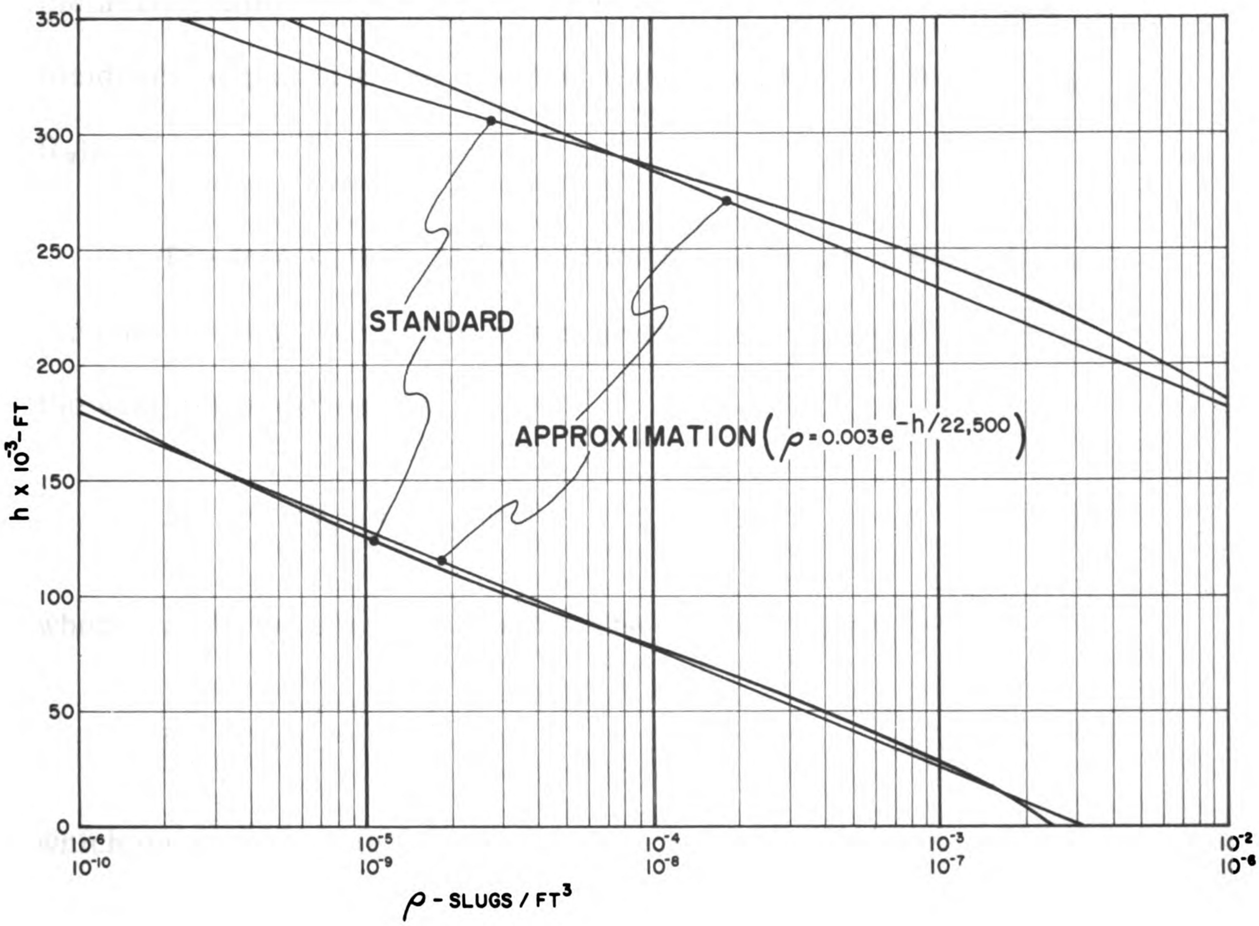

FIGURE 3. 6

1959 ARDC STANDARD ATMOSPHERE
AIR DENSITY

phere. For atmospheric variations refer to [4].

Other aerodynamic parameters that are used to express the aerodynamics of the vehicle are Mach number (M), the flow incidence angles (α, β, η), and the B-frame angular rates (P_a, Q_a, R_a).

The free stream Mach number (free stream refers to the air surrounding the vehicle that is undisturbed by the presence of the vehicle) is defined by

$$M = V_a / a \tag{3.22}$$

where, a, is the speed of sound. The speed of sound is

$$a = \sqrt{\gamma R T} \tag{3.23}$$

which over the possible atmospheric conditions where the speed of sound is of significance is (γ = 1.4, R = 1715 ft-lb/slug°R)

$$a = 49.1 (T)^{1/2} \tag{3.24}$$

Using a standard atmosphere with temperature being a function of altitude, the speed of sound becomes a function of altitude as shown in Figure 3.7.

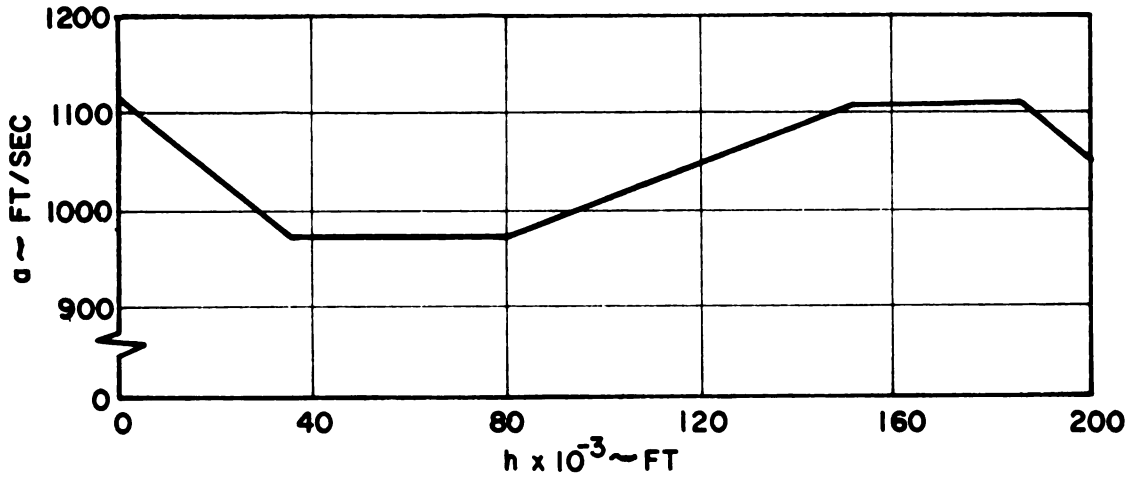

FIGURE 3. 7

SPEED OF SOUND IN STANDARD ATMOSPHERE

For many applications, when simplicity is desired as is the case in preliminary design studies, the variation of the speed of sound is neglected and assumed to be constant at some average value over the flight conditions being considered. In this study it is assumed to be

$$a = 1000 \text{ fps} \tag{3.25}$$

The flow incidence angles, α and β, in standard aircraft terminology, are referred to as the "angle of attack" and the "sideslip angle." For convenience in referring to these angles these terms are also used here where the terms are associated with the arbitrarily chosen B-frame reference axes. As shown in

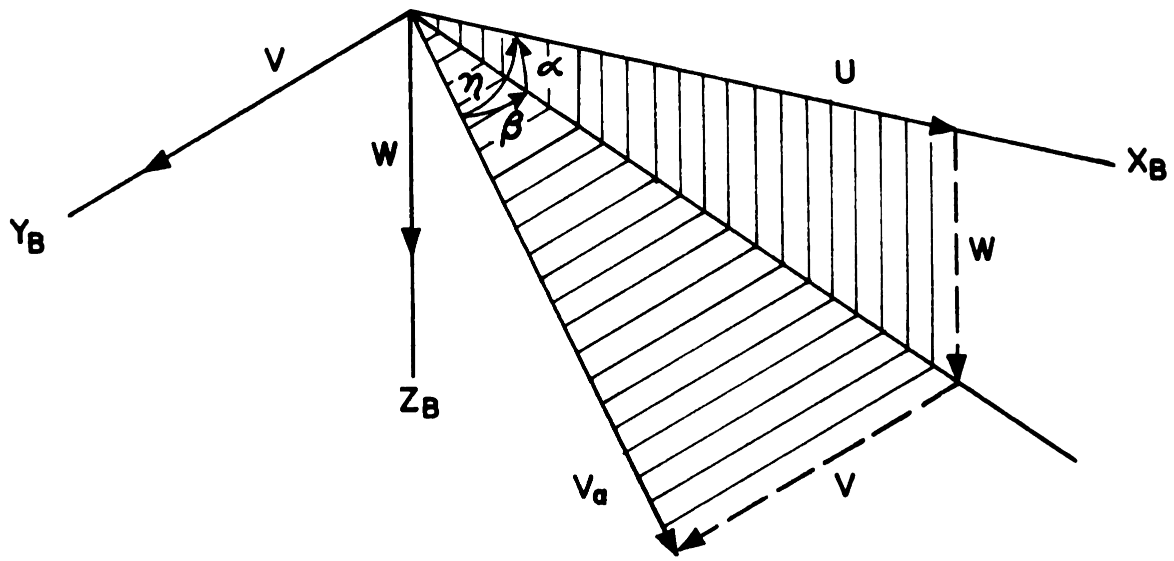

FIGURE 3. 8

FLOW INCIDENCE ANGLES

Figure 3. 8, the angle of attack is measured in the X_B-Z_B plane with

$$\sin \alpha = \frac{W}{V_\alpha \cos \beta} \tag{3.26}$$

The sideslip angle is measured in a plane which contains the total velocity vector with respect to the air mass, V_α, and is perpendicular to the X_B-Z_B plane as

$$\sin \beta = \frac{V}{V_\alpha} \tag{3.27}$$

With small angle assumptions

$$\alpha = \frac{W}{V_a}$$
$$\beta = \frac{V}{V_a} \tag{3.28}$$

The total flow incidence angle (Refer to Figure 3. 8) is

$$\sin \eta = \frac{(V^2 + W^2)^{1/2}}{V_a} \tag{3.29}$$

which for small angles in terms of α and β becomes

$$\eta = (\alpha^2 + \beta^2)^{1/2} \tag{3.30}$$

The angular rate terms, (P_a , Q_a, R_a), are the angular rates of the vehicle with respect to the air mass measured around the B-frame axes. Since the differences between these rates and the rates measured with respect to inertial space are small, it is assumed in the computation of the aerodynamic effects due to these terms that

$$P_a = P$$
$$Q_a = Q \tag{3.31}$$
$$R_a = R$$

A single force coefficient, as defined by Equation 3.18, is used for each of the three B-frame axes with

$$
\begin{aligned}
F_{xa} &= C_x \, q \, A \\
F_{ya} &= C_y \, q \, A \\
F_{za} &= C_z \, q \, A
\end{aligned}
\tag{3.32}
$$

Also, as defined by Equation 3.19, individual moment coefficients are used for the three B-frame axes with

$$
\begin{aligned}
M_{xa} &= C_{\ell} \, q \, Ad \\
M_{ya} &= C_m \, q \, Ad \\
M_{za} &= C_n \, q \, Ad
\end{aligned}
\tag{3.33}
$$

In general, each of the aerodynamic coefficients are highly non-linear functions of the parameters, M, α, β, P_a, Q_a, and R_a. (In addition, if aerodynamic control surfaces were used in the system, the surface deflections would also be included -- increasing the non-linearity.)

The aerodynamic data is often given, as in [1, pp. 5-9 through 5-26] for example, in terms of "lift" and "drag" coefficients. Referring to Figure 3.9, both can be considered as being applied at the center of pressure (c.p.) with the drag coefficient acting along the direction of the vehicle velocity with respect to the

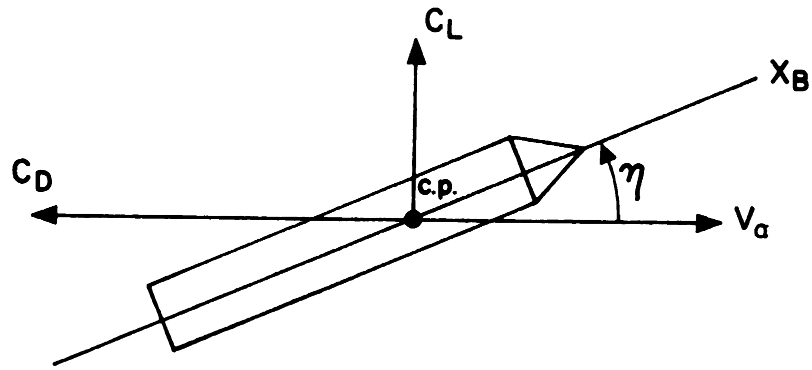

FIGURE 3.9

BODY LIFT AND DRAG COEFFICIENTS

air mass, V_a , and the lift coefficient acting perpendicular to this velocity. The positive directions are as shown by Figure 3.9. From Figure 3.10, using spherical triangle relationships, the

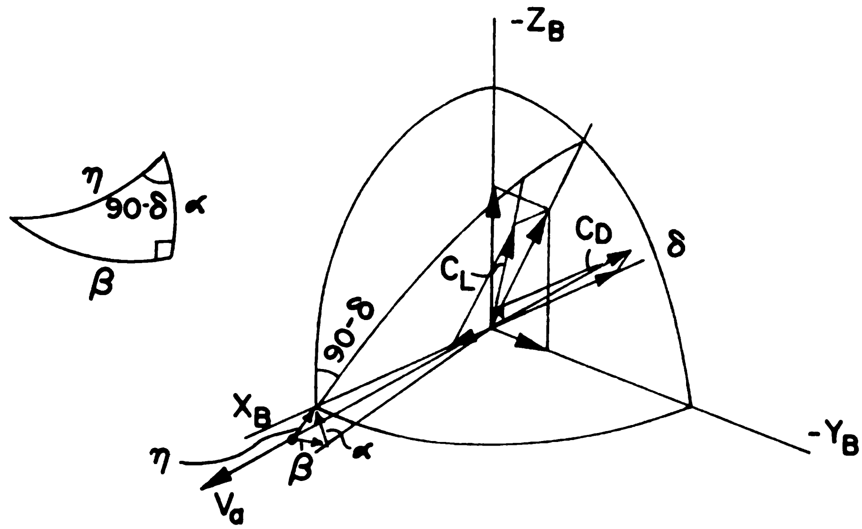

FIGURE 3.10

FORCE COEFFICIENT COORDINATE TRANSFORMATION

B-frame body force coefficients in terms of body lift and drag become

$$C_{xb} = C_L \sin\eta - C_D \cos\eta$$

$$C_{yb} = -\frac{\sin\beta}{\sin\eta} (C_L \cos\eta + C_D \sin\eta) \tag{3.34}$$

$$C_{zb} = -\frac{\tan\alpha}{\tan\eta} (C_L \cos\eta + C_D \sin\eta)$$

With small angle assumptions

$$C_{xb} = - C_L - C_D$$

$$C_{yb} = -\left(\frac{C_L}{\eta} + C_D\right)\beta \tag{3.35}$$

$$C_{zb} = -\left(\frac{C_L}{\eta} + C_D\right)\alpha$$

For the lift and drag of the tail it is assumed that the pair of surfaces which lie in the X_B-Z_B plane are influenced by β only and that the pair which lie in the X_B-Y_B plane are influenced by α only. Thus, from Figure 3.11 the force coefficients for the two

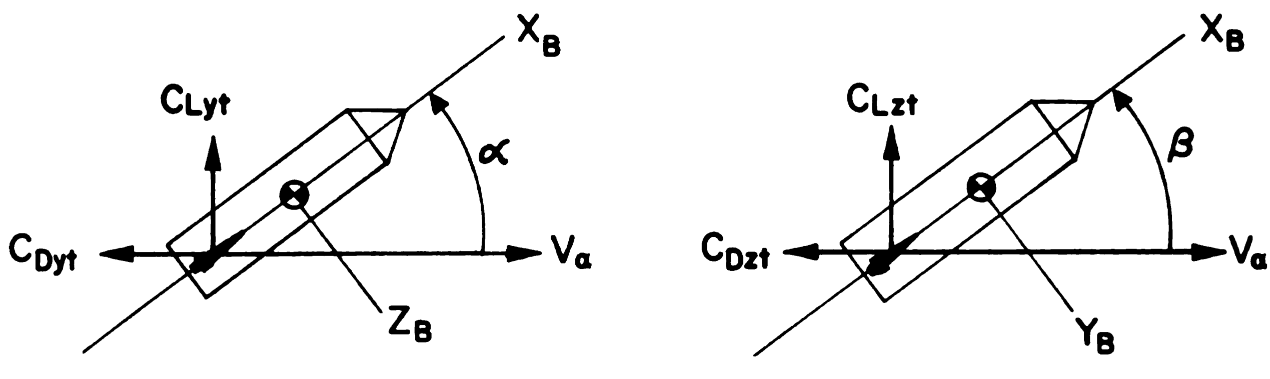

FIGURE 3.11

TAIL FORCE COEFFICIENTS

pairs of identical fins with small angles are

$$C_{xt} = C_{Lyt}\alpha + C_{Lzt}\beta - C_{Dyt} - C_{Dzt}$$

$$C_{yt} = -(C_{Lzt} + C_{Dzt}\beta) \tag{3.36}$$

$$C_{zt} = -(C_{Lyt} + C_{Dyt}\alpha)$$

Summing Equations 3. 35 and 3. 36 yields the total aerodynamic force coefficients as

$$C_x = C_L\eta - C_D + C_{Lyt}\alpha + C_{Lzt}\beta - C_{Dyt} - C_{Dzt}$$

$$C_y = -\left(\frac{C_L}{\eta} + C_D + C_{Dzt}\right)\beta - C_{Lzt} \tag{3.37}$$

$$C_z = -\left(\frac{C_L}{\eta} + C_D + C_{Dyt}\right)\alpha - C_{Lyt}$$

The moments that act around the body axes are assumed to be made up of the lift and drag terms acting on the body and on the tail. The body forces act at the center of pressure of the body and the tail forces act at the center of pressure of the tail. Each acts around the center of gravity of the vehicle which, by definition, is the center of the B-frame. Thus, from Figure 3. 12, the moments around the B-frame axes, including non-dimensional viscous damp-

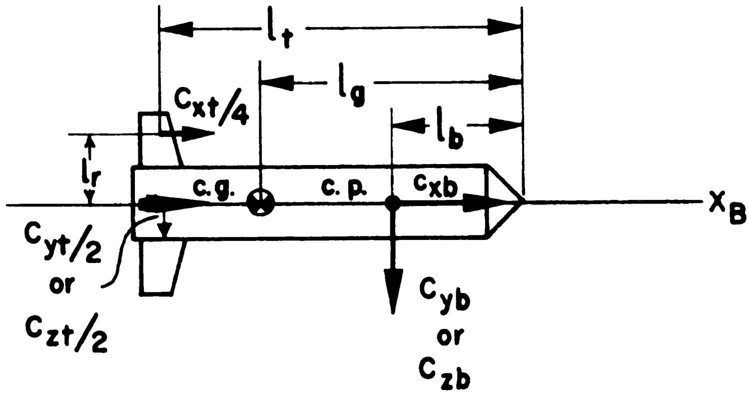

FIGURE 3.12

MOMENT COEFFICIENTS

ing terms (refer to Appendix C), are,

$$C_{\ell} = \left[\frac{d}{2V_a}\right] C_{\ell_p} P$$

$$C_m = -(\ell_g - \ell_b)\, C_{zb} - (\ell_g - \ell_t)\, C_{zt} + \left[\frac{d}{2V_a}\right] C_{m_q} Q \qquad (3.38)$$

$$C_n = (\ell_g - \ell_b)\, C_{yb} + (\ell_g - \ell_t)\, C_{yt} + \left[\frac{d}{2V_a}\right] C_{n_r} R$$

The c. p. and c. g. location data necessary to obtain the force and moment coefficients is developed and given in Appendix C. As is shown in Appendix C, the lift and drag coefficients for the body are

$$C_L = C_{L_\eta}\,\eta$$

$$C_D = C_{D_o} + \frac{\partial C_D}{\partial C_L{}^2}\left(C_{L_\eta}\right)^2 \eta^2 \tag{3.39}$$

and for the tail are

$$C_{Lyt} = C_{Lt_\alpha}\,\alpha$$

$$C_{Lzt} = C_{Lt_\alpha}\,\beta$$

$$C_{Dyt} = C_{Dt_o} + \frac{\partial C_{Dt}}{\partial C_{Lt}{}^2}\left(C_{Lt_\alpha}\right)^2 \alpha^2 \tag{3.40}$$

$$C_{Dzt} = C_{Dt_o} + \frac{\partial C_{Dt}}{\partial C_{Lt}{}^2}\left(C_{Lt_\alpha}\right)^2 \beta^2$$

Upon solution of Equations 3.35, 3.36, 3.37, 3.38, 3.39, and 3.40, the aerodynamic coefficient matrix becomes

$$\begin{bmatrix} C_x \\ C_y \\ C_z \\ C_l \\ C_m \\ C_n \end{bmatrix} = \begin{bmatrix} -\left(C_{D_o} + 2C_{Dt_o}\right) + \left(C_{L_\eta} - \frac{\partial C_D}{\partial C_L{}^2} C_{L_\eta}{}^2\right)\eta^2 + \left(C_{Lt_\alpha} - \frac{\partial C_{Dt}}{\partial C_{Lt}{}^2} C_{Lt_\alpha}{}^2\right)\eta^2 \\ -\left\{\left[C_{D_o} + C_{Dt_o}\right] + C_{L_\eta}\left[1 + \frac{\partial C_D}{\partial C_L{}^2} C_{L_\eta}\eta^2\right] + C_{Lt_\alpha}\left[1 + \frac{\partial C_{Dt}}{\partial C_{Lt}{}^2} C_{Lt_\alpha}\beta^2\right]\right\}\beta \\ -\left\{\left[C_{D_o} + C_{Dt_o}\right] + C_{L_\eta}\left[1 + \frac{\partial C_D}{\partial C_L{}^2} C_{L_\eta}\eta^2\right] + C_{Lt_\alpha}\left[1 + \frac{\partial C_{Dt}}{\partial C_{Lt}{}^2} C_{Lt_\alpha}\alpha^2\right]\right\}\alpha \\ \frac{d}{2V} C_{l_p} P \\ \left\{\left[l_g - l_b\right]\left[C_{D_o} + C_{L_\eta}\left(1 + \frac{\partial C_D}{\partial C_L{}^2} C_{L_\eta}\eta^2\right)\right] + \left[l_g - l_t\right]\left[C_{Dt_o} + C_{Lt_\alpha}\left(1 + \frac{\partial C_{Dt}}{\partial C_{Lt}{}^2} C_{Lt_\alpha}\alpha^2\right)\right]\right\}\alpha + \left(\frac{d}{2V_e}\right) C_{m_q} Q \\ -\left\{\left[l_g - l_b\right]\left[C_{D_o} + C_{L_\eta}\left(1 + \frac{\partial C_D}{\partial C_L{}^2} C_{L_\eta}\eta^2\right)\right] + \left[l_g - l_t\right]\left[C_{Dt_o} + C_{Lt_\alpha}\left(1 + \frac{\partial C_{Dt}}{\partial C_{Lt}{}^2} C_{Lt_\alpha}\beta^2\right)\right]\right\}\beta + \left(\frac{d}{2V_e}\right) C_{m_r} R \end{bmatrix} \tag{3.41}$$

Upon consideration of the magnitudes of the drag terms that are due to lift at small angles it is found that at subsonic speeds the error in leaving these terms out of the C_x term is about 7% at η = 10 degrees and 1.75% at η = 5 degrees. At supersonic speeds the error is zero. In the remaining terms for all speeds, the error in leaving the drag due to lift out is about 3% at angles of 10 degrees and 0.75% at 5 degrees. Tolerating these errors (as can be done in preliminary design studies)

$$\begin{bmatrix} C_x \\ C_y \\ C_z \\ C_\ell \\ C_m \\ C_n \end{bmatrix} = \begin{bmatrix} -(C_{D_0} + 2C_{Dt_0}) \\ -(C_{D_0} + C_{Dt_0} + C_{L\eta} + C_{Lt\alpha})\beta \\ -(C_{D_0} + C_{Dt_0} + C_{L\eta} + C_{Lt\alpha})\alpha \\ \left(\frac{d}{2V_a}\right)C_{\ell_p}\ P \\ \left[(\ell_g - \ell_b)(C_{D_0} + C_{L\eta}) + (\ell_g - \ell_t)(C_{Dt_0} + C_{Lt\alpha})\right]\alpha + \left(\frac{d}{2V_a}\right)C_{m_q}\,Q \\ -\left[(\ell_g - \ell_b)(C_{D_0} + C_{L\eta}) + (\ell_g - \ell_t)(C_{Dt_0} + C_{Lt\alpha})\right]\beta + \left(\frac{d}{2V_a}\right)C_{n_r}\,R \end{bmatrix} \tag{3.42}$$

The terms on the right hand side of Equation 3.42 can be re-written considering Equations 3.22 and 3.25 and the data in Appendix C as

$$\begin{aligned}
\phi_1(V_a) &= -(C_{D_0} + 2C_{Dt_0}) \\
\phi_2(V_a) &= -(C_{D_0} + C_{Dt_0} + C_{L\eta} + C_{Lt\alpha}) \\
\phi_3(V_a) &= -(C_{D_0} + C_{Dt_0} + C_{L\eta} + C_{Lt\alpha}) \\
\phi_4(V_a) &= \left(\frac{d}{2V_a}\right) C_{\ell_p} \\
\phi_5(V_a, t_b) &= (\ell_g - \ell_b)(C_{D_0} + C_{L\eta}) + (\ell_g - \ell_t)(C_{Dt_0} + C_{Lt\alpha}) \\
\phi_6(V_a) &= \left(\frac{d}{2V_a}\right) C_{m_q} \\
\phi_7(V_a, t_b) &= -\left[(\ell_g - \ell_b)(C_{D_0} + C_{L\eta}) + (\ell_g - \ell_t)(C_{Dt_0} + C_{Lt\alpha})\right] \\
\phi_8(V_a) &= \left(\frac{d}{2V_a}\right) C_{n_r}
\end{aligned} \tag{3.43}$$

with

$$\begin{bmatrix} C_x \\ C_y \\ C_z \\ C_\ell \\ C_m \\ C_n \end{bmatrix} = \begin{bmatrix} \phi_1(V_a) & 0 & 0 & 0 & 0 & 0 \\ 0 & \phi_2(V_a) & 0 & 0 & 0 & 0 \\ 0 & 0 & \phi_3(V_a) & 0 & 0 & 0 \\ 0 & 0 & 0 & \phi_4(V_a) & 0 & 0 \\ 0 & 0 & \phi_5(V_a, t_b) & 0 & \phi_6(V_a) & 0 \\ 0 & \phi_7(V_a, t_b) & 0 & 0 & 0 & \phi_8(V_a) \end{bmatrix} \begin{bmatrix} 1 \\ \beta \\ a \\ P \\ Q \\ R \end{bmatrix} \tag{3.44}$$

3.3.2 Propulsion and Control Forces

For propulsion and control, as given in Section 2.2, the first stage uses five (5) engines of the F-1 type, the second stage uses five (5) engines of the J-2 type, and the third stage uses one (1) engine of the J-2 variety and a set of reaction jets. As shown in Figure 3.13, the engines of the first stage are arranged in a cluster about the fifth engine with each of the outside four gimballed around one axis to provide attitude control of the vehicle. Each engine assembly is rotated about an appropriate axis to change the direction of the thrust vector, and thus provide a moment (and an unwanted side force) about a desired axis. The choice of the B-frame axes provides for control around the yaw (Z_B) axis with rotations of the number 1 and number 3 engines, and around the

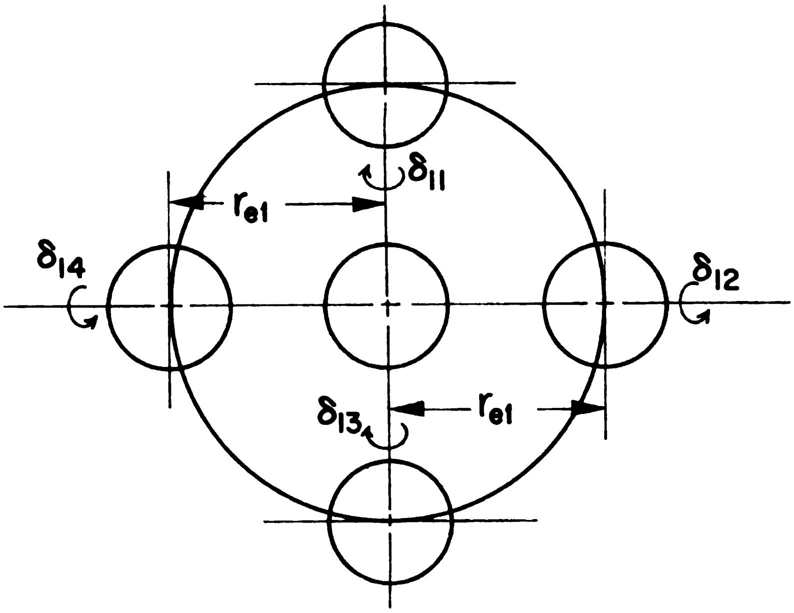

FIGURE 3. 13

FIRST STAGE ENGINE CONFIGURATION

pitch (Y_B) axis with rotations of the number 2 and number 4 engines. As shown in Figure 3. 13, positive rotations of the engines through the angles δ_{11}, δ_{12}, δ_{13}, and δ_{14} are defined by positive rotations of the engine with respect to the vehicle body around the B-Frame axes. Also, with rotations of the number 2 and number 4 engines in opposite directions a moment with a moment arm, r_{e1}, is developed for roll (X_B) axis control.

The second stage, as the first stage, uses a cluster of four gimballed engines around a fifth stationary engines. The arrangement for control is the same as that shown in Figure 3. 13 for the first stage but with deflection angles δ_{21}, δ_{22}, δ_{23}, and δ_{24} with a moment arm for the number 2 and number 4 engines of r_{e2}.

The third stage used a single engine which is gimballed around two axes as shown in Figure 3.14. The rotation around the

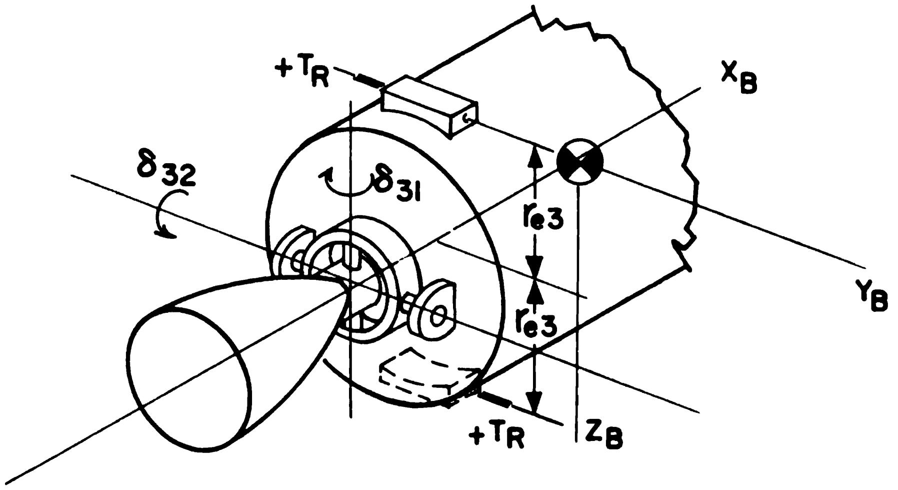

FIGURE 3.14

THIRD STAGE ENGINE CONFIGURATION

axis parallel to Z_B is δ_{31}, and the rotation around the axis parallel to Y_B is δ_{32}, giving yaw and pitch control respectively.

Since it is not possible to obtain a rolling moment from a single engine mounted on the X_B axis, it is necessary to add a second type of control to provide rolling moments. Four (4) reaction jets are used, located as shown in Figure 3.14, which operating in pairs produce, it as assumed, equal plus and minus forces, and hence, no side force.

From Figure 3.15, the X_B and Y_B forces and the

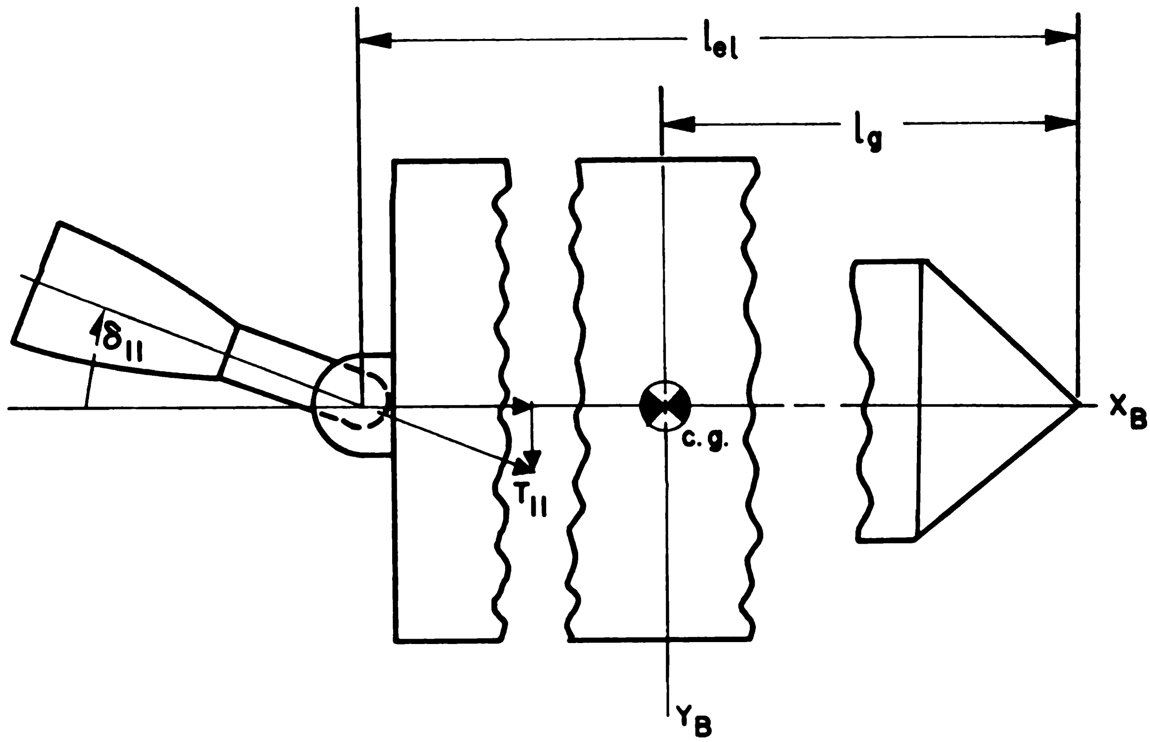

FIGURE 3.15

ENGINE FORCES AND MOMENTS

Z_B moment produced by the first stage number 1 engine are

$$
\begin{aligned}
F_{xe11} &= T_{11} \cos \delta_{11} \\
F_{ye11} &= T_{11} \sin \delta_{11} \qquad (3.45) \\
M_{ze11} &= -(T_{11} \sin \delta_{11})(\ell_{e1} - \ell_g)
\end{aligned}
$$

A moment would also be produced about the Y_B axis if the engine were not canted so that the thrust vector passed through the c.g. of the vehicle. It is assumed that all of the engines are canted, and in addition, that the moments from each caused by the shifting of the c.g. (due to expulsion of fuel for example) exactly cancel each other. The small reduction in effective thrust for each of the engines due to canting is assumed to be insignificant. Also, it is assumed that the forces and moments produced by misalignment of the engines are zero.

Assuming the thrust from each of the first stage engines to be identical and calling this thrust T_1 , the forces and moments produced by all of the first stage engines, similar to Equations 3.45 with small angle assumption, using Figures 3.13 and 3.15, are

$$\begin{bmatrix} F_{xe1} \\ F_{ye1} \\ F_{ze1} \\ M_{xe1} \\ M_{ye1} \\ M_{ze1} \end{bmatrix} = T_1 \begin{bmatrix} 5 \\ (\delta_{11} + \delta_{13}) \\ -(\delta_{12} + \delta_{14}) \\ (\delta_{14} - \delta_{12})\, r_{e1} \\ -(\delta_{12} + \delta_{14})(\ell_{e1} - \ell_g) \\ -(\delta_{11} + \delta_{13})(\ell_{e1} - \ell_g) \end{bmatrix} \tag{3.46}$$

The arrangement of the second stage engines is the same as that of the first stage. Using the same approximations and assumptions, the forces and moments for the second stage engines become

$$\begin{bmatrix} F_{xe2} \\ F_{ye2} \\ F_{ze2} \\ M_{xe2} \\ M_{ye2} \\ M_{ze2} \end{bmatrix} = T_2 \begin{bmatrix} 5 \\ (\delta_{21} + \delta_{23}) \\ -(\delta_{22} + \delta_{24}) \\ (\delta_{24} - \delta_{22})\, r_{e2} \\ -(\delta_{22} + \delta_{24})\,(\ell_{e2} - \ell_g) \\ -(\delta_{21} + \delta_{23})\,(\ell_{e2} - \ell_g) \end{bmatrix} \tag{3.47}$$

For the third stage, roll control is accomplished with reaction jets. Assuming identical thrust from each of the reaction jet engines (Figure 3.14) and an equal distance of each from the X_B axis, the rolling moment is

$$M_{xe3} = 2\,(r_{e3}\,T_R)\,\delta_{33} \tag{3.48}$$

where T_R is the magnitude of the thrust of each of the jets and δ_{33} represents the non-linear command function of the jets (on-off with a dead zone) as shown in Figure 3.16. The remaining forces and moments are produced by the single J-2 engine in a manner similar to the first and second stage engines except that the third stage engine is gimballed around two axes rather than one (Refer to Figure 3.14). Using the same approximations and assumptions

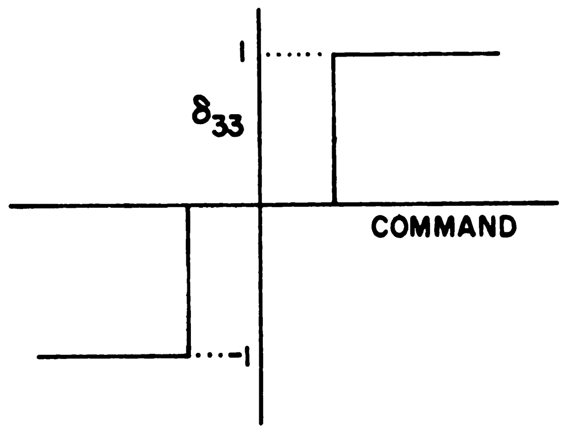

FIGURE 3. 16

REACTION JET COMMAND FUNCTION

as used for the first and second stages and including the reaction jets, the third stage forces and moments become

$$\begin{bmatrix} F_{xe3} \\ F_{ye3} \\ F_{ze3} \\ M_{xe3} \\ M_{ye3} \\ M_{ze3} \end{bmatrix} = T_3 \begin{bmatrix} 1 \\ \delta_{31} \\ -\delta_{32} \\ 2\dfrac{T_R}{T_3}\delta_{33} r_{e3} \\ -\delta_{32}(\ell_{e3} - \ell_g) \\ -\delta_{31}(\ell_{e3} - \ell_g) \end{bmatrix} \tag{3.49}$$

The thrust of a rocket engine can be represented by a momentum term and a pressure term as

$$T = \overbrace{\dot{m} V_e}^{\text{Momentum Term}} + \overbrace{(P_e - P_a) A_e}^{\text{Pressure Term}} \qquad (3.50)$$

Owing to such things as ejection of part of the exhaust gases in a non-axial direction with respect to the engine, correction factors should applied to Equation 3.50 (Refer to 1 , p. 20-10). Assuming these corrections are included, the effective thrust for each of the engines of the first stage is

$$T_I = T_{VI} - (P_a A_{eI}) \qquad (3.51)$$

The vacuum thrust term, T_{VI} (thrust outside the earth's atmosphere), includes the momentum term and the exist pressure term with correction factors; and the atmospheric pressure term, $P_a A_{eI}$, consists of the free stream atmospheric pressure and the effective nozzle exist area. The free stream atmospheric pressure term by the equation of state of a thermally perfect gas is

$$P_a = \rho RT \qquad (3.52)$$

and in terms of the speed of sound is

$$P = \frac{1}{\gamma} \rho a^2 \tag{3.52}$$

With a constant speed of sound as given by Equation 3. 24 and with $\gamma = 1.4$, the free stream atmospheric pressure is

$$P_a = 0.714 \times 10^6 \rho \tag{3.53}$$

(Equation 3. 53 is accurate to within 3% of total engine thrust if the exponential approximations for air density is used.)

Since the second and third stage engines are used only when the vehicle is outside the effective atmosphere, the thrust from these engines can be represented by a vacuum thrust term as

$$\begin{aligned} T_2 &= T_{v2} \\ T_3 &= T_{v3} \end{aligned} \tag{3.54}$$

With parameter values of

$$\begin{aligned} T_{v1} &= 1{,}740{,}000 \text{ lbs} \\ A_{e1} &= 113 \text{ feet}^2 \\ T_{v2} &= 260{,}000 \text{ lbs} \\ T_{v3} &= 260{,}000 \text{ lbs} \end{aligned} \tag{3.55}$$

the thrust equations become

$$
\begin{aligned}
T_1 &= 1.74 \times 10^6 - 80.8 \times 10^6 \rho \\
T_2 &= 260{,}000 \qquad\qquad (3.56) \\
T_3 &= 260{,}000
\end{aligned}
$$

3.4 GRAVITATION

In general, gravitational forces between the vehicle and every other body in the universe tend to accelerate the vehicle. Common practice is to call the center of the earth the center of the inertial reference frame for terrestrial vehicle considerations. Since the center of the earth and the vehicle are accelerating in space by very nearly the same amount, this is a good assumption. The inertial and gravitational forces are exactly equal, and hence an accelerometer would not sense the acceleration (it only senses external forces), and thus, would not inject an error into the guidance system. Also, the difference between the acceleration due to gravitational attraction between the earth and all other bodies of the universe, and the vehicle and all other bodies of the universe is a function of the distance between the vehicle and the mass center of the earth. As illustrated in Appendix A, the difference between the accelerations due to attraction between the sun and the earth, and the sun and the vehicle are insignificant ($<10^{-7}$ g's). The only gravitational attraction necessary to consider is that between the vehicle and the earth.

As the earth is not a perfect sphere, the gravitational attraction between the earth and a vehicle near the surface of the earth will not, in general, be directed radially between the center of the earth and the vehicle. A good first order approximation is given in [5, p. 61] as a function of geocentric latitude, and upon application to the coordinate system used here becomes

$$
\begin{aligned}
G_X &= -\frac{\mu R_{eq}^{2}}{Z^{4}} J \sin 2\Phi \cos\Psi \\
G_Y &= -\frac{\mu R_{eq}^{2}}{Z^{4}} J \sin 2\Phi \sin\Psi \qquad (3.57) \\
G_Z &= -\frac{\mu}{Z^{2}}\left[1 + J\frac{R_{eq}^{2}}{Z^{2}}(1 - 3\sin^{2}\Phi)\right]
\end{aligned}
$$

where from [2, p. 108] with conversion of units

$$
\begin{aligned}
\mu &= 1.40770 \times 10^{16}\ \text{ft}^{3}/\text{sec}^{2} \\
R_{eq} &= 20{,}925{,}732\ \text{ft} \\
J &= 1.6241 \times 10^{-3} \qquad (3.58) \\
e &= 1/298.26
\end{aligned}
$$

For a still more accurate expression of the earth's gravitational field, with data obtained by using earth satellites, see [1, p. 4-30].

For a particular mission it is possible to greatly simplify the gravitational computations (no need for Φ and Ψ) by using

$$
\begin{aligned}
G_x &= G_{xo} \frac{Z_o^2}{Z^2} + \frac{\partial G_x}{\partial \sigma} \\
G_y &= G_{yo} \frac{Z_o^2}{Z^2} + \frac{\partial G_y}{\partial \sigma} \\
G_z &= G_{zo} \frac{Z_o^2}{Z^2} + \frac{\partial G_z}{\partial \sigma}
\end{aligned}
\qquad (3.59)
$$

For rough preliminary design studies it is reasonable to approximate the acceleration due to gravitation as

$$
\begin{aligned}
G_X &= G_Y = 0 \\
G_Z &= -\frac{\mu}{Z^2}
\end{aligned}
\qquad (3.60)
$$

3.5 VEHICLE MASS AND INERTIA

The mass of the vehicle at any time after launch is a function of its own initial mass, the amount of fuel that has burned, and the number of stages remaining. The mass, assuming a constant burning rate, is

$$
m = m_{1_o} + m_{2_o} + m_{3_o} - \dot{m}_1 t_{b1} - \dot{m}_2 t_{b2} - \dot{m}_3 t_{b3} \qquad (3.61)
$$

From Appendix C the initial masses of the three stages (where m_{3_0} consists of the third stage dry weight plus the payload and the guidance and control sections) are

$$m_{1_0} = 153,600 \text{ slugs}$$
$$m_{2_0} = 27,200 \text{ slugs} \qquad (3.62)$$
$$m_{3_0} = 14,280 \text{ slugs}$$

and the mass flow rates which are assumed to be constant, are

$$\dot{m}_1 = 900 \text{ slugs/sec}$$
$$\dot{m}_2 = 90 \text{ slugs/sec} \qquad (3.63)$$
$$\dot{m}_3 = 18 \text{ slugs/sec}$$

The three body-axis inertias of the vehicle depend upon the dry weight of the stages remaining and upon the amount of fuel remaining. The inertias are given in Appendix C in Figures C-4, C-5, C-6, and C-7. Each was calculated using a constant burning rate assuming all of the fuel contributed to the inertia with the fuel moving toward engine end of the vehicle as the fuel is expended.

3.6 VEHICLE EQUATIONS OF MOTION

In defining the motions of the vehicle, it is necessary to have a single equation for each of its six degrees of freedom. There are three equations expressing the translational motions and three expressing the rotational motions.

The equations for the translational motions are derived in Appendix A. These equations are based on Newton's second law. The results (Equations A-47) are expressed in V-frame coordinates, and thus, rotations of the V-frame with respect to the I-frame, where Newton's laws are valid, are taken into account. The center of the V-frame, by necessity, is located at the c. g. of the vehicle.

Since the forces that act on the vehicle (Equations A-47) are expressed in B-frame coordinates, it is necessary to transform the forces from the B-frame to the V-frame. This can be done by using the inverse relationships of the direction cosine transformation that is given in Equations 3.9 and 3.10 as

$$\begin{bmatrix} F_X \\ F_Y \\ F_Z \end{bmatrix} = \begin{bmatrix} \ell_1 & m_1 & n_1 \\ \ell_2 & m_2 & n_2 \\ \ell_3 & m_3 & n_3 \end{bmatrix} \begin{bmatrix} F_x \\ F_y \\ F_z \end{bmatrix} \tag{3.64}$$

The rotational motions of the vehicle are derived in Appendix B. The equations expressing these motions are based on the moment of momentum referred to the B-frame, whose center is located at the mass center of the vehicle. The external moments are given in B-frame coordinates and, thus, no coordinate transformation is required.

Combining the results of Appendices A and B into one matrix yields

$$\begin{bmatrix} \dot{X} \\ \dot{Y} \\ \dot{Z} \\ P \\ Q \\ R \end{bmatrix} = \begin{bmatrix} -\dot{X}\dot{Z}/Z \\ -\dot{Y}\dot{Z}/Z \\ (\dot{X}^2 + \dot{Y}^2)/Z \\ 0 \\ PR\,(I_{zz} - I_{xx})/I_{yy} \\ RQ\,(I_{xx} - I_{yy})/I_{zz} \end{bmatrix} + \begin{bmatrix} F_X/m \\ F_Y/m \\ F_Z/m \\ M_x/I_{xx} \\ M_y/I_{yy} \\ M_z/I_{zz} \end{bmatrix} + \begin{bmatrix} G_X \\ G_Y \\ G_Z \\ 0 \\ 0 \\ 0 \end{bmatrix} \quad (3.65)$$

Solutions to these equations can be obtained using the aerodynamic and propulsion system moment and transformed force inputs. The body axis forces and moments are defined by Equations 3. 32, 3. 33, 3. 42, 3. 46, 3. 47, 3. 49, 3,56, and 3. 60 with data from Appendix C.

4. GUIDANCE AND CONTROL SYSTEM COMPONENTS

The basic electromechanical components used in the guidance and control system are gyros, a three-gimbal platform, accelerometers, and servos. The basic expressions for the dynamics of these components are developed from fundamental concepts.

4.1 GYROS

The dynamics of a gyro can be considered through the use of the rotational form of Newton's second law. As developed in Appendix B and given by Equation B-13, this expression is

$$\overline{T} = \left[\frac{d\overline{H}}{dt}\right]_I \tag{4.1}$$

where $\overline{T}$ is the applied torque vector. The rate of change of angular momentum of a gyro wheel referred to the gimbal within which the wheel is mounted, herein called the float, is

$$\overline{T}_w = \left[\frac{d\,\overline{H}_w}{dt}\right]_I = \left[\frac{d\,\overline{H}_w}{dt}\right]_f + \overline{\omega}_{If} \times \overline{H}_w \tag{4.2}$$

(This gimbal is called the float because in many gyros it is suspended in a fluid for purposes of load relief of the supports under

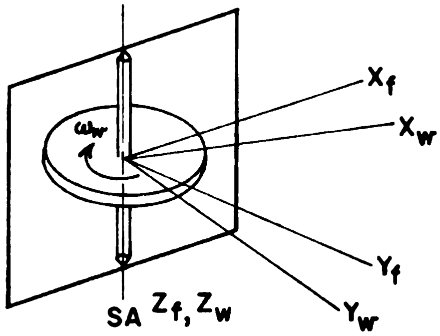

FIGURE 4. 1

BASIC GYRO

high environment accelerations and for the addition of viscous friction.) The angular momentum of the wheel is

$$\overline{H}_w = I_w \overline{\omega}_w \tag{4.3}$$

where I_w about principle axes is a matrix as

$$I_w = \begin{bmatrix} I_{wx} & 0 & 0 \\ 0 & I_{wy} & 0 \\ 0 & 0 & I_{wz} \end{bmatrix} \tag{4.4}$$

The coordinate systems are shown in Figure 4. 1 where the common z axis about which the wheel rotates is called the spin axis (SA). Assuming that the wheel is non-accelerating with respect to the float

$$\left[\frac{d\,\bar{H}_w}{dt}\right]_f = 0 \tag{4.5}$$

and

$$\bar{T}_w = \bar{\omega}_{If} \times \bar{H}_w \tag{4.6}$$

This is the basic gyro law where the applied torque is equal to the cross product of the angular rate of the gimbal within which the wheel is mounted and the wheel angular momentum.

The addition of an axis of freedom to the gyro as shown in Figure 4.2 yields a gyro known as a "single-degree-of-freedom gyro." The coordinate system of the case is referred to as the c-frame where the X_c axis is called the "input axis" (IA), and the Z_c axis is called the "spin reference axis" (SRA).

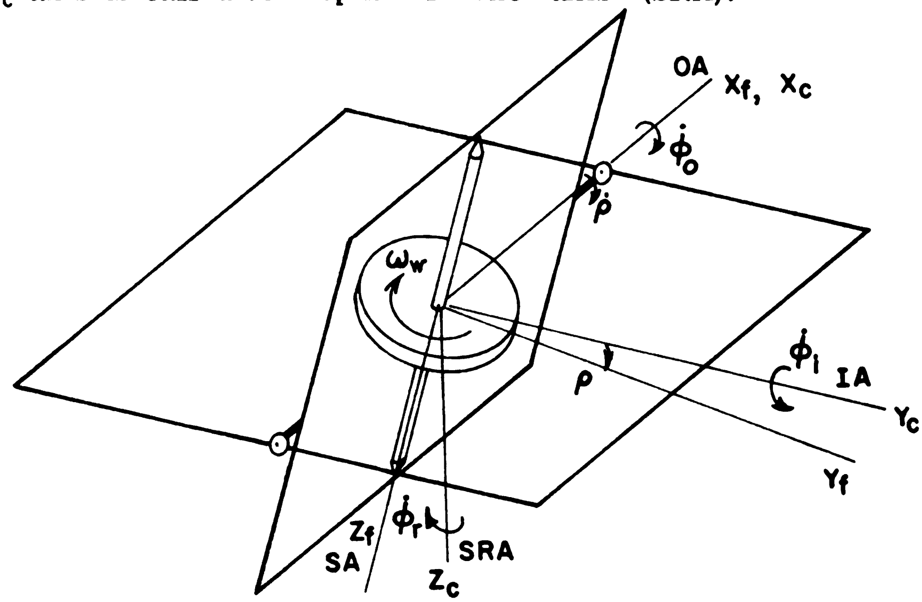

FIGURE 4.2

SINGLE-DEGREE-OF-FREEDOM GYRO

The torque applied to the float is

$$\bar{T}_f = \left[\frac{d\,\bar{H}_f}{dt}\right]_I = \left[\frac{d\,\bar{H}_f}{dt}\right]_f + \bar{\omega}_{If} \times \bar{H}_f \tag{4.7}$$

where the angular momentum at the float is

$$\bar{H}_f = H_w\, k_f + I_f \bar{\omega}_{If} \tag{4.8}$$

The angular rate input is

$$\bar{\omega}_{If} = \begin{bmatrix} \dot{\phi}_o \\ \dot{\phi}_i \\ \dot{\phi}_r \end{bmatrix}_c + \begin{bmatrix} \dot{\rho} \\ 0 \\ 0 \end{bmatrix}_f \tag{4.9}$$

which, in the f-frame, by coordinate transformation with small angle assumptions is

$$\bar{\omega}_{If} = \begin{bmatrix} \dot{\phi}_o + \dot{\rho} \\ \dot{\phi}_i + \rho\dot{\phi}_r \\ \dot{\phi}_r - \rho\dot{\phi}_i \end{bmatrix}_f \tag{4.10}$$

(Positive gyro and platform angles are defined as rotations of the inside member with respect to the outside member in a positive direction as defined by the inner member coordinate system.)

Combining Equations 4. 8 and 4. 10, with the assumption that the inertias are about principle axes, the float angular momentum in float coordinates becomes

$$\bar{H}_f = \begin{bmatrix} I_{fx} \ (\dot{\phi}_o + \dot{\rho}) \\ I_{fy} \ (\dot{\phi}_i + \rho\dot{\phi}_r) \\ I_{fz} \ (\dot{\phi}_r - \rho\dot{\phi}_i) + H_w \end{bmatrix}_f \tag{4.11}$$

The expression for the torque about 0A from Equation 4. 7 using Equations 4. 10 and 4. 11 is

$$T_{fx} = I_{fx} (\ddot{\phi}_o + \ddot{\rho}) + H_w (\dot{\phi}_i + \rho\dot{\phi}_r) + (I_{fz} - I_{fy})(\dot{\phi}_i + \rho\dot{\phi}_r)(\dot{\phi}_r - \rho\dot{\phi}_i) \tag{4.12}$$

With a viscous damper torque, a spring (or flex-leads to the gyro motor) torque, and other drift disturbance torques on the output axis expressed as

$$T_{fx} = -D_\rho \dot{\rho} - K_\rho \rho + T_\rho \tag{4.13}$$

Equation 4. 12 becomes

$$I_{fx}\ddot{\rho} + D_\rho\dot{\rho} + K_\rho\rho = -H_w\dot{\phi}_i - I_{fx}\ddot{\phi}_o - H_w\rho\dot{\phi}_r + T_\rho - (I_{fz} - I_{fy})(\dot{\phi}_i + \rho\dot{\phi}_r)(\dot{\phi}_r - \rho\dot{\phi}_i) \tag{4.14}$$

The last term in Equation 4. 14 is generally small (by design) and can be ignored. The term, $H_w\rho\dot{\phi}_r$, is involved in a phenomenon known as "kinematic rectification." Periodic motion of ϕ_r and ϕ_i, or ϕ_o, at the same frequencies and in certain phase relationship will appear as an input through the term $H_w \rho \dot{\phi}_r$ which will always be of one sign. As will be shown in Section 4.2, Equation 4.25, a torque on the gyro output axis causes a drift of the stabilized platform gimbal and thus an error in its reference position. To limit this effect, the excursion of ρ is held to a minimum. Neglecting this term, the general single-degree-of-freedom gyro state model becomes

$$\frac{d}{dt}\begin{bmatrix} \dot{\rho} \\ \rho \end{bmatrix} = \begin{bmatrix} -\dfrac{D_\rho}{I_{fx}} & -\dfrac{K_\rho}{I_{fx}} \\ 1 & 0 \end{bmatrix}\begin{bmatrix} \dot{\rho} \\ \rho \end{bmatrix} + \begin{bmatrix} \dfrac{-H_w}{I_{fx}} \\ 0 \end{bmatrix}\dot{\phi}_i + \begin{bmatrix} -\ddot{\phi}_o \\ 0 \end{bmatrix} + \begin{bmatrix} \dfrac{T_\rho}{I_{fx}} \\ 0 \end{bmatrix} \tag{4.15}$$

Classifications of single-degree-of-freedom gyros are related to the physical parameters of the gyro as given in Equation 4.15. If K_ρ is large, the gyro is known as a "rate gyro" since in steady state the output axis angle, ρ, is proportional to the input rate, $\dot{\phi}_i$. If K_ρ is small and D_ρ is large, it is known as an "integrating rate gyro" and if both K_ρ and D_ρ are small, it is known as a "doubly integrating rate gyro."

Rate gyros are used in the system herein described to provide vehicle body axis rate information for control system damping. This is done by hard mounting three rate gyros with their sensitive axes mutually perpendicular and parallel to the B-frame axes. The rate gyro state model is given by Equation 4.15.

Doubly integrating rate gyros are used with the stable platform.

4.2 PLATFORM

The stable platform as shown in Figure 4.3 consists of three gimbals, the inner one of which is stabilized with respect to inertial space by three doubly integrating rate gyros. The gyros are mounted orthogonally with each of the three gyros stabilizing one axis of the inner gimbal. If the gyros and gimbals are oriented as shown in Figure 4.3, each gyro can be considered as a two-degree-of-freedom gyro where the axes of freedom for the A gyro are about ρ_A and α, for the B gyro about ρ_B and β, and for the C gyro about ρ_C and γ. Thus, the dynamics of the A gyro, for example, can be derived considering it to be a two-degree-of-freedom gyro as shown in Figure 4.4.

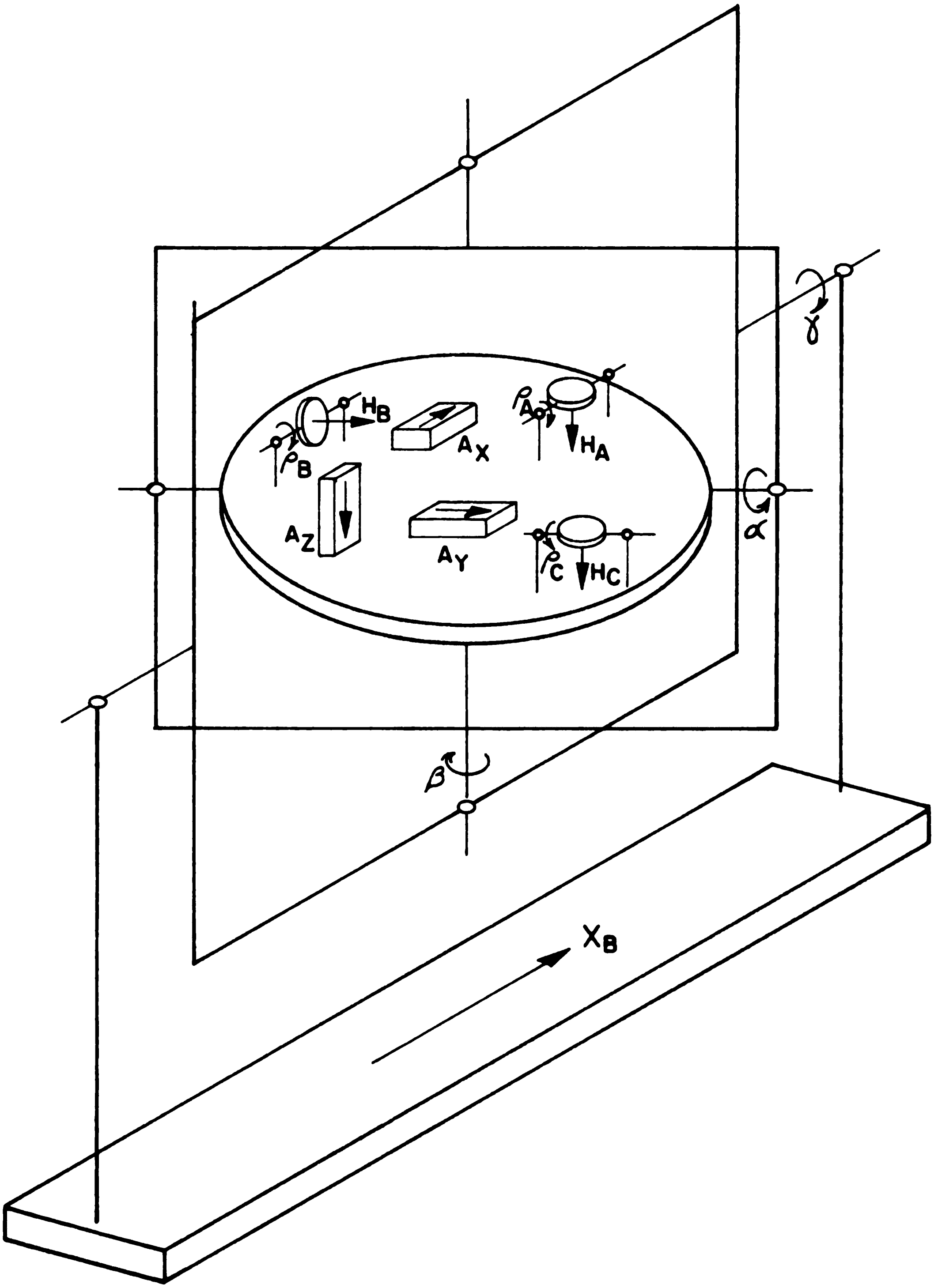

FIGURE 4. 3

<u>THREE-AXIS STABLE PLATFORM</u>

The torque equation for the gimbal is

$$\bar{T}_g = \left[\frac{d\,\bar{H}_g}{dt}\right]_I = \left[\frac{d\,\bar{H}_g}{dt}\right]_g + \bar{\omega}_{Ig} \times \bar{H}_g \tag{4.16}$$

where the angular momentum is

$$\bar{H}_g = \bar{H}_f + I_g \bar{\omega}_{Ig} \tag{4.17}$$

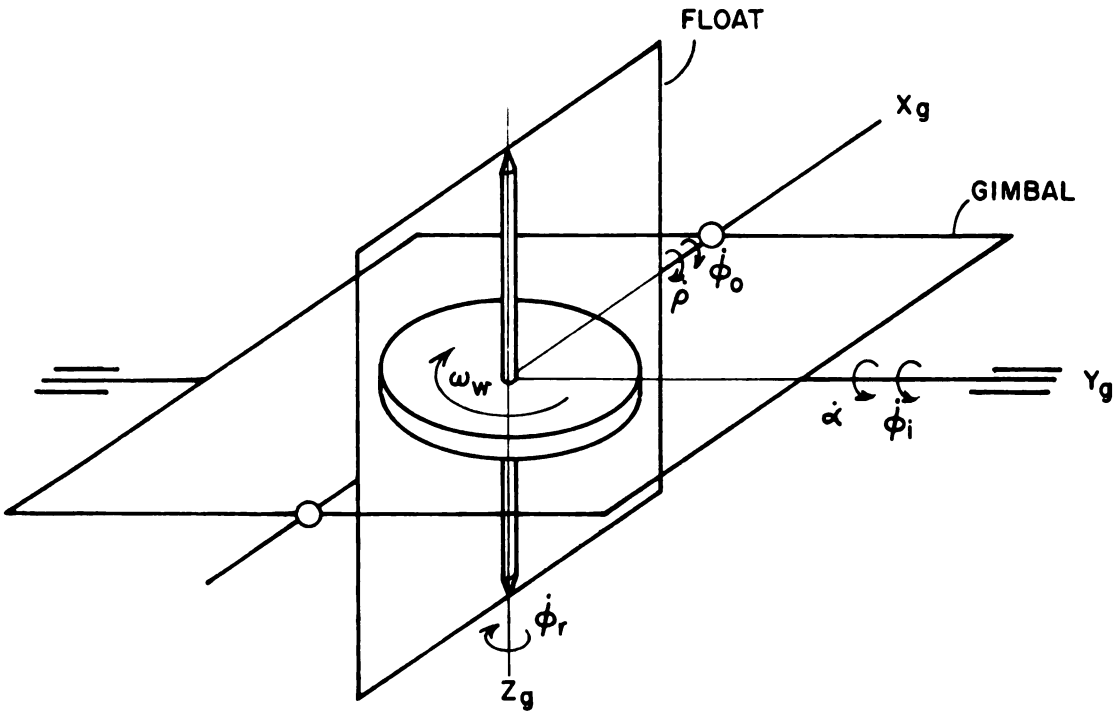

FIGURE 4.4

TWO-DEGREE-OF-FREEDOM GYRO

and

$$I_g = \begin{bmatrix} I_{gx} & 0 & 0 \\ 0 & I_{gy} & 0 \\ 0 & 0 & I_{gz} \end{bmatrix} \tag{4.18}$$

Upon coordinate transformation of the float angular momentum (Equation 4. 11) through the angle ρ and summing with $I_g \, \overline{\omega}_{Ig}$, Equation 4. 17 becomes

$$\overline{H}_g = \begin{bmatrix} (I_{fx} + I_{gx})\dot{\phi}_o + I_{fx}\dot{\rho} \\ (I_{fy} + I_{gy})\dot{\phi}_i - H_w \rho + (I_{fy} - I_{fz})\dot{\phi}_r \rho + I_{fz}\dot{\phi}_i \rho^2 \\ (I_{fz} + I_{gz})\dot{\phi}_r + H_w + (I_{fy} - I_{fz})\dot{\phi}_i \rho + I_{fy}\dot{\phi}_r \rho^2 \end{bmatrix} \tag{4.19}$$

Assuming the terms involving $(I_{fy} - I_{fz})$ and ρ^2 are small and considering only the Y_g component, Equation 4.16 with no case motions, or,

$$\alpha = \phi_i \tag{4.20}$$

becomes

$$T_{gy} = (I_{fy} + I_{gy})\ddot{\alpha} - H_w(\dot{\rho} + \dot{\phi}_o) + (I_{fx} + I_{gx} - I_{fz} - I_{gz})\dot{\phi}_o \dot{\phi}_r + I_{fx}\dot{\phi}_r \dot{\rho} \tag{4.21}$$

With

$$T_{gy} = -D_\alpha \dot{\alpha} + T_\alpha \tag{4.22}$$

and assuming the non-linear terms and $\dot{\phi}_o$ are small, the expression for gimbal motion in state model form becomes

$$\frac{d}{dt}\left[\dot{\alpha}\right] = \left[-D_\alpha/(I_{fy} + I_{gy})\right]\left[\dot{\alpha}\right] + \left[H_w/(I_{fy} + I_{gy})\right]\left[\dot{\rho}\right] + \left[1/(I_{fy} + I_{gy})\right]\left[T_\alpha\right] \tag{4.23}$$

Combining Equations 4. 15, 4. 20, and 4. 23, the state model for the two-degree-of-freedom gyro becomes

$$\frac{d}{dt}\begin{bmatrix} \dot{\rho} \\ \rho \\ \dot{\alpha} \end{bmatrix} = \begin{bmatrix} -\dfrac{D_\rho}{I_{fx}} & -\dfrac{K_\rho}{I_{fx}} & -\dfrac{H_w}{I_{fx}} \\ 1 & 0 & 0 \\ \dfrac{H_w}{(I_{fy} + I_{gy})} & 0 & \dfrac{-D_\alpha}{(I_{fy} + I_{gy})} \end{bmatrix} \begin{bmatrix} \dot{\rho} \\ \rho \\ \dot{\alpha} \end{bmatrix} + \begin{bmatrix} \dfrac{T_\rho}{I_{fx}} \\ 0 \\ \dfrac{T_\alpha}{(I_{fy} + I_{gy})} \end{bmatrix} \tag{4.24}$$

Neglecting the inertia, damping, and spring terms, the two-degree-of-freedom gyro terminal equations by rearrangement become

$$\begin{bmatrix} T_\rho \\ T_\alpha \end{bmatrix} = \begin{bmatrix} 0 & H_w \\ -H_w & 0 \end{bmatrix} \begin{bmatrix} \dot{\rho} \\ \dot{\alpha} \end{bmatrix} \tag{4.25}$$

These are the terminal equations of an "ideal gyro."

Equations 4. 25 show that if a torque exists on the ρ axis, for instance, a "precession rate" will appear on the α axis. Since torques are always present about all of the axes of a stable platform due to friction, motion of the vehicle, etc., the axes will all move from their respective reference positions at rates inversely proportional to the stabilizing gyro's angular momentum. In the design of gyros and platforms one of the most important objectives is to keep these "drift torques" as low as possible.

Although it is not possible to correct for torques acting about the gyro output axes by "closing the loop", it is possible to control the torques on the gyro input axes by using a technique known as "torque compensation." This consists of measuring the gyro output-axis angle and applying a torque about the proper gimbal axis in a direction which will drive the gyro back toward its reference position. In effect, an average torque is applied which exactly cancels the torque which would otherwise cause the gyro to drift. If the vehicle is not oriented so that the platform gimbal positions are as shown in Figure 4. 3, however, but say with a 90-degree pitch angle ($\alpha = 90°$), the gimbal axes that are stabilized by the B and C gyros are interchanged. (A yaw angle will have a similar effect but since the expected yaw motions of the vehicle herein considered are small, this decoupling is ignored.) The decoupling with α must be corrected, and can be, by simply resolving the gyro output axis angles as shown in Figure 4.5 through the angle α. In this way, under steady-state conditions, torques are produced that exactly cancel the drift torques. For an example of an analysis of a stable platform torque compensation system refer to Appendix D.

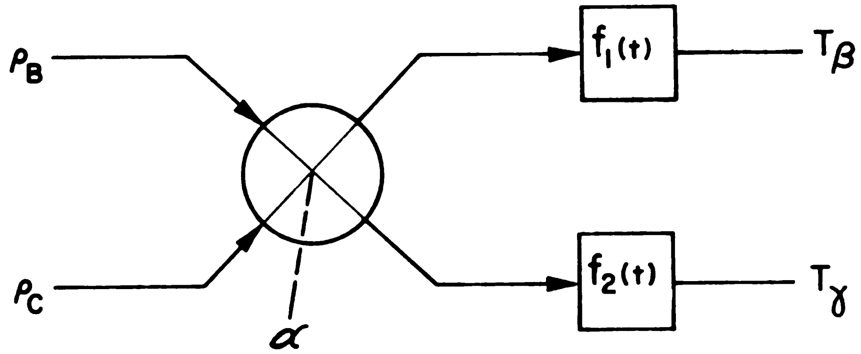

FIGURE 4. 5

CODING FOR TORQUE COMPENSATION

4. 3 ACCELEROMETERS

Ther are many types of accelerometers that can be used to sense the linear accelerations of a vehicle. All of them rely on the inertial reaction of a known mass to an applied acceleration. A simple example of an accelerometer would be a spring-mass system where the mass is mounted between two springs on a viscous slide as shown in Figure 4. 6. The state model for this system is

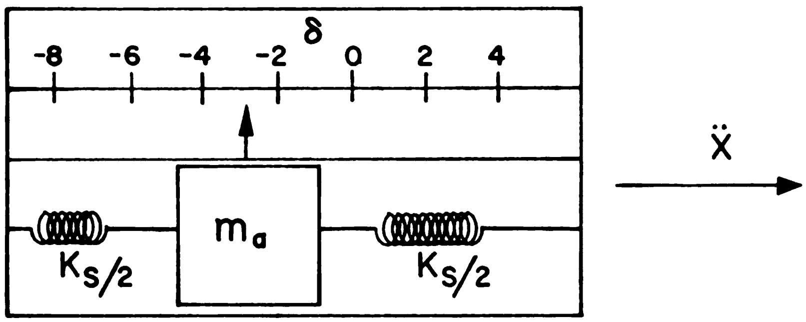

FIGURE 4. 6

SPRING-MASS ACCELEROMETER

$$\frac{d}{dt}\begin{bmatrix} \dot{\delta} \\ \\ \delta \end{bmatrix} = \begin{bmatrix} -D_a/m_a & -K_S/m_a \\ \\ 1 & 0 \end{bmatrix} \begin{bmatrix} \dot{\delta} \\ \\ \delta \end{bmatrix} + \begin{bmatrix} -1 \\ \\ 0 \end{bmatrix} \ddot{x} \tag{4.26}$$

where

$$\ddot{x}_m = -\frac{K_S}{m_a}\delta \tag{4.27}$$

A second type of accelerometer that could be used is one which has a pendulous mass that is forced back to a reference position by a torquer-pickoff combination as shown in Figure 4. 7. The state model for this accelerometer is

$$\frac{d}{dt}\begin{bmatrix} \dot{\delta} \\ \\ \delta \end{bmatrix} = \begin{bmatrix} -D_a/I_a & -K_P K_A K_T/I_a \\ \\ 1 & 0 \end{bmatrix} \begin{bmatrix} \dot{\delta} \\ \\ \delta \end{bmatrix} + \begin{bmatrix} -m_a r/I_a \\ \\ 0 \end{bmatrix} \ddot{x} \tag{4.28}$$

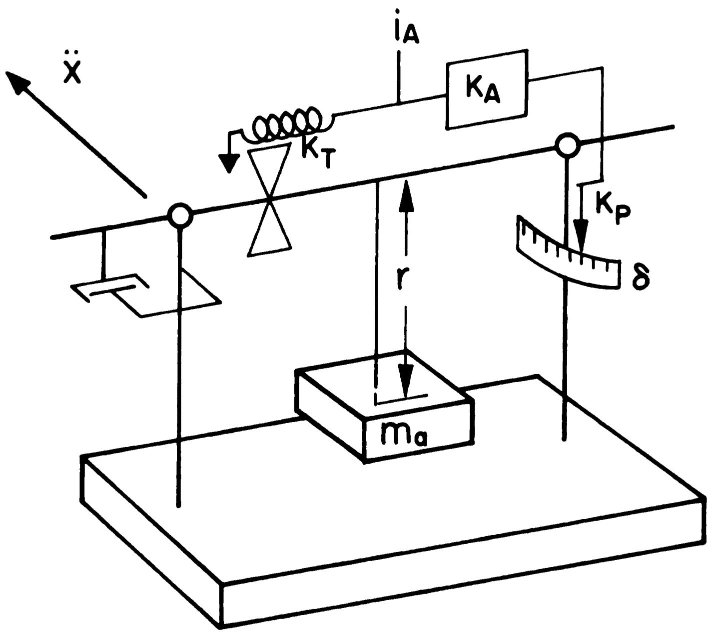

FIGURE 4. 7

PENDULOUS ACCELEROMETER

where

$$\ddot{x}_m = -\frac{K_T}{m_a r} i_A \tag{4.29}$$

An example of an integrating accelerometer is a "pendulous integrating gyro accelerometer" known as a PIGA. As shown in Figure 4. 8, the PIGA consists of a two-degree-of-freedom gyro with the acceleration sensitive axis along the gyro input axis. A small, known, unbalanced mass is located on the spin axis which, coupled with an acceleration, produces a torque about the gyro output axis. By Equation 4. 25 this torque products a rate around the gyro input axis where by integration

$$\int \dot{\alpha}\, dt \approx \int \ddot{X}\, dt$$

$$\alpha \approx \dot{X} \tag{4.30}$$

with no initial conditions. Thus, measurement of the angle, α, by

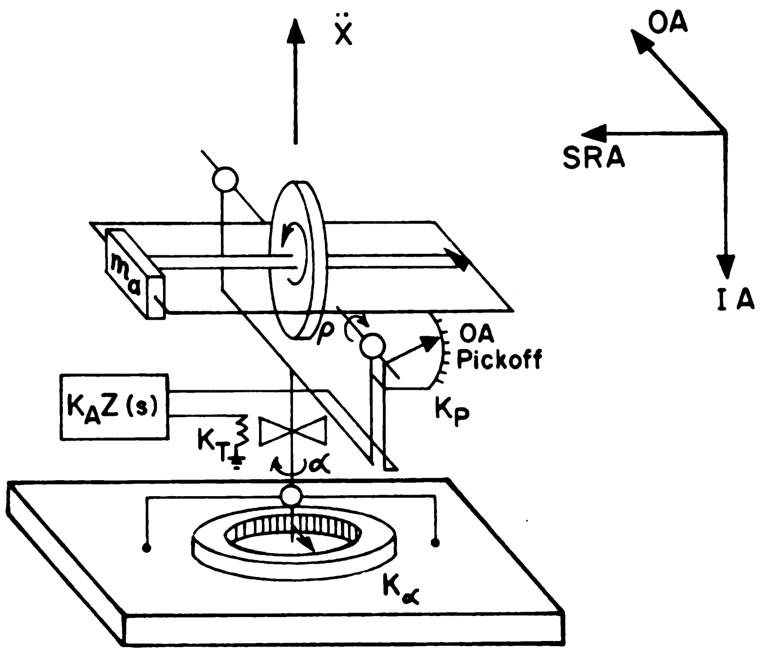

FIGURE 4. 8

PENDULOUS INTEGRATING GYRO ACCELEROMETER

a digital pickoff for example, yields an output which is proportional to velocity.

To eliminate input axis torques and to hold the sensitive axis along IA, it is necessary to "close the loop" by measuring the output axis angle and driving the input axis with a torquer. For stability, because of the high loop gain, it may be necessary to add a compensation network, Z(s).

The linearized state model of the PIGA, including the gyro dynamics from Equation 4. 24 and the compensation network is

$$\frac{d}{dt}\begin{bmatrix} \dot{\rho} \\ \rho \\ \dot{\alpha} \end{bmatrix} = \begin{bmatrix} -\dfrac{D\rho}{I_{fx}} & -\dfrac{K\rho}{I_{fx}} & -\dfrac{H_w}{I_{fx}} \\ 0 & 1 & 0 \\ \dfrac{H_w}{(I_{fy}+I_{gy})} & \dfrac{K_P K_A K_T Z(s)}{(I_{fy}+I_{gy})} & \dfrac{-D_\alpha}{(I_{fx}+I_{gy})} \end{bmatrix} \begin{bmatrix} \dot{\rho} \\ \rho \\ \dot{\alpha} \end{bmatrix} + \begin{bmatrix} -\dfrac{mr}{I_{fx}} \\ 0 \\ 0 \end{bmatrix} \ddot{x} \tag{4.31}$$

where

$$\dot{x}_m = K_\alpha \alpha \tag{4.32}$$

4.4 ENGINE SERVOS

In the design of the actuating systems for controlling the angular position of the engines, the first considerations are the determination of the maximum deflection angles, maximum velocities, and maximum accelerations that are necessary. These requirements are defined by the vehicle attitude control system requirements, in addition to engine thrust misalignments, vehicle side and longitudinal accelerations, frictions, and restraints due to such things as propellant lines leading to the engines.

In general, hydraulic actuators are used to position large booster engines (Figure 4.9). The servo loop that is used is a

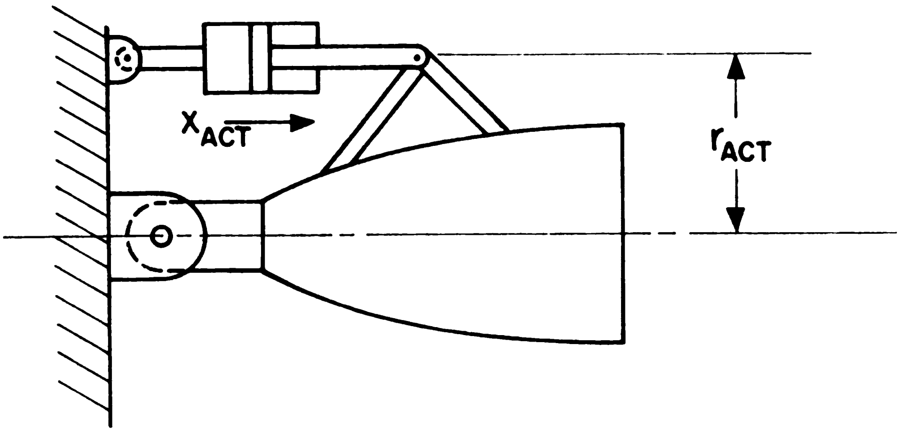

FIGURE 4.9

ENGINE SERVO

simple position servo with a position feedback as shown in Figure 4-10. The design of this type of servo system necessarily includes many non-linearities and is much beyond the scope of this thesis. A simplified state model of this servo would be of the form given by Equation 4.33.

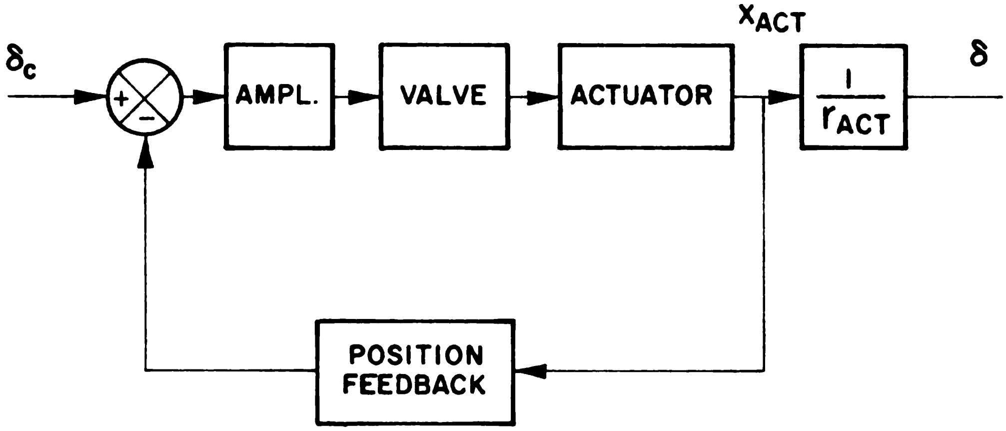

FIGURE 4.10

BLOCK DIAGRAM OF ENGINE SERVO

$$\frac{d}{dt}\begin{bmatrix}\dot{\delta}\\ \delta\end{bmatrix} = \begin{bmatrix}a_{11} & a_{12}\\ 1 & 0\end{bmatrix}\begin{bmatrix}\dot{\delta}\\ \delta\end{bmatrix} + \begin{bmatrix}b_{11}\\ 0\end{bmatrix}\delta_c \qquad (4.33)$$

where

$$a_{11} = -2\ \zeta\ \omega_n$$

$$a_{12} = -b_{11} = -\omega_n^{\,2}$$

For a comprehensive analysis of a booster hydraulic servo system refer to [1, pp. 14-40 to 14-49].

5. GUIDANCE AND CONTROL EQUATIONS

As described in Section 2 and shown in Figure 2.3, information provided by sensors and by the on-board computer is processed to determine the necessary commands to properly guide and control the vehicle. These commands are expressed in equation form as functions of the sensed and computed information.

5.1 CONTROL SYSTEM EQUATIONS

The control system, or more accurately the attitude control system, is a simple position servo type of system where position and rate information are fed back and summed with the command angle, and then used to drive the system. As shown in Figure 5.1

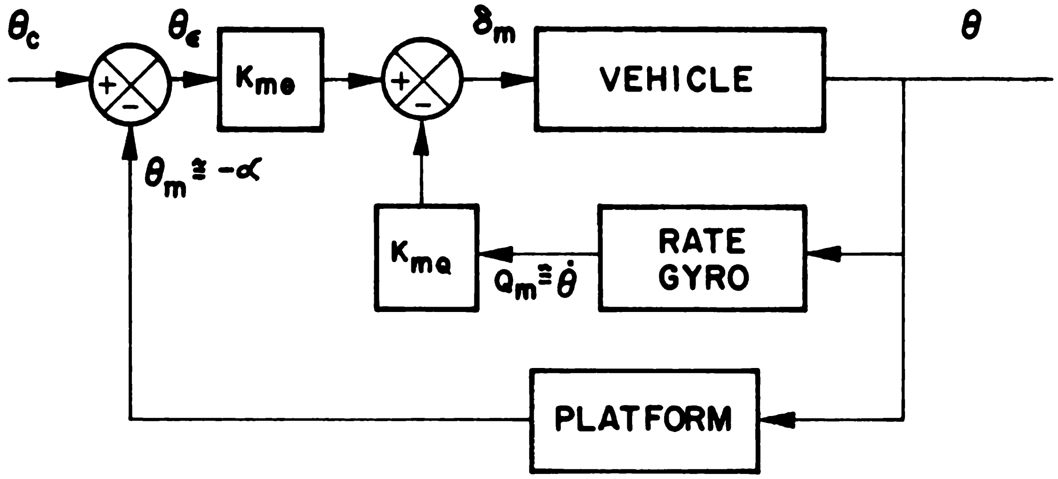

FIGURE 5.1

PITCH AXIS CONTROL SYSTEM

for the pitch axis of the control system

$$\delta_m = -K_{mQ} Q_m + K_{m\theta} (\theta_c - \theta_m) \tag{5.1}$$

where the gains K_{mQ} and $K_{m\theta}$ are used to provide the desired system stability and response. These gains change as a function of the vehicle parameters and, therefore, must be determined as a function of these parameters. A simplified approach which can be used in finding the necessary gains is given in Section 7. A block diagram similar to that of Figure 5.1 describes the control system for each axis, yielding a complete set of equations as

$$\begin{bmatrix} \delta_\ell \\ \delta_m \\ \delta_n \end{bmatrix} = \begin{bmatrix} -K_{\ell P} P_m + K_{\ell\phi} (\phi_c - \phi_m) \\ -K_{mQ} Q_m + K_{m\theta} (\theta_c - \theta_m) \\ -K_{nR} R_m + K_{n\Psi} (\Psi_c - \Psi_m) \end{bmatrix} \tag{5.2}$$

where by the proper choice of the platform gimbal order (refer to Figure 4.3), the gimbal angles for small roll and yaw motions of the vehicles yield

$$\begin{aligned} \phi_m &= -\gamma \cong \phi \\ \theta_m &= -\alpha \cong \theta \\ \Psi_m &= -\beta \cong \Psi \end{aligned} \tag{5.3}$$

5.2 GUIDANCE SYSTEM EQUATIONS

The objective of the guidance system is to provide commands to the control system so that the vehicle will reach the desired end conditions at the time of orbit injection. First, it is necessary to know where the vehicle is, and second, it is necessary to know what corrections to make to cause the vehicle to perform as desired.

In determining where the vehicle is, it is necessary to have a defined coordinate system in which measurements and computations can be made. The V-frame as defined in Section 3.1.3 is used as the computational and measurement frame. The platform accelerometers are, at the instant of liftoff, aligned with these axes, and during the flight are driven to remain aligned by torquers on the output axes of the platform gyros. The technique and equations used for this operation are given in Section 6.3.

Since the desired vehicle trajectory is in the T-frame (see Figure 2.4) and computations are made in the V-frame, it is necessary to relate these two coordinate systems. Referring to Figure 5.2, the location of the V-frame in the T-frame is defined by the angles σ and λ. An auxiliary coordinate frame, the d-frame, is attached to the plane which contains i_T and the point V where i_d is perpendicular to this plane, k_d is directed radially away from the center of the earth, and j_d completes the d-frame forming a right hand orthogonal coordinate system. The angular separation of the V-frame from the d-frame around their common z axis is defined by the angle ξ.

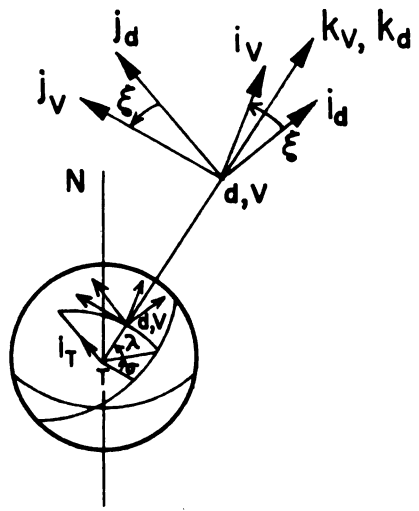

FIGURE 5. 2

RELATIONS BETWEEN THE T-, d-, AND V-FRAMES

From Figure 5. 2 the angular rate of the V-frame measured in V-frame coordinates as observed from inertial space is

$$\bar{\omega}_{IV} \quad = \quad \dot{\sigma}\, i_T \; - \; \dot{\lambda}\, i_d \; + \; \dot{\xi}\, k_V \tag{5.4}$$

Now, since

$$i_T \quad = \quad (\cos\lambda)\, j_d \; + \; (\sin\lambda)\, k_d \tag{5.5}$$

Equation 5.4 becomes

$$\overline{\omega}_{IV} = -\dot{\lambda} i_d + (\dot{\sigma}\cos\lambda)\, j_d + (\dot{\sigma}\sin\lambda)\, k_d + \dot{\xi}\, k_V \qquad (5.6)$$

The coordinate transformation from the V-frame to the d-frame is

$$\begin{bmatrix} i_d \\ j_d \\ k_d \end{bmatrix} = \begin{bmatrix} \cos\xi & -\sin\xi & 0 \\ \sin\xi & \cos\xi & 0 \\ 0 & 0 & 1 \end{bmatrix} \begin{bmatrix} i_V \\ j_V \\ k_V \end{bmatrix} \qquad (5.7)$$

Combining Equation 5.6 and 5.7 yields

$$\overline{\omega}_{IV} = \begin{bmatrix} \dot{\sigma}\cos\lambda\sin\xi - \dot{\lambda}\cos\xi \\ \dot{\sigma}\cos\lambda\cos\xi + \dot{\lambda}\sin\xi \\ \dot{\xi} + \dot{\sigma}\sin\lambda \end{bmatrix} \qquad (5.8)$$

By definition of the V-frame, the z component of angular velocity is zero (Equation A-40). Thus

$$\overline{\omega}_{IV} = \begin{bmatrix} \dot{\sigma}\cos\lambda\sin\xi - \dot{\lambda}\cos\xi \\ \dot{\sigma}\cos\lambda\cos\xi + \dot{\lambda}\sin\xi \\ 0 \end{bmatrix} \qquad (5.9)$$

with

$$\dot{\xi} = -\dot{\sigma}\sin\lambda \qquad (5.10)$$

As shown in Section 6.3 these equations can be solved for $\dot{\sigma}$, σ, $\dot{\lambda}$, and λ using the components of $\overline{\omega}_{IV}$ that are computed for torquing the platform.

Using parameters which can be obtained from Equations 5.9 and 5.10, the yaw guidance command is

$$\Psi_c = K_{n\dot{\lambda}} \dot{\lambda} + K_{n\lambda} \lambda \tag{5.11}$$

and the pitch guidance command is

$$\theta_c = \theta_o - K_{m\dot{Z}} \dot{Z}_T - K_{mZ} (Z - Z_N) \tag{5.12}$$

where Z_N is the desired nominal vertical distance and θ_o is a constant pitch angle used in computing the nominal trajectory. (A constant pitch angle is sometimes used with vehicles of this type.) The velocity which is normal to the desired flight path is

$$\dot{Z}_T = \dot{Z} \cos \gamma_N - \dot{X} \sin \gamma_N \tag{5.13}$$

where γ_N is the desired nominal flight path angle. The gains in Equations 5.11 and 5.12 must be selected to give the desired stability and response of the system. As shown in Section 7.3, these equations must be considered along with the control system equations to determine optimum system stability and response. The desired nominal flight path angle γ_N and the desired nominal vertical distance are programmed parameters where each is a function of σ. Precomputed functions based on a nominal flight are obtained from the on-board computer.

6. ON-BOARD COMPUTER

To guide the vehicle in the desired manner, it is necessary to have an on-board computer, preferably a digital computer, to perform computations as required by the guidance and control systems. The computer must generate platform torquing commands, engine cutoff and ignition signals, and attitude commands.

6.1 PLATFORM TORQUING COMMANDS

In the guidance scheme it was decided to drive the platform on which the accelerometers are mounted, so that the sensitive axes of the accelerometers are always aligned with the axes of the V-frame. Thus, it is necessary to solve the vehicle translational equations of motion using inputs from the accelerometers. The output axes of the gyros must then be torqued at rates, as determined from these equations, equal to the angular rates of the V-frame with respect to inertial space.

The set of accelerometers sense the negative of the acceleration due to the inertial reaction force and that due to gravitation

$$\bar{A} = -\left[\frac{\sum \bar{F}_I}{m} + \bar{G}\right] \tag{6.1}$$

which by Equation A-11 yields

$$\bar{A} = \frac{\sum \bar{F}_E}{m} \tag{6.2}$$

where

$$\bar{A} = \begin{bmatrix} A_X \\ A_Y \\ A_Z \end{bmatrix} = \frac{1}{m} \begin{bmatrix} F_X \\ F_Y \\ F_Z \end{bmatrix} \tag{6.3}$$

Upon rearrangement of Equations A-47 and substitution of Equations 6.3, the expressions that must be solved by the computer are

$$\frac{d}{dt} \begin{bmatrix} \dot{X} \\ \dot{Y} \\ \dot{Z} \end{bmatrix} = \begin{bmatrix} -\dot{X}\dot{Z}/Z \\ -\dot{Y}\dot{Z}/Z \\ (\dot{X}^2 + \dot{Y}^2)/Z \end{bmatrix} + \begin{bmatrix} A_X \\ A_Y \\ A_Z \end{bmatrix} + \begin{bmatrix} G_X \\ G_Y \\ G_Z \end{bmatrix} \tag{6.4}$$

The (A_X, A_Y, A_Z) inputs come from the accelerometers and the components of gravitation must be derived by the computer. The simplified gravitation equations (from Section 3.4) are

$$\begin{bmatrix} G_X \\ G_Y \\ G_Z \end{bmatrix} = \begin{bmatrix} 0 \\ 0 \\ -\mu / Z^2 \end{bmatrix} \tag{6.5}$$

The angular rate of the V-frame with respect to inertial space, and, therefore, the necessary rate of the stable platform (from Appendix A) is

$$\bar{\omega}_{IV} = \begin{bmatrix} \omega_X \\ \omega_Y \\ 0 \end{bmatrix} = \begin{bmatrix} -\dot{Y}/Z \\ \dot{X}/Z \\ 0 \end{bmatrix} \tag{6.6}$$

Arrangement of the gyros and accelerometers so as to have one gyro stabilize each of the axes of the V-frame and one accelerometer sense along each axis of the V-frame (see Figure 4.3), allows for direct computation and torquing of each gyro for rotation of the V-frame. A functional diagram of the platform gyros and accelerometers with the solution of Equations 6.4 is shown in Figure 6.1. The two loops that are obtained -- the one including the X_V axis accelerometer and gyro and the other including the Y_V axis accelerometer and gyro -- are known as "Schuler loops." The mechanical equivalent of a Schuler loop would be a pendulum with an arm length equal to Z where because of this length, the arm will always define the Z_V axis regardless of applied accelerations. (The gravitational component of acceleration acting on the pendulum is that which is acting on the vehicle.)

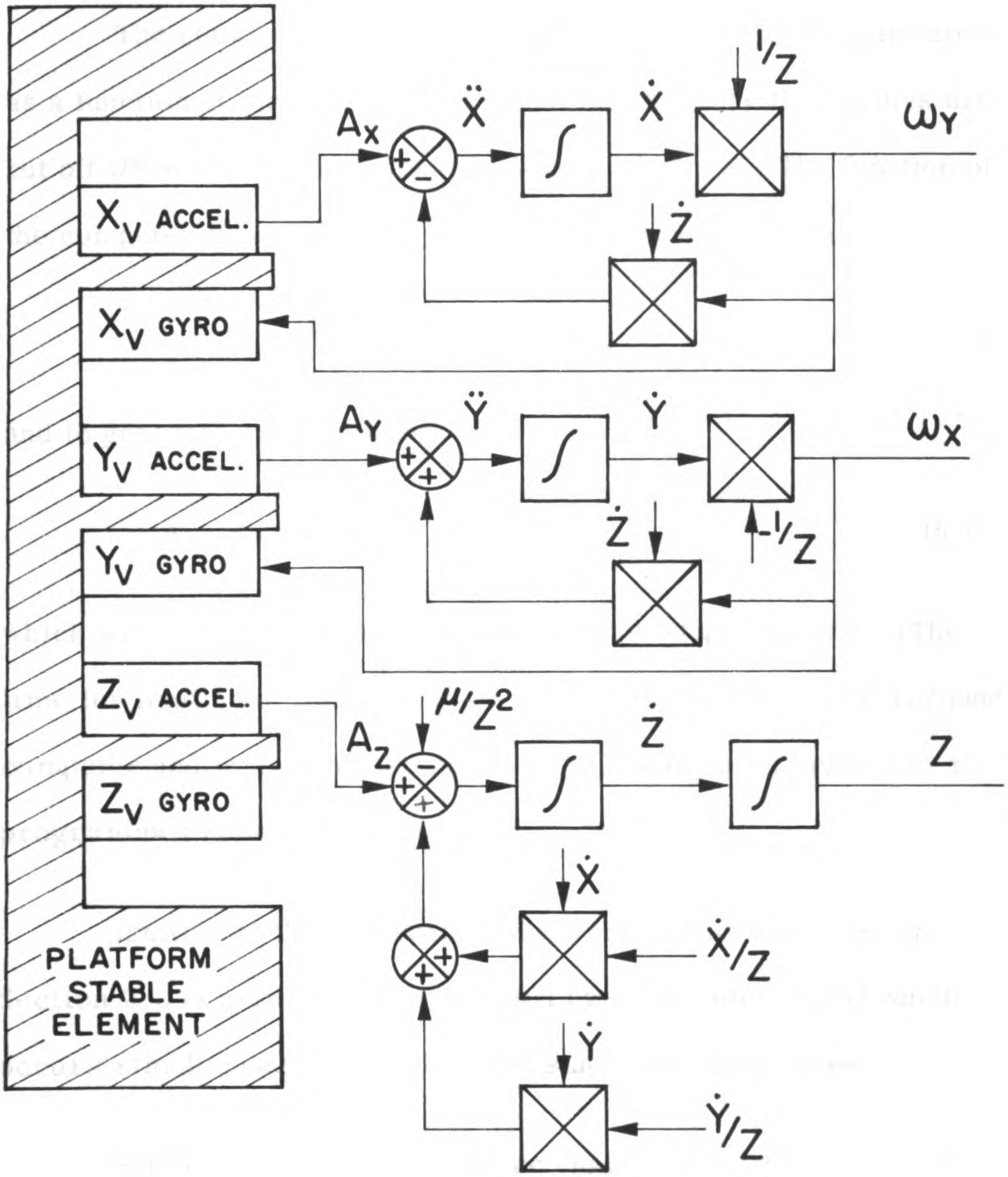

FIGURE 6.1

FUNCTIONAL DIAGRAM OF PLATFORM TORQUING SYSTEM

6.2 ENGINE CUTOFF AND IGNITION SIGNALS

The cutoff command for the first stage engines is generated as a function of the vehicle total acceleration where the engines are cut off when the total acceleration reaches 5.4 g's. The function of the computer then is to compute the total acceleration as

$$A_T = (A_X^2 + A_Z^2)^{1/2} \tag{6.7}$$

and to generate a signal when

$$A_T \geq 5.4 \text{ g's} \tag{6.8}$$

which will initiate shut down of the five first stage engines. (The time for ignition of the first stage engines is determined by a ground computer and is herein assumed to be at the instant required by the programmed nominal trajectory.)

Ignition of the five second stage engines as described in Section 2.2 is assumed to be initiated by a computer signal which occurs simultaneously with the first stage shut down signal.

Shut down of the second stage engines is commanded by the computer when the total velocity reaches the second stage cutoff velocity of the nominal vehicle. Thus, the computer must determine the velocity as

$$V_T = (\dot{X}^2 + \dot{Z}^2)^{1/2} \tag{6.9}$$

and generate a cutoff signal when

$$V_T \geq V_{NOM} \tag{6.10}$$

which will shut down the five second stage engines.

After coasting until the vehicle reaches an altitude as determined by the nominal trajectory

$$Z \geq Z_{NOM} \tag{6.11}$$

a signal is generated which commands ignition of the third stage engine. (It is assumed that the vehicle attitude is close to nominal.)

The third stage engine cutoff signal must be generated as a function of the total vehicle velocity. Since the vehicle, if properly controlled, will have velocity along the X_V axis only, it is necessary only to monitor the velocity along this axis. The cutoff signal of the third stage (ignoring shut down time) must then be generated when

$$\dot{X} \geq V_{ORB} \tag{6.12}$$

where from Equation 2.3 at the equator

$$V_{ORB} = 24,875.9 \text{ fps} \tag{2.3}$$

6.3 ATTITUDE COMMANDS

According to the launch sequence given in Section 2.2, the vehicle must be rolled to zero roll angle during the first 20 seconds of flight. Thus, for purposes of limiting the motions of the engines and for minimum structural loading, the computer must provide a programmed roll rate of 1 deg/sec until zero roll angle is reached. (A maximum initial ϕ of 20 degrees is assumed.) Then, the command is removed and from there on, for the remainder of the flight, the roll axis becomes a nulling loop.

After 20 seconds, the launch sequence calls for a kick angle of 6 degrees. To do this, the computer must provide a pitch command, beginning at 20 seconds after liftoff, increasing up to 6 degrees at a rate of 1 deg/sec. When

$$90 - \theta_m = 6 \text{ degrees} \tag{6.13}$$

the pitch command must be switched over to the gravity turn command which, as described in Section 2.2, causes the angle of attack to be zero. The pitch command which must be given by the computer is

$$\theta_c = \tan^{-1}\left(\frac{A_z}{A_x}\right) \tag{6.14}$$

This command is used until the end of the first stage burning period.

For the remainder of the flight, the pitch and yaw commands are determined by Equations 5.11 and 5.12. The values for γ_N and Z_N are stored in the computer where each is a function of the distance σ. The values for these parameters must be obtained from a previously simulated flight of the nominal vehicle.

The remaining parameters in Equations 5.11 and 5.12 are obtained by solution with the on-board computer of Equations 5.9 and 5.10. The angular rate of the V-frame as given by Equation 6.6 can be used to solve for the trajectory plane angles as given by Equations 5.9 and 5.10. A functional diagram illustrating the computer solution of these equations is given in Figure 6.2.

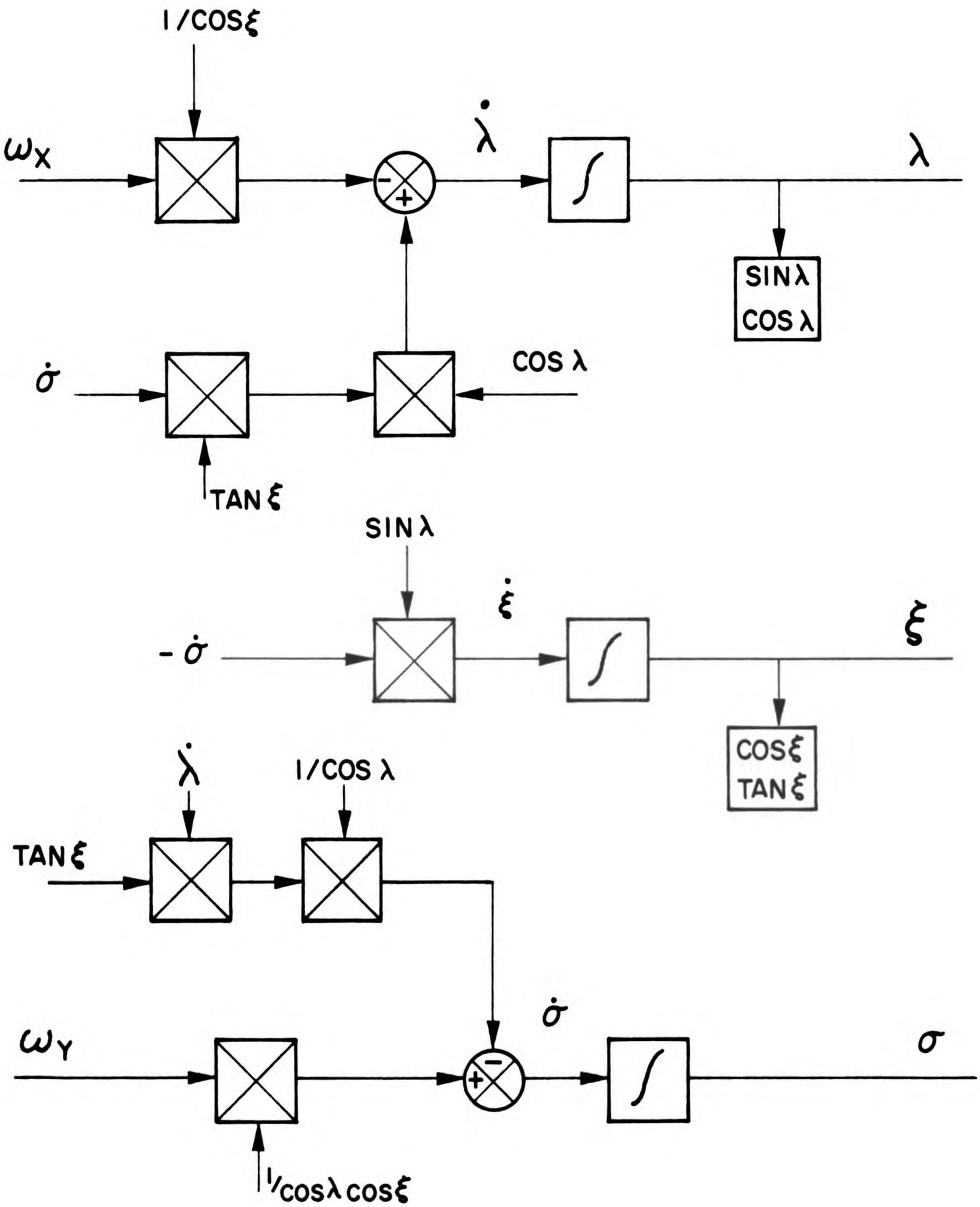

FIGURE 6. 2

FUNCTIONAL DIAGRAM OF SOLUTION OF NAVIGATION EQUATIONS

7. SYSTEM OPTIMIZATION

In the optimization of vehicle guidance and control systems it is generally desired to first obtain a stable system and second to have a system which controls the attitude and trajectory of the vehicle in an optimum manner. For most systems it is desired to have the system respond to a command as rapidly as possible but not so fast as to excite such things as sloshing, bending, or compliance modes; to structurally damage the vehicle; or to use excessive amounts of fuel.

7.1 FLIGHT CONDITIONS

For preliminary design studies, the system can be investigated using linear analysis techniques by linearizing the control system components, by defining vehicle "flight conditions", and by assuming small perturbations of the vehicle parameters. The parameters that are time dependent and do not appreciably influence the dynamic response are assumed to be constants where sets of these parameters over the possible flight regime define the vehicle flight conditions. In doing so, sets of constant values for the vehicle mass, inertias, c. g. and c. p. distances, altitude, and speed are defined. (The assumption that speed is constant eliminates a long period oscillation known in aircraft terminology as a "phugoid oscillation." Since the period is usually on the order of 30 to 130 seconds it is assumed to have a small effect on stability and response and is ignored.)

7.2 SIMPLIFIED SYSTEM EQUATIONS

The translational dynamics of the vehicle can be expressed by

$$\left[\frac{d\,\overline{V}_T}{dt}\right]_I = \left[\frac{d\,\overline{V}_T}{dt}\right]_B + \overline{\omega}_{IB} \times \overline{V}_T \tag{7.1}$$

where

$$\overline{\omega}_{IB} = \begin{bmatrix} P \\ Q \\ R \end{bmatrix} \tag{7.2}$$

and by ignoring earth rate and winds

$$\overline{V}_T = \begin{bmatrix} U \\ V \\ W \end{bmatrix} \tag{7.3}$$

Also, similar to Equation A-15 considering only the gravitation of the earth

$$\left[\frac{d\,\overline{V}_T}{dt}\right]_I = \frac{\overline{F}_{EX}}{m} + \overline{G}_E \tag{7.4}$$

where in B-frame coordinates

$$\frac{\overline{F}_{EX}}{m} = \frac{1}{m}\begin{bmatrix} F_x \\ F_y \\ F_z \end{bmatrix}$$

$$\overline{G}_E = \begin{bmatrix} G_x \\ G_y \\ G_z \end{bmatrix} \tag{7.5}$$

Combining Equations 7.1 and 7.4 and expanding with Equations 7.2, 7.3 and 7.5, the vehicle translational equations in body axes become

$$\frac{d}{dt}\begin{bmatrix} U \\ V \\ W \end{bmatrix} \cong \begin{bmatrix} VR - WQ \\ WP - UR \\ UQ - VP \end{bmatrix} + \frac{1}{m}\begin{bmatrix} F_x \\ F_y \\ F_z \end{bmatrix} + \begin{bmatrix} G_x \\ G_y \\ G_z \end{bmatrix} \tag{7.6}$$

The components of $\overline{V}_a$ can be expressed in terms of initial values and small perturbations around these initial value as

$$\begin{aligned} U &= U_o + u \\ V &= V_o + v \\ W &= W_o + w \end{aligned} \tag{7.7}$$

Similarly, assuming $\phi \cong 0$, the angular rates can be expressed as

$$\begin{aligned} P &\cong \dot{\phi} \\ P &\cong \dot{\phi}_o + \dot{\phi}' \\ Q &\cong \dot{\theta} \\ Q &\cong \dot{\theta}_o + \dot{\theta}' \\ R &\cong \dot{\Psi} \\ R &\cong \dot{\Psi}_o + \dot{\Psi}' \end{aligned} \tag{7.8}$$

With

$$\begin{aligned} \dot{U} &= V_o = W_o = \dot{\phi}_o = \dot{\theta}_o = \dot{\Psi}_o = 0 \\ U &\cong U_o \cong V_{o_o} \end{aligned} \tag{7.9}$$

upon substitution of Equations 7.7 and 7.8 and by elimination of products of small numbers, the expressions for the translational and rotational dynamics (Equations 7.6 and B-31) reduce to

$$\frac{d}{dt}\begin{bmatrix} v \\ w \\ \dot{\phi}' \\ \dot{\theta}' \\ \dot{\Psi}' \end{bmatrix} = \begin{bmatrix} -V_{a_0}\ \dot{\Psi}' \\ V_{a_0}\ \dot{\theta}' \\ 0 \\ 0 \\ 0 \end{bmatrix} + \begin{bmatrix} F_y/m \\ F_z/m \\ M_x/I_{xx} \\ M_y/I_{yy} \\ M_z/I_{zz} \end{bmatrix} + \begin{bmatrix} G_y \\ G_z \\ 0 \\ 0 \\ 0 \end{bmatrix} \tag{7.10}$$

The forces and moments consist of aerodynamic and control forces which upon consideration of Equations 7.7, 7.8, and 7.9 with Equations 3.28, 3.44 and, 3.46 become for the first stage

$$\begin{bmatrix} \frac{F_y}{m} \\ \frac{F_z}{m} \\ \frac{M_x}{I_{xx}} \\ \frac{M_y}{I_{yy}} \\ \frac{M_z}{I_{zz}} \end{bmatrix} = \begin{bmatrix} \frac{\phi_2 q_0 A}{m} & & 0 & 0 & 0 \\ 0 & \frac{\phi_3 q_0 A}{m} & 0 & 0 & 0 \\ 0 & 0 & \frac{\phi_4 q_0 Ad}{I_{xx}} & 0 & 0 \\ 0 & \frac{\phi_5 q_0 Ad}{I_{yy}} & 0 & \frac{\phi_6 q_0 Ad}{I_{yy}} & 0 \\ \frac{\phi_7 q_0 Ad}{I_{zz}} & 0 & 0 & 0 & \frac{\phi_8 q_0 Ad}{I_{zz}} \end{bmatrix} \begin{bmatrix} v \\ w \\ \dot{\phi}' \\ \dot{\theta}' \\ \dot{\Psi}' \end{bmatrix} + T_1 \begin{bmatrix} (\delta_{11} + \delta_{13})/m \\ -(\delta_{12} + \delta_{14})/m \\ (\delta_{14} - \delta_{12})\, r_{e1}/I_{xx} \\ -(\delta_{12} + \delta_{14})(\ell_{e1} - \ell_g)/I_{yy} \\ -(\delta_{11} + \delta_{13})(\ell_{e1} - \ell_g)/I_{zz} \end{bmatrix} \tag{7.11}$$

With

$$\begin{aligned} \phi &= \phi' \\ \theta &= \theta_0 + \theta' \\ \Psi &= \Psi' \end{aligned} \tag{7.12}$$

the components of gravitation (G_y , G_z), by coordinate transformation using Equation 3.9 with small angle assumptions and considering only G_z (and dropping the constant term in the G_z expression), become

$$\begin{bmatrix} G_y \\ \\ G_z \end{bmatrix} = \begin{bmatrix} \phi' \cos\theta_0 + \Psi' \sin\theta_0 \\ \\ \theta' \sin\theta_0 \end{bmatrix} G_{Z_0} \qquad (7.13)$$

where

$$G_{Z_0} = -\mu/Z_0^2 \qquad (7.14)$$

7.3 CONTROL SYSTEM

The control system operates on the rate gyro and the platform outputs where, from Equations 5.2, the control system commands are

$$\begin{bmatrix} \delta_\ell \\ \delta_m \\ \delta_n \end{bmatrix} = \begin{bmatrix} -K_{\ell P} \, P_m + K_{\ell\phi} \, \phi_\epsilon \\ -K_{mQ} \, Q_m + K_{m\theta} \, \theta_\epsilon \\ -K_{nR} \, R_m + K_{n\Psi} \, \Psi_\epsilon \end{bmatrix} \qquad (7.15)$$

with error angles, assuming small motions and that $\phi_0 = \Psi_0 = 0$, of

$$\begin{bmatrix} \phi_\epsilon \\ \theta_\epsilon \\ \Psi_\epsilon \end{bmatrix} = \begin{bmatrix} \phi_c - \phi' \\ \theta_c - (\theta_0 + \theta') \\ \Psi_c - \Psi' \end{bmatrix} \qquad (7.16)$$

Assuming the response time of the rate gyros to be insignificant

$$P_m = P = \dot{\phi}' \qquad Q_m = Q = \dot{\theta}' \qquad R_m = R = \dot{\Psi}' \tag{7.17}$$

To simplify the equations, it is also assumed that the response time of the servos is insignificant and perfect, and that

$$\begin{bmatrix} \delta_\ell \\ \delta_m \\ \delta_n \end{bmatrix} = \begin{bmatrix} (\delta_{14} - \delta_{12}) \\ -(\delta_{12} + \delta_{14}) \\ -(\delta_{11} + \delta_{13}) \end{bmatrix} \tag{7.18}$$

Substitution of Equation 7.16, 7.17, and 7.18 into 7.15 yields

$$\begin{bmatrix} (\delta_{14} - \delta_{12}) \\ -(\delta_{12} + \delta_{14}) \\ -(\delta_{11} + \delta_{13}) \end{bmatrix} = \begin{bmatrix} -K_{\ell P}\,\dot{\phi}' - K_{\ell\phi}\,\phi' \\ -K_{mQ}\,\dot{\theta}' - K_{m\theta}\,\theta' \\ -K_{nR}\,\dot{\Psi}' - K_{n\Psi}\,\Psi' \end{bmatrix} + \begin{bmatrix} K_{\ell\phi}\ \phi_c \\ K_{m\theta}\ (\theta_c - \theta_o) \\ K_{n\Psi}\ \Psi_c \end{bmatrix} \tag{7.19}$$

Combining Equations 7.10, 7.11, 7.13, 7.14, 7.17, and 7.19 and observing that these equations can be split into three sets, the simplified state models for the vehicle and control system become:

for the yaw axis,

$$\frac{d}{dt}\begin{bmatrix} v \\ \dot{\Psi}' \\ \Psi' \end{bmatrix} = \begin{bmatrix} a_{11} & a_{12} & a_{13} \\ a_{21} & a_{22} & a_{23} \\ 0 & a_{32} & 0 \end{bmatrix}\begin{bmatrix} v \\ \dot{\Psi}' \\ \Psi' \end{bmatrix} + \begin{bmatrix} a_{18} \\ 0 \\ 0 \end{bmatrix}\phi' + \begin{bmatrix} b_{13} \\ b_{23} \\ 0 \end{bmatrix}\Psi_c \tag{7.20}$$

for the pitch axis,

$$\frac{d}{dt}\begin{bmatrix} w \\ \dot{\theta}' \\ \theta' \end{bmatrix} = \begin{bmatrix} a_{44} & a_{45} & a_{46} \\ a_{54} & a_{55} & a_{56} \\ 0 & a_{65} & 0 \end{bmatrix}\begin{bmatrix} w \\ \dot{\theta}' \\ \theta' \end{bmatrix} + \begin{bmatrix} b_{46} \\ b_{56} \\ 0 \end{bmatrix}(\theta_c - \theta_o) \tag{7.21}$$

and for the roll axis,

$$\frac{d}{dt}\begin{bmatrix} \dot{\phi}' \\ \phi' \end{bmatrix} = \begin{bmatrix} a_{77} & a_{78} \\ a_{87} & 0 \end{bmatrix}\begin{bmatrix} \dot{\phi}' \\ \phi' \end{bmatrix} + \begin{bmatrix} b_{78} \\ 0 \end{bmatrix}\phi_c \tag{7.22}$$

where

$$a_{11} = \phi_2 \frac{q_o A}{m} \tag{7.23}$$

$$a_{12} = T_1 \frac{K_{nR}}{m} - V_{a_0} \tag{7.24}$$

$$a_{13} = T_1 \frac{K_{n\Psi}}{m} - \frac{\mu}{Z_0^{\,2}} \sin \theta_0 \tag{7.25}$$

$$a_{18} = -\frac{\mu}{Z_0^{\,2}} \cos \theta_0 \tag{7.26}$$

$$a_{21} = \phi_7 \frac{q_0 Ad}{I_{zz}} \tag{7.27}$$

$$a_{22} = \phi_8 \frac{q_0 Ad}{I_{zz}} - T_1 \frac{(\ell_{e1} - \ell_g)}{I_{zz}} K_{nR} \tag{7.28}$$

$$a_{23} = - T_1 \frac{(\ell_{e1} - \ell_g)}{I_{zz}} K_{n\Psi} \tag{7.29}$$

$$a_{32} = 1 \tag{7.30}$$

$$a_{44} = \phi_3 \frac{q_0 A}{m} \tag{7.31}$$

$$a_{45} = V_{a_0} - T_1 \frac{K_{mQ}}{m} \tag{7.32}$$

$$a_{46} = -\frac{\mu}{Z_o^{\,2}} \sin \theta_o - T_1 \frac{K_{m\theta}}{m} \tag{7.33}$$

$$a_{54} = \phi_5 \frac{q_o Ad}{I_{yy}} \tag{7.34}$$

$$a_{55} = -T_1 \frac{(\ell_{el} - \ell_g)}{I_{yy}} K_{mQ} \tag{7.35}$$

$$a_{56} = -T_1 \frac{(\ell_{el} - \ell_g)}{I_{yy}} K_{m\theta} \tag{7.36}$$

$$a_{65} = 1 \tag{7.37}$$

$$a_{77} = \phi_4 \frac{q_o Ad}{I_{xx}} - T_1 \left(\frac{r_{el} \quad K_{\ell P}}{I_{xx}} \right) \tag{7.38}$$

$$a_{78} = -T_1 \frac{r_{el} \quad K_{\ell\phi}}{I_{xx}} \tag{7.39}$$

$$a_{87} = 1 \tag{7.40}$$

$$b_{13} = -T_1 \frac{K_{n\Psi}}{m} \tag{7.41}$$

$$b_{23} = T_1 \frac{(\ell_{el} - \ell_g)}{I_{zz}} K_{n\Psi} \tag{7.42}$$

$$b_{46} = T_1 \frac{K_{m\theta}}{m} \tag{7.43}$$

$$b_{56} = T_1 \frac{(\ell_{e1} - \ell_g)}{I_{yy}} K_{m\theta} \tag{7.44}$$

$$b_{78} = T_1 \frac{r_{e1} \ K_{\ell\phi}}{I_{xx}} \tag{7.45}$$

All of the terms in the coefficient matrices are constants under specified flight conditions with data given by Equations 3.21, 3.43, 3.56 and Appendix C. Computation of the control system gain constants, $K_{\ell P}$, $K_{\ell\phi}$, K_{mQ}, etc., necessary for given flight conditions can be accomplished by finding the characteristic equations for each of the three vehicle axes (Equations 7.20, 7.21 and 7.22) and adjusting the gains to give the desired system stability and response characteristics.

7.4 SAMPLE PROBLEM

As a sample problem, consider the roll axis equations. The characteristic equation is

$$\lambda^2 + \left(T_1 \frac{r_{e1} \ K_{\ell P}}{I_{xx}} - \phi_4 \frac{q_0 \ Ad}{I_{xx}}\right)\lambda + T_1 \frac{r_{e1} \ K_{\ell\phi}}{I_{xx}} = 0 \tag{7.46}$$

From [6, p. 88] because of sloshing and bending modes, etc., it is desirable to have a natural frequency of

$$\omega_n = 0.6\,\pi \text{ rad/sec} \tag{7.47}$$

Thus, from Equation 7.46 the position feedback gain must be

$$K_{\ell\phi} = \frac{I_{xx}\,(0.6\pi)^2}{T_1\ r_{e1}} \tag{7.48}$$

and, for say $\zeta = 1.0$, the rate feedback gain must be

$$K_{\ell P} = \frac{I_{xx}\,(1.2\pi)}{T_1\ r_{e1}} + \frac{\phi_4\, q_0\, Ad}{T_1\ r_{e1}} \tag{7.49}$$

At launch with $q_0 = 0$, using a value for I_{xx} from Figure C-4 of

$$I_{xx} = 2.55 \times 10^7 \text{ slug-ft}^2 \tag{7.50}$$

a thrust from Equation 3.56 of

$$T_1 = 1.5 \times 10^6 \text{ lbs} \tag{7.51}$$

and

$$r_{e1} = 15 \text{ feet} \tag{7.52}$$

the necessary position gain constant becomes

$$K_{\ell\phi} = 4.03 \text{ rad/rad} \tag{7.53}$$

and the rate gain constant becomes

$$K_{\ell_P} = 4.27 \text{ rad/rad/sec} \qquad (7.54)$$

Simiarly, the remaining first stage roll axis gains can be computed as a function of burning time, speed, and altitude using Equations 3.21, 3.43, 3.56, C-16 and Figure C-4.

The second and third stage control systems are identical to the first stage control system, except that the third stage roll control has an on-off bang-bang system, and therefore solutions for each can be obtained using Equations 7.20 through 7.45 with the appropriate parameters for each stage.

For a complete mechanization of the control system gains in the airborne system, it would be necessary to make each a function of elapsed burning time, speed, and altitude. However, since the vehicle would very likely follow close to the nominal trajectory, the gains could probably be made a function of flight time only. Studies considering all possible parameter variations would have to be made to determine the practicality of this approach.

7.5 GUIDANCE SYSTEM

Preliminary guidance system investigations can be made simultaneously with the control system by including the guidance commands as given by Equations 6.14, 5.11, 5.12 and 5.13 and the ramp commands as required for the roll-out and kick angle. From Figure 7.1, with small angle assumptions,

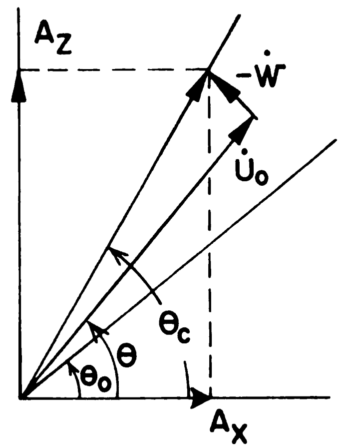

FIGURE 7.1

ACCELERATIONS IN A GRAVITY TURN

$$\theta_c - \theta_0 \cong (\theta - \theta_0) - \frac{\dot{w}}{\dot{U}_0} \tag{7.55}$$

which upon substitution of Equation 7.12 is

$$(\theta_c - \theta_0) \cong \theta' - \frac{\dot{w}}{\dot{U}_0} \tag{7.56}$$

Upon combining Equations 7.56 and 7.21, where $\dot{U}_0$ is the initial acceleration (assumed to be constant for each flight condition), the expressions for pitch axis guidance and control can be found and used to study the stability and response during the gravity turn. Roll and yaw are simply nulling loops during the atmospheric phase and thus no guidance loops are involved.

The guidance system for the remaining phase of flight (the vacuum phase) can be investigated using the guidance equations as given by Equations 5.11, 5.12, and 5.13. By coordinate transformation using small perturbations as given by Equations 7.7 and 7.12 with

$$\gamma_N = \theta_o \tag{7.57}$$

and

$$\dot{Z}_N = U_o \sin\theta_N \tag{7.58}$$

the yaw guidance command is

$$\psi_c = -K_{n\lambda}(U_o \psi' + v) - K_{n\lambda}\int (U_o \psi' + v)\, dt \tag{7.59}$$

and the pitch guidance command is

$$(\theta_c - \theta_o) = K_{m\dot{z}}(U_o \theta' - w) + K_{mZ} \cos\theta_o \int (U_o \theta' - w)\, dt \tag{7.60}$$

Combining Equations 7.59 and 7.60 with Equations 7.20 and 7.21, respectively, solutions for the pitch and yaw guidance systems together with the control systems can be obtained.

8. SIMULATION

Simulation of the complete system can be accomplished using analog and digital computers along with the actual hardware for some of the components as shown in Figure 8.1. If hardware is used, the simulated part of the system must operate in real time so that the dynamic properties of the hardware are properly included. All of the equations necessary for simulation are listed in this section so that solutions using equations only can be made, but allowing for substitution of hardware as desired. These equations are grouped as indicated by the block diagram of Figure 8.2.

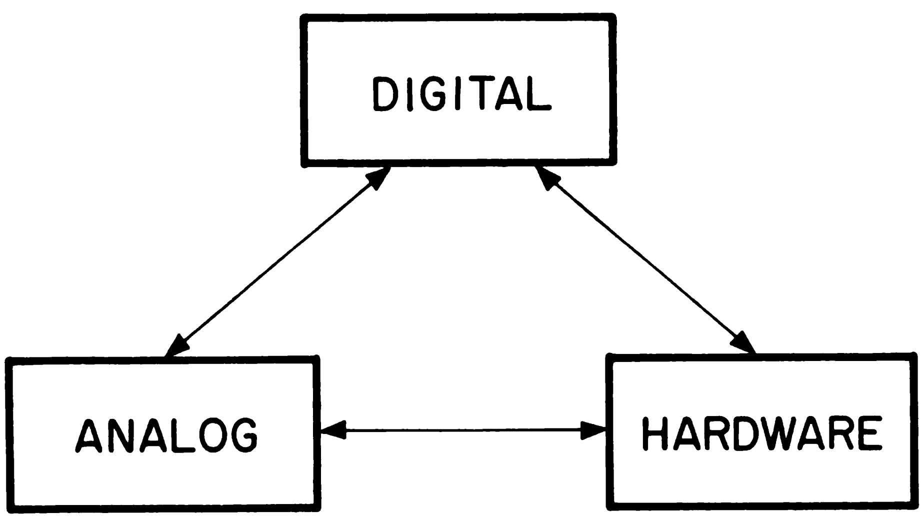

FIGURE 8.1

BASIC SYSTEM DIAGRAM

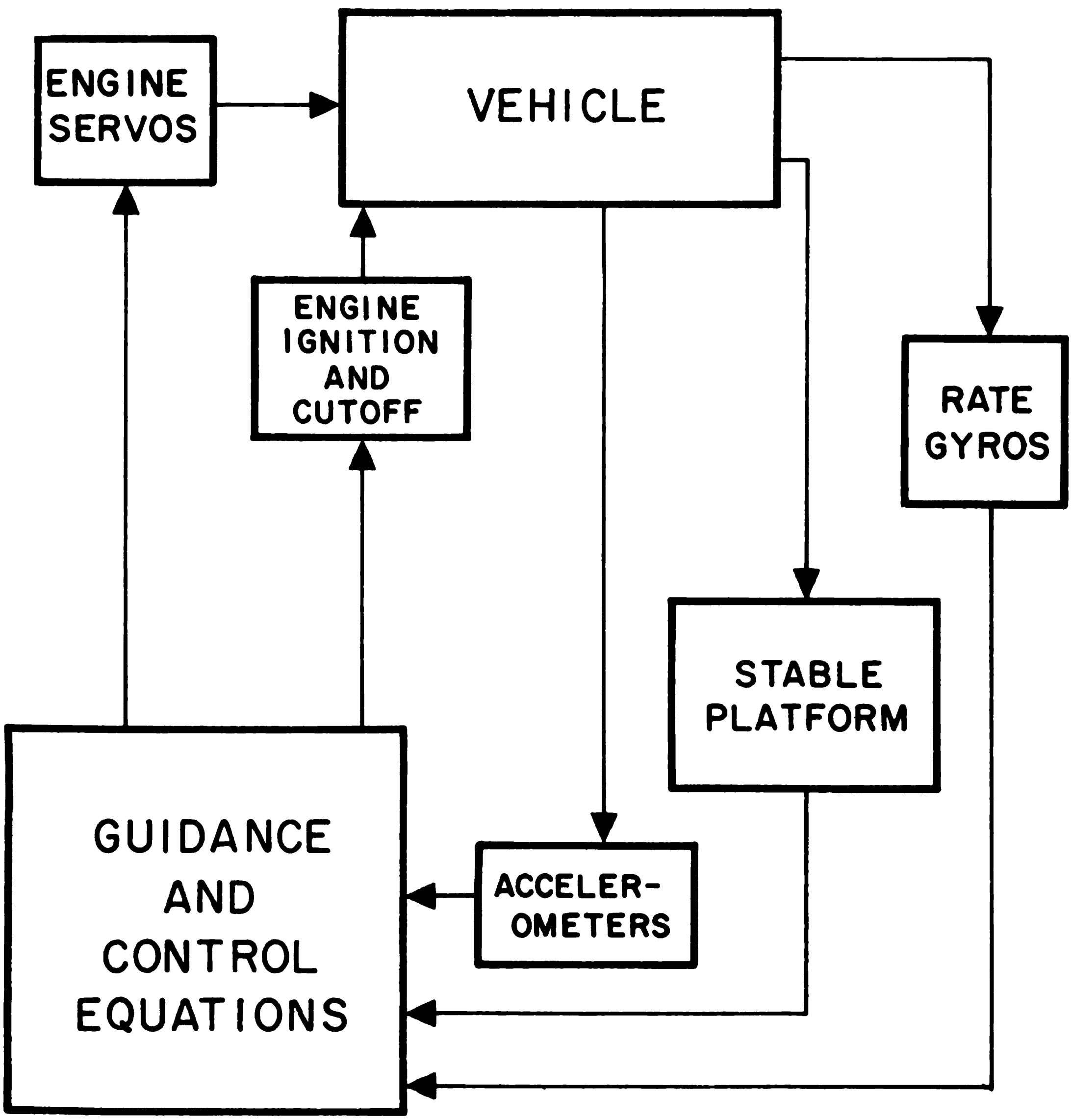

FIGURE 8.2

SIMULATION BLOCK DIAGRAM

8.1 VEHICLE

All of the equations necessary for simulation of the vehicle are listed; numerical data for the aerodynamic coefficients, and the inertias are given in Appendix C. First, the vehicle translational dynamics are given where the aerodynamic force coefficients are

$$\begin{bmatrix} C_x \\ C_y \\ C_z \end{bmatrix} = \begin{bmatrix} -(C_{D_o} + 2C_{Dt_o}) \\ -(C_{D_o} + C_{Dt_o} + C_{L\eta} + C_{Lt\alpha})\beta \\ -(C_{D_o} + C_{Dt_o} + C_{L\eta} + C_{Lt\alpha})\alpha \end{bmatrix} \qquad (3.42)$$

and the incidence angles are

$$\begin{aligned} \alpha &= W/V_a \\ \beta &= V/V_a \end{aligned} \qquad (3.28)$$

The body axis forces are

$$\begin{bmatrix} F_x \\ F_y \\ F_z \end{bmatrix} = qA \begin{bmatrix} C_x \\ C_y \\ C_z \end{bmatrix} + \begin{bmatrix} F_{xe} \\ F_{ye} \\ F_{ze} \end{bmatrix}_{1,2,3}$$

where the reference area is

$$A = 855 \text{ ft}^2 \qquad (C\text{-}17)$$

The engine forces are

$$\begin{bmatrix} F_{xe1} \\ F_{ye1} \\ F_{ze1} \end{bmatrix} = T_1 \begin{bmatrix} 5 \\ (\delta_{11} + \delta_{13}) \\ -(\delta_{12} + \delta_{14}) \end{bmatrix} \tag{3.46}$$

$$\begin{bmatrix} F_{xe2} \\ F_{ye2} \\ F_{ze2} \end{bmatrix} = T_2 \begin{bmatrix} 5 \\ (\delta_{21} + \delta_{23}) \\ -(\delta_{22} + \delta_{24}) \end{bmatrix} \tag{3.47}$$

$$\begin{bmatrix} F_{xe3} \\ F_{ye3} \\ F_{ze3} \end{bmatrix} = T_3 \begin{bmatrix} 1 \\ \delta_{31} \\ \delta_{32} \end{bmatrix} \tag{3.49}$$

The engine thrusts are

$$\begin{bmatrix} T_1 \\ T_2 \\ T_3 \end{bmatrix} = \begin{bmatrix} 1.74 \text{x } 10^6 - 80.8 \text{ x } 10^6 \rho \\ 260,000 \\ 260,000 \end{bmatrix} \tag{3.56}$$

The forces in V-frame coordinates are

$$\begin{bmatrix} F_X \\ F_Y \\ F_Z \end{bmatrix} = \begin{bmatrix} \ell_1 & m_1 & n_1 \\ \ell_2 & m_2 & n_2 \\ \ell_3 & m_3 & n_3 \end{bmatrix} \begin{bmatrix} F_x \\ F_y \\ F_z \end{bmatrix} \tag{3.64}$$

where the direction cosines are

$$\begin{bmatrix} \ell_1 \\ \ell_2 \\ \ell_3 \\ m_1 \\ m_2 \\ m_3 \\ n_1 \\ n_2 \\ n_3 \end{bmatrix} = \begin{bmatrix} \cos\psi \cos\theta \\ -\sin\psi \\ \cos\psi \sin\theta \\ \sin\phi \sin\theta - \cos\phi \sin\psi \cos\theta \\ -\cos\phi \cos\psi \\ -\sin\phi \cos\theta - \cos\phi \sin\psi \sin\theta \\ \cos\phi \sin\theta + \sin\phi \sin\psi \cos\theta \\ \sin\phi \cos\psi \\ -\cos\phi \cos\theta + \sin\phi \sin\psi \sin\theta \end{bmatrix} \tag{3.9}$$

The vehicle mass is

$$m = m_{1_0} + m_{2_0} + m_{3_0} - \dot{m}_1 t_{b1} - \dot{m}_2 t_{b2} - \dot{m}_3 t_{b3} \tag{3.61}$$

where

$$m_{1_0} = 153,600 \text{ slugs}$$

$$m_{2_0} = 27,200 \text{ slugs}$$

$$m_{3_0} = 14,280 \text{ slugs} \quad (3.62)$$

$$\dot{m}_1 = 900 \text{ slugs/sec} \quad (3.63)$$

$$\dot{m}_2 = 90 \text{ slugs/sec}$$

$$\dot{m}_3 = 18 \text{ slugs/sec}$$

The V-frame translational equations are

$$\frac{d}{dt}\begin{bmatrix} \dot{X} \\ \dot{Y} \\ \dot{Z} \end{bmatrix} = \begin{bmatrix} -\dot{X}\,\dot{Z}/Z \\ -\dot{Y}\,\dot{Z}/Z \\ (\dot{X}^2 + \dot{Y}^2)/Z - \mu/Z^2 \end{bmatrix} + \begin{bmatrix} F_X/m \\ F_Y/m \\ F_Z/m \end{bmatrix} \quad (3.65)$$

where

$$\mu = 1.4077 \times 10^{16} \text{ ft}^3/\text{sec}^2 \quad (3.58)$$

The V-frame angular rates are

$$\bar{\omega}_{IV} = \begin{bmatrix} \omega_X \\ \omega_Y \\ 0 \end{bmatrix} = \begin{bmatrix} -\dot{Y}/Z \\ \dot{X}/Z \\ 0 \end{bmatrix} \quad (6.6)$$

where

$$(\bar{\omega}_{IV})_o = \omega_{IE} \begin{bmatrix} \cos \Phi_o \cos \Psi_o \\ \cos \Phi_o \sin \Psi_o \\ 0 \end{bmatrix}$$

and

$$\begin{aligned} X_o &= Y_o = 0 \\ Z_o &= 20,925,732 \text{ ft (at equator)} \end{aligned} \qquad (3.58)$$

and

$$\omega_{IE} = 0.72921 \times 10^{-4} \text{ rad/sec} \qquad (3.2)$$

The body axis velocities relative to air mass are approximately

$$\begin{bmatrix} U \\ V \\ W \end{bmatrix} = \begin{bmatrix} \ell_1 & \ell_2 & \ell_3 \\ m_1 & m_2 & m_3 \\ n_1 & n_2 & n_3 \end{bmatrix} \begin{bmatrix} \dot{X} - \dot{X}_o \\ \dot{Y} - \dot{Y}_o \\ \dot{Z} \end{bmatrix}$$

The total velocity relative to air mass (Figure 3.8) is

$$V_a = (U^2 + V^2 + W^2)^{1/2}$$

the air density is

$$\rho = 0.003\, e^{-h/22,500} \qquad (3.21)$$

where the altitude is

$$h = (Z - Z_o) \tag{3.21}$$

and the dynamic pressure is

$$q = \frac{1}{2} \rho V_a^2 \tag{3.20}$$

The rotational dynamics are given below where the aerodynamic moment coefficients are

$$\begin{bmatrix} C_\ell \\ C_m \\ C_n \end{bmatrix} = \begin{bmatrix} \frac{d}{2V_a} C_{\ell_p} P \\ \left[(\ell_g - \ell_b)(C_{D_o} + C_{L_\eta}) + (\ell_g - \ell_t)(C_{Dt_o} + C_{Lt_\alpha}) \right] \alpha + \frac{d}{2V_a} C_{m_q} Q \\ - \left[(\ell_g - \ell_b)(C_{D_o} + C_{L_\eta}) + (\ell_b - \ell_t)(C_{Dt_o} + C_{Lt_\alpha}) \right] \beta + \frac{d}{2V_a} C_{n_r} R \end{bmatrix} \tag{3.42}$$

the body axis moments are

$$\begin{bmatrix} M_x \\ M_y \\ M_z \end{bmatrix} = qAd \begin{bmatrix} C_\ell \\ C_m \\ C_n \end{bmatrix} + \begin{bmatrix} M_{xe} \\ M_{ye} \\ M_{ze} \end{bmatrix}_{1,2,3}$$

and the reference length is

$$d = 33 \text{ feet} \tag{C-18}$$

The engine moments are

$$\begin{bmatrix} M_{xe1} \\ M_{ye1} \\ M_{ze1} \end{bmatrix} = T_1 \begin{bmatrix} (\delta_{14} - \delta_{12})\, r_{e1} \\ -(\delta_{12} + \delta_{14})(\ell_{e1} - \ell_g) \\ -(\delta_{11} + \delta_{13})(\ell_{e1} - \ell_g) \end{bmatrix} \qquad (3.46)$$

$$\begin{bmatrix} M_{xe2} \\ M_{ye2} \\ M_{ze2} \end{bmatrix} = T_2 \begin{bmatrix} (\delta_{24} - \delta_{22})\, r_{e2} \\ -(\delta_{22} + \delta_{24})(\ell_{e2} - \ell_g) \\ -(\delta_{21} + \delta_{23})(\ell_{e2} - \ell_g) \end{bmatrix} \qquad (3.47)$$

$$\begin{bmatrix} M_{xe3} \\ M_{ye3} \\ M_{ze3} \end{bmatrix} = T_3 \begin{bmatrix} 2\dfrac{T_R}{T_3}\, \delta_{33}\, r_{e3} \\ -\delta_{32}\, (\ell_{e3} - \ell_g) \\ -\delta_{31}\, (\ell_{e3} - \ell_g) \end{bmatrix} \qquad (3.49)$$

where

$$r_{e3} = 11 \text{ feet} \qquad (C\text{-}23)$$

and for a $\ddot{\phi}_{MIN}$ of $2°/\sec^2$

$$T_R = 300 \text{ lbs}$$

The B-frame rotational equations are

$$\frac{d}{dt}\begin{bmatrix} P \\ Q \\ R \end{bmatrix} = \begin{bmatrix} 0 \\ PR\,(I_{zz} - I_{xx})/I_{yy} \\ RQ\,(I_{xx} - I_{yy})/I_{zz} \end{bmatrix} + \begin{bmatrix} M_x/I_{xx} \\ M_y/I_{yy} \\ M_z/I_{zz} \end{bmatrix} \tag{3.65}$$

and the Euler rates are

$$\begin{bmatrix} \dot{\phi} \\ \dot{\theta} - \omega_Y \\ \dot{\psi} \end{bmatrix} = \begin{bmatrix} 1 & -\cos\phi \tan\psi & \sin\phi \tan\psi \\ 0 & \dfrac{\cos\phi}{\cos\psi} & -\dfrac{\sin\phi}{\cos\psi} \\ 0 & \sin\phi & \cos\phi \end{bmatrix} \begin{bmatrix} P \\ Q \\ R \end{bmatrix} \tag{3.17}$$

8.2 RATE GYROS

Three rate gyros are necessary to measure the three body axis rates. Choosing orientations such that the roll and pitch gyro output axes are along Z_B and the yaw gyro output axis is along Y_B, the state models from Equation 4.15 become: for the roll axis,

$$\frac{d}{dt}\begin{bmatrix} \dot{\rho} \\ \rho \end{bmatrix} = \begin{bmatrix} -D_\rho/I_{fx} & -K_\rho/I_{fx} \\ 1 & 0 \end{bmatrix} \begin{bmatrix} \dot{\rho} \\ \rho \end{bmatrix} + \begin{bmatrix} -H_w/I_{fx} \\ 0 \end{bmatrix} P + \begin{bmatrix} -\dot{R} \\ 0 \end{bmatrix}$$

$$P_m = -\frac{K_\rho}{H_w}\rho$$

for the pitch axis,

$$\frac{d}{dt}\begin{bmatrix} \dot{\rho} \\ \rho \end{bmatrix} = \begin{bmatrix} -D_\rho/I_{fx} & -K_\rho/I_{fx} \\ 1 & 0 \end{bmatrix}\begin{bmatrix} \dot{\rho} \\ \rho \end{bmatrix} + \begin{bmatrix} -H_w/I_{fx} \\ 0 \end{bmatrix} Q + \begin{bmatrix} -\dot{R} \\ 0 \end{bmatrix}$$

$$Q_m = -\frac{K_\rho}{H_w}\rho$$

and for the yaw axis,

$$\frac{d}{dt}\begin{bmatrix} \dot{\rho} \\ \rho \end{bmatrix} = \begin{bmatrix} -D_\rho/I_{fx} & -K_\rho/I_{fx} \\ 1 & 0 \end{bmatrix}\begin{bmatrix} \dot{\rho} \\ \rho \end{bmatrix} + \begin{bmatrix} -H_w/I_{fx} \\ 0 \end{bmatrix} R + \begin{bmatrix} -\dot{Q} \\ 0 \end{bmatrix}$$

$$R_m = -\frac{K_\rho}{H_w}\rho$$

8.3 STABLE PLATFORM

Because a stable platform must remain stationary in the computational coordinate system to assure accuracy, it can be assumed that

$$\phi_m = -\gamma$$

$$\theta_m = -\alpha$$

$$\psi_m = -\beta$$

8.4 ACCELEROMETERS

For purposes of illustration, the simple spring-mass accelerometer is used with

$$\frac{d}{dt}\begin{bmatrix}\dot{\delta}\\ \delta\end{bmatrix} = \begin{bmatrix}-D_a/m_a & -K_S/m_a\\ 1 & 0\end{bmatrix}\begin{bmatrix}\dot{\delta}\\ \delta\end{bmatrix} + \begin{bmatrix}-1\\ 0\end{bmatrix}\ddot{x} \qquad (4.28)$$

where for the X_V axis accelerometer,

$$\ddot{X} = \ddot{x}$$

$$A_X = -\frac{K_S}{m_a}\delta$$

for the Y_V axis accelerometer,

$$\ddot{Y} = \ddot{x}$$

$$A_Y = -\frac{K_S}{m_a}\delta$$

and for the Z_V axis accelerometer,

$$\ddot{Z} = \ddot{x}$$

$$A_Z = -\frac{K_S}{m_a}\delta$$

8.5 ENGINE SERVOS

The state model for a typical engine servo is

$$\frac{d}{dt}\begin{bmatrix} \dot{\delta} \\ \delta \end{bmatrix} = \begin{bmatrix} -2\zeta\omega_n & -\omega_n^2 \\ 1 & 0 \end{bmatrix} \begin{bmatrix} \dot{\delta} \\ \delta \end{bmatrix} + \begin{bmatrix} -\omega_n^2 \\ 0 \end{bmatrix} \delta_c$$

where δ corresponds with δ_{11} , δ_{12} , $\cdots$, δ_{21} , δ_{22} , $\cdots$, δ_{31} for each servo, and δ_c is the input command for each servo and corresponds with δ_{11_c} , δ_{12_c} , $\cdots$, δ_{21_c} , δ_{22_c} , $\cdots$, δ_{31_c} .

8.6 GUIDANCE AND CONTROL EQUATIONS

The control system equations are

$$\begin{bmatrix} \delta_\ell \\ \delta_m \\ \delta_n \end{bmatrix} = \begin{bmatrix} -K_{\ell P}\ P_m + K_{\ell\phi}(\phi_c - \phi_m) \\ -K_{mQ}\ Q_m + K_{m\theta}(\theta_c - \theta_m) \\ -K_{nR}\ R_m + K_{n\psi}(\psi_c - \psi_m) \end{bmatrix} \tag{5.2}$$

where

$$\begin{bmatrix} \delta_\ell \\ \delta_m \\ \delta_n \end{bmatrix} = \begin{bmatrix} (\delta_{14c} - \delta_{12c}) \\ -(\delta_{12c} + \delta_{14c}) \\ -(\delta_{11c} + \delta_{13c}) \end{bmatrix}$$

The guidance equations for the vertical rise period are

$$\theta_c = \psi_c = 0$$

and

$$\dot{\phi}_c = 1 \text{ degree/sec}$$

till

$$\phi_m = 0$$

then

$$\phi_c = 0$$

The guidance equations for the gravity turn are

$$\phi_c = \psi_c = 0$$

and

$$\theta_c = \tan^{-1}\left(\frac{A_Z}{A_X}\right)$$

The guidance commands during the vacuum phase are

$$\phi_c = 0$$

$$\psi_c = K_{n\dot{\lambda}}\,\dot{\lambda} + K_{n\lambda}\,\lambda$$

$$\theta_c = \theta_o - K_{m\dot{Z}}\,\dot{Z}_T - K_{mZ}\,(Z - Z_N)$$

where

$$\dot{Z}_T = \dot{Z}\cos\gamma_N - \dot{X}\sin\gamma_N$$

and θ_o , γ_N , and Z_N are values as determined by a nominal trajectory. It is also necessary to use the vehicle translational dynamics equations where

$$\frac{d}{dt}\begin{bmatrix}\dot{X}\\ \dot{Y}\\ \dot{Z}\end{bmatrix} = \begin{bmatrix}-\dot{X}\dot{Z}/Z\\ -\dot{Y}\dot{Z}/Z\\ (\dot{X}^2+\dot{Y}^2)/Z - \mu/Z^2\end{bmatrix} + \begin{bmatrix}A_X\\ A_Y\\ A_Z\end{bmatrix}$$

and

$$\mu = 1.4077 \times 10^{16}\ \text{ft}^3/\text{sec}^2 \qquad (3.58)$$

$$\bar{\omega}_{IV} = \begin{bmatrix}\omega_X\\ \omega_Y\\ 0\end{bmatrix} = \begin{bmatrix}-\dot{Y}/Z\\ \dot{X}/Z\\ 0\end{bmatrix} \qquad (6.6)$$

$$\left(\bar{\omega}_{IV}\right)_o = \omega_{IE}\begin{bmatrix}\cos\Phi_o \cos\Psi_o\\ \cos\Phi_o \sin\Psi_o\\ 0\end{bmatrix}$$

$$\omega_{IE} = 0.72921 \times 10^{-4}\ \text{rad/sec} \qquad (3.2)$$

$$X_o = Y_o = 0$$

$$Z_o = 20{,}925{,}732\ \text{feet} \qquad (3.58)$$

The trajectory plane angles are defined by

$$\dot{\xi} = -\dot{\sigma} \sin \lambda$$

$$\dot{\lambda} = \dot{\sigma} \cos \lambda \tan \xi - \frac{\omega_X}{\cos \xi}$$

$$\dot{\sigma} = \frac{\omega_Y}{\cos \lambda \cos \xi} - \frac{\dot{\lambda} \tan \xi}{\cos \lambda}$$

8.7 ENGINE IGNITION AND CUTOFF

Ignition of the first stage engines is initiated at the start of the program. Cutoff of the first stage engines and ignition of the second stage engines occurs when

$$(A_X^2 + A_Z^2)^{1/2} \geq 5.4 \text{ g's}$$

Cutoff of the second stage engines occurs when

$$(\dot{X}^2 + \dot{Z}^2)^{1/2} \geq V_{NOM}$$

where V_{NOM} is a number determined from nominal trajectory computations. Likewise, ignition of the third stage engine occurs after a coasting period as determined by nominal trajectory computations when

$$Z \geq Z_{NOM}$$

so that h will be at 300 N.M. when third stage cutoff occurs at

$$\dot{X} = 24,875.9 \text{ fps} \qquad (2.3)$$

9. CONCLUSIONS

State models for a space carrier vehicle and a guidance and control system for this vehicle have been derived and are summarized in Section 8. The basic aerodynamics and gyrodynamics have been developed beginning with fundamental concepts (Sections 3 and 4) so that more comprehensive expressions for the individual components can be derived and incorporated as required. The complete mission, the vehicle, and the systems necessary to accomplish the mission have been defined.

As briefly described in Section 8, analog computers, digital computers, and component hardware can be used to simulate the complete system for purposes of preliminary design studies. To do so, it would be necessary to program the given system state models for analog and/or digital computers and to include hardware as dictated by desire and availability of equipment.

The state models that are given are meant to provide a framework within which the individual systems can be studies. In the future, if desired a more sophisticated guidance system or control system could be used instead of the system described. It might be desired, for example to replace the vacuum phase guidance system with a self optimizing system, or the position control system with a rate command control system. In addition, the vehicle state models could be expanded to include such things as fuel sloshing, and vehicle bending and compliance modes. These tasks could be done by simply adding expressions for these effects to the appropriate state models.

In general, the system models that are given are adequate for simulated preliminary design studies but if more detailed investigations are needed expansion of the individual models may become necessary.

APPENDIX A

VEHICLE TRANSLATIONAL DYNAMICS

The development of expressions for the translational, or linear, dynamics of the vehicle is begun by consideration of Newton's second law of motion -- that the rate of change of linear momentum of an element of mass, as observed from inertial space, is equal to the force acting on the element of mass. Referring to Figure A-1

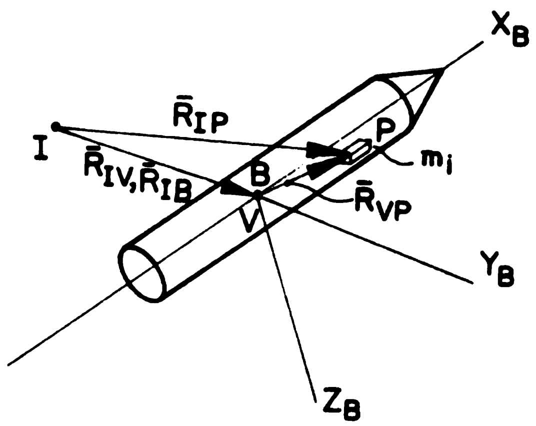

FIGURE A-1

LOCATION OF ELEMENT OF MASS

the force, F_i , on an element of mass, m_i , is

$$\bar{F}_i = \left[\frac{d}{dt} \left(m_i \; \bar{V}_{IP} \right) \right]_I \qquad \text{(A-1)}$$

as observed from inertial space, where

$$\bar{V}_{IP} = \left[\frac{d\,\bar{R}_{IP}}{dt}\right]_I \tag{A-2}$$

The sum of the forces acting on the elements of mass consists of externally applied forces plus the forces acting between the elements of mass. Since the forces between each of the elements of mass cancel, by Newton's third law (for every action there is an equal and opposite reaction), the total force, and thus the total applied force, and the total rate of change of linear momentum are obtained by summation over the i elements of the vehicle (from Eq. A-1) as

$$\bar{F}_A = \sum_i \bar{F}_i = \sum_i \left[\frac{d}{dt}\left(m_i\ \bar{V}_{IP}\right)\right]_I \tag{A-3}$$

From Figure A-1

$$\bar{R}_{IP} = \bar{R}_{IV} + \bar{R}_{VP}$$

which upon differentiation with respect to time yields

$$\left[\frac{d\,\bar{R}_{IP}}{dt}\right]_I = \left[\frac{d\,\bar{R}_{IV}}{dt}\right]_I + \left[\frac{d\,\bar{R}_{VP}}{dt}\right]_I \tag{A-4}$$

Interchanging the differentiation and the summation, Equation A-3 becomes

$$\overline{F}_A = \left[\frac{d}{dt} \sum_i m_i \overline{V}_{IP}\right]_I \tag{A-5}$$

and upon combination with Equations A-2 and A-4 becomes

$$\overline{F}_A = \left\{\frac{d}{dt} \sum_i m_i \left(\left[\frac{d\,\overline{R}_{IV}}{dt}\right]_I + \left[\frac{d\,\overline{R}_{VP}}{dt}\right]_I\right)\right\}_I$$

As each of the individual elements of mass is invariant with time

$$\overline{F}_A = \left[\frac{d^2}{dt^2} \sum_i m_i \overline{R}_{IV}\right]_I + \left[\frac{d^2}{dt^2} \sum_i m_i \overline{R}_{VP}\right]_I \tag{A-6}$$

Since by definition of the mass center with V at the c. g. of the vehicle

$$\sum_i m_i \overline{R}_{VP} = 0 \tag{A-7}$$

and Equation A-6 becomes

$$\overline{F}_A = \left[\frac{d^2}{dt^2} \sum_i m_i \overline{R}_{IV}\right]_I \tag{A-8}$$

Again, considering each element of mass to be invariant with time, and since $\overline{R}_{IV}$ is not affected by the summation, Equation A-8 reduces to

$$\bar{F}_A = m \left[\frac{d^2 \bar{R}_{IV}}{dt^2} \right]_I \qquad \text{(A-9)}$$

where

$$m = \sum_i m_i \qquad \text{(A-10)}$$

Note that Equation A-9 is valid even if the elements of mass are moving with respect to the mass center as would be the case with vehicle bending modes, longitudinal compliance modes, and propellent sloshing. Also, it is valid if the vehicle mass is changing as would be the case during the expulsion of propellant during the thrusting phases.

The forces that act on the vehicle sum to zero as

$$\bar{F}_I + \bar{F}_{EX} + \sum_i m_i \bar{G} = 0 \qquad \text{(A-11)}$$

where

$$\bar{F}_A = -\bar{F}_I \qquad \text{(A-12)}$$

Upon substitution of Equation A-12 into Equation A-11, the applied force becomes

$$\bar{F}_A = \bar{F}_{EX} + \sum_i m_i \bar{G} \qquad \text{(A-13)}$$

$$= \bar{F}_{EX} + m\bar{G} \qquad \text{(A-14)}$$

where, $\overline{F}_{EX}$ consists of the propulsion, aerodynamic, and control inputs to the vehicle and $\overline{G}$ is the total acceleration due to gravitational forces. Equating Equations A-9 and A-14 yields

$$\left[\frac{d^2\,\overline{R}_{IV}}{dt^2}\right]_I = \frac{\overline{F}_{EX}}{m} + \overline{G} \tag{A-15}$$

Figure A-2 shows the vector relationships between the centers of the I, E, and V coordinate frames with

$$\overline{R}_{IV} = \overline{R}_{IE} + \overline{R}_{EV} \tag{A-16}$$

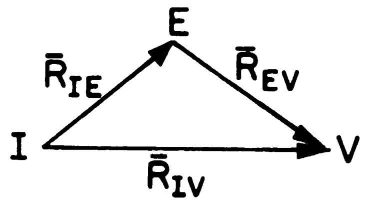

FIGURE A-2

COORDINATE SYSTEM VECTOR DIAGRAM

Differentiation of Equation A-16 with respect to time gives

$$\left[\frac{d\,\overline{R}_{IV}}{dt}\right]_I = \left[\frac{d\,\overline{R}_{IE}}{dt}\right]_I + \left[\frac{d\,\overline{R}_{EV}}{dt}\right]_I \tag{A-17}$$

with

$$\left[\frac{d\,\overline{R}_{EV}}{dt}\right]_I = \left[\frac{d\,\overline{R}_{EV}}{dt}\right]_V + \overline{\omega}_{IV} \times \overline{R}_{EV} \tag{A-18}$$

Differentiating Equation A-17 after substitution of Equation A-18 yields

$$\left[\frac{d^2\,\bar{R}_{IV}}{dt^2}\right]_I = \left[\frac{d^2\,\bar{R}_{IE}}{dt^2}\right]_I + \left\{\frac{d}{dt}\left[\frac{d\,\bar{R}_{EV}}{dt}\right]_V\right\}_I \tag{A-19}$$

$$+ \left[\frac{d\,\bar{\omega}_{IV}}{dt}\right]_I \times \bar{R}_{EV} + \bar{\omega}_{IV} \times \left[\frac{d\,\bar{R}_{EV}}{dt}\right]_I$$

where

$$\left\{\frac{d}{dt}\left[\frac{d\,\bar{R}_{EV}}{dt}\right]_V\right\}_I = \left[\frac{d^2\,\bar{R}_{EV}}{dt^2}\right]_V + \bar{\omega}_{IV} \times \left[\frac{d\,\bar{R}_{EV}}{dt}\right]_V \tag{A-20}$$

and

$$\left[\frac{d\,\bar{\omega}_{IV}}{dt}\right]_I = \left[\frac{d\bar{\omega}_{IV}}{dt}\right]_V + \bar{\omega}_{IV} \times \bar{\omega}_{IV} \tag{A-21}$$

which reduces to

$$\left[\frac{d\,\bar{\omega}_{IV}}{dt}\right]_I = \left[\frac{d\,\bar{\omega}_{IV}}{dt}\right]_V \tag{A-22}$$

Upon combining Equations A-19, A-20, and A-22

$$\left[\frac{d^2\bar{R}_{IV}}{dt^2}\right]_I = \left[\frac{d^2\bar{R}_{IE}}{dt^2}\right]_I + \left[\frac{d^2\bar{R}_{EV}}{dt^2}\right]_V + \left[\frac{d\bar{\omega}_{IV}}{dt}\right]_V \times \bar{R}_{EV}$$

(A-23)

$$+ \quad 2\bar{\omega}_{IV} \times \left[\frac{d\,\bar{R}_{EV}}{dt}\right]_V + \bar{\omega}_{IV} \times (\bar{\omega}_{IV} \times \bar{R}_{EV})$$

For the I-frame to be an inertial reference frame where Newton's laws apply, it is necessary and sufficient that this frame be non-accelerating and non-rotating. A constant linear velocity is acceptable as shown in [7, pp. 67-69]. In considering the solution of Equation A-23, it is necessary to define the acceleration terms, $\left[d^2\,\bar{R}_{IV}/dt^2\right]_I$ and $\left[d^2\,\bar{R}_{IE}/dt^2\right]_I$.

The acceleration of the earth with respect to inertial space, it is assumed, is caused only by gravitational forces. Considering the point E to be at the mass center of the earth,

$$\bar{G}_U = \left[\frac{d^2\,\bar{R}_{IE}}{dt^2}\right]_I \qquad \text{(A-24)}$$

Assuming that the vehicle is "close enough" to the mass center to the earth, this same gravitational attraction will be acting on the vehicle. Also, assuming the vehicle to be a point mass, a vector sum for the total attraction accelerations can be written, including the gravitational attraction between the vehicle and the earth, as

$$\overline{G} = \overline{G}_U + \overline{G}_E \tag{A-25}$$

Substitution of Equation A-25 into A-15 and the result, along with Equation A-24, into A-23, yields

$$\frac{\overline{F}_{EX}}{m} + \overline{G}_U + \overline{G}_E = \overline{G}_U + \left[\frac{d^2 \overline{R}_{EV}}{dt^2}\right]_V + \left[\frac{d\overline{\omega}_{IV}}{dt}\right]_V \times \overline{R}_{EV}$$

$$+ 2\,\overline{\omega}_{IV} \times \left[\frac{d\,\overline{R}_{EV}}{dt}\right]_V + \overline{\omega}_{IV} \times (\overline{\omega}_{IV} \times \overline{R}_{EV}) \tag{A-26}$$

$$\frac{\overline{F}_{EX}}{m} + \overline{G}_E = \left[\frac{d^2 \overline{R}_{EV}}{dt^2}\right]_V + \left[\frac{d\,\overline{\omega}_{IV}}{dt}\right]_V \times \overline{R}_{EV}$$

$$+ 2\overline{\omega}_{IV} \times \left[\frac{d\,\overline{R}_{EV}}{dt}\right]_V + \overline{\omega}_{IV} \times (\overline{\omega}_{IV} \times \overline{R}_{EV}) \tag{A-27}$$

To qualitatively verify the assumption of being "close enough" to the mass center of the earth, consider the error in attraction due to the sun. For a vehicle not at the mass center of the earth, but say on or near the surface of the earth, and on the far side with respect to the sun as shown in Figure A-3, a net acceleration would exist. The path of the earth around the sun is very nearly circular

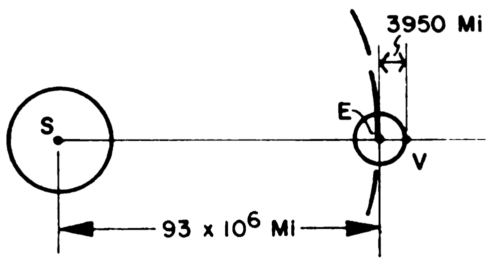

FIGURE A-3

VEHICLE ACCELERATION RELATED TO SUN

(eccentricity of 0.01673) where if it were exactly circular, the centrifugal and gravitational accelerations would be equal as

$$\frac{(V_{SE})^2}{R_{SE}} - G_{SE} = 0 \tag{A-28}$$

For the vehicle on the surface of the earth (ignoring effects due to the earth and the moon), the net acceleration on the vehicle due to its orbit around the sun is

$$A_{SV} = \frac{V_{SV}^2}{R_{SV}} - G_{SV} \tag{A-29}$$

where by the inverse-square gravitational law,

$$G_{SV} = G_{SE} \left(\frac{R_{SE}}{R_{SV}} \right)^2 \tag{A-30}$$

Assuming that the angular rate of the earth and the vehicle around the sun are the same

$$V_{SV} = \left(\frac{R_{SV}}{R_{SE}} \right) V_{SE} \tag{A-31}$$

Solution of Equations A-28, A-29, A-30, and A-31 yields

$$A_{SV} = V_{SE}^2 \left[\frac{R_{SV}}{R_{SE}^2} - \frac{R_{SE}}{R_{SV}^2} \right] \tag{A-32}$$

$$A_{SV} \cong \frac{3\, V_{SE}^2\, R_{EV}}{R_{SV}^2} \tag{A-33}$$

Upon substitution of parameter values

$$V_{SE} = \frac{2\,(93 \times 10^6)\,\pi\,(5280)}{365\,(24)\,(3600)} \tag{A-34}$$

$$V_{SE} = 98{,}000 \text{ fps} \tag{A-35}$$

and

$$A_{SV} \cong 0.85 \times 10^{-7} \text{ g's} \tag{A-36}$$

As it turns out, the accuracy that is necessary (and available) for the most accurate present day guidance systems is on the order of 10^{-5} g's. Therefore, the unbalanced acceleration on the vehicle at or near the surface of the earth due to the effects of the earth's orbit around the sun can be neglected.

Observing the definitions of the V-frame coordinate system

$$\overline{R}_{EV} = \begin{bmatrix} 0 \\ 0 \\ Z \end{bmatrix}_V \tag{A-37}$$

$$\left[\frac{d\,\overline{R}_{EV}}{dt}\right]_V = \begin{bmatrix} 0 \\ 0 \\ \dot{Z} \end{bmatrix}_V \tag{A-38}$$

$$\left[\frac{d^2\,\overline{R}_{EV}}{dt^2}\right]_V = \begin{bmatrix} 0 \\ 0 \\ \ddot{Z} \end{bmatrix}_V \tag{A-39}$$

and

$$\overline{\omega}_{IV} = \begin{bmatrix} \omega_X \\ \omega_Y \\ 0 \end{bmatrix}_V \tag{A-40}$$

$$\left[\frac{d\,\bar{\omega}_{IV}}{dt}\right]_V = \begin{bmatrix} \dot{\omega}_X \\ \dot{\omega}_Y \\ 0 \end{bmatrix}_V \tag{A-41}$$

Define

$$\bar{G}_E = \begin{bmatrix} G_X \\ G_Y \\ G_Z \end{bmatrix} \tag{A-42}$$

and

$$\bar{F}_{EX} = \begin{bmatrix} F_X \\ F_Y \\ F_Z \end{bmatrix} \tag{A-43}$$

Upon completion of the cross products of Equation A-27 using Equations A-37, A-38, A-40, and A-41, and upon substitution of these products and Equations A-39, A-42, and A-43, Equation A-27 becomes

$$\frac{1}{m}\begin{bmatrix} F_X \\ F_Y \\ F_Z \end{bmatrix} + \begin{bmatrix} G_X \\ G_Y \\ G_Z \end{bmatrix} = \begin{bmatrix} 0 \\ 0 \\ \ddot{Z} \end{bmatrix} + \begin{bmatrix} \dot{\omega}_Y Z \\ -\dot{\omega}_X Z \\ 0 \end{bmatrix} + \begin{bmatrix} 2\,\omega_Y \dot{Z} \\ -2\,\omega_X \dot{Z} \\ 0 \end{bmatrix} + \begin{bmatrix} 0 \\ 0 \\ -(\omega_X^2 + \omega_Y^2)\,Z \end{bmatrix}$$

(A-44)

$$= \frac{d}{dt}\begin{bmatrix} \omega_Y Z \\ -\omega_X Z \\ \dot{Z} \end{bmatrix} + \begin{bmatrix} \omega_Y \dot{Z} \\ -\omega_X \dot{Z} \\ 0 \end{bmatrix} + \begin{bmatrix} 0 \\ 0 \\ -(\omega_X^2 + \omega_Y^2) Z \end{bmatrix} \tag{A-45}$$

After rearrangement and expressing $\bar{\omega}_{IV}$ as viewed from the point E as

$$\bar{\omega}_{IV} = \bar{\omega}_{EV} = \begin{bmatrix} -\dot{Y}/Z \\ \dot{X}/Z \\ 0 \end{bmatrix} \tag{A-46}$$

Equations A-45 become

$$\frac{d}{dt}\begin{bmatrix} \dot{X} \\ \dot{Y} \\ \dot{Z} \end{bmatrix} = \begin{bmatrix} -\dot{X}\dot{Z}/Z \\ -\dot{Y}\dot{Z}/Z \\ (\dot{X}^2 + \dot{Y}^2)/Z \end{bmatrix} + \frac{1}{m}\begin{bmatrix} F_X \\ F_Y \\ F_Z \end{bmatrix} + \begin{bmatrix} G_X \\ G_Y \\ G_Z \end{bmatrix} \tag{A-47}$$

Equations A-47 are the basic set of translational equations that are used both for the simulation of the vehicle and for use in the guidance computer. In the simulation of the vehicle the external forces, (F_X, F_Y, F_Z), are computed as functions of the aerodynamics of the vehicle, the thrust, and the control inputs, while in the guidance computer the accelerations, $\left(\frac{F_X}{m}, \frac{F_Y}{m}, \frac{F_Z}{m}\right)$, represents the inputs from the accelerometers.

The components of (X, Y, Z) and their derivatives, the forces, and the gravitational accelerations are measured, as defined, in the directions of the three components of the V-frame as viewed by an observer located at the center of the earth in a non-rotating coordinate system.

APPENDIX B

VEHICLE ROTATIONAL DYNAMICS

The rotational dynamics of the vehicle can be developed by considering the moment of momentum (angular momentum). The coordinate system that is used is one which has its center at B and its axes fixed to the vehicle (this is the B-frame as shown in Figure A-1). By definition the moment of momentum of an element of mass is (refer to Figure A-1)

$$\bar{H}_i = \bar{R}_{BP} \times (m_i \, \bar{V}_{IP}) \tag{B-1}$$

Upon differentiation (each element of mass is invariant with time) Equation B-1 becomes

$$\left[\frac{d\,\bar{H}_i}{dt}\right]_I = \left[\frac{d\,\bar{R}_{BP}}{dt}\right]_I \times (m_i \, \bar{V}_{IP}) + \bar{R}_{BP} \times m_i \left[\frac{d\,\bar{V}_{IP}}{dt}\right]_I \tag{B-2}$$

By definition the moment of an element of mass about the point B is

$$\bar{M}_i = \bar{R}_{BP} \times \bar{F}_i \tag{B-3}$$

which upon substitution of Equation A-1, and again considering m_i to be unchanging with time, becomes

$$\bar{M}_i = \bar{R}_{BP} \times m_i \left[\frac{d\,\bar{V}_{IP}}{dt}\right]_I \qquad \text{(B-4)}$$

Substitution of Equation B-4 into Equation B-2 yields the expression for the moment of an element of mass,

$$\bar{M}_i = \left[\frac{d\,\bar{H}_i}{dt}\right]_I - \left[\frac{d\,\bar{R}_{BP}}{dt}\right]_I \times m_i\,\bar{V}_{IP} \qquad \text{(B-5)}$$

Summation of all of the moments yields a total moment of

$$\bar{M} = \sum_i \bar{M}_i = \left[\frac{d\bar{H}}{dt}\right]_I - \sum_i \left[\frac{d\,\bar{R}_{BP}}{dt}\right]_I \times m_i\,\bar{V}_{IP}$$

(B-6)

From Figure A-1

$$\bar{R}_{IP} = \bar{R}_{IB} + \bar{R}_{BP} \qquad \text{(B-7)}$$

and by differentiation

$$\left[\frac{d\,\bar{R}_{IP}}{dt}\right]_I = \bar{V}_{IP} = \left[\frac{d\,\bar{R}_{IB}}{dt}\right]_I + \left[\frac{d\,\bar{R}_{BP}}{dt}\right]_I \qquad \text{(B-8)}$$

The last term of Equation B-6, upon substitution of Equation B-8, becomes

$$\sum_i \left[\frac{d\,\bar{R}_{BP}}{dt}\right]_I \times m_i\,\bar{V}_{IP} = \sum_i \left[\frac{d\,\bar{R}_{BP}}{dt}\right]_I \times m_i \left[\frac{d\,\bar{R}_{IB}}{dt}\right]_I$$

$$+ \sum_i \left[\frac{d\,\bar{R}_{BP}}{dt}\right]_I \times m_i \left[\frac{d\,\bar{R}_{BP}}{dt}\right]_I \qquad \text{(B-9)}$$

Since $\left[\frac{d\,\bar{R}_{IB}}{dt}\right]_I$ is independent of the summation and the last term is zero, the expression reduces to

$$\sum_i \left[\frac{d\,\bar{R}_{BP}}{dt}\right]_I \times m_i\,\bar{V}_{IP} = \left\{\sum_i m_i \left[\frac{d\,\bar{R}_{BP}}{dt}\right]_I\right\} \times \left[\frac{d\,\bar{R}_{IB}}{dt}\right]_I \qquad \text{(B-10)}$$

If the point B is at the mass center of the vehicle, and since m is constant, the summation on the right hand side of Equation B-10 becomes

$$\frac{d}{dt}\left[\sum_i m_i\,\bar{R}_{BP}\right]_I = 0 \qquad \text{(B-11)}$$

and Equation B-10 becomes

$$\sum_i \left[\frac{d\,\bar{R}_{BP}}{dt}\right]_I \times m_i\,\bar{V}_{IP} = 0 \qquad \text{(B-12)}$$

Thus, with the assumption that B is at the mass center of the vehicle, Equation B-6 reduces to the well known expression

$$\bar{M} = \left[\frac{d\bar{H}}{dt}\right]_I \tag{B-13}$$

Returning to Equation B-1 and summing over all of the elements of mass, the total moment of momentum is

$$\bar{H} = \sum_i \bar{H}_i = \sum_i \bar{R}_{BP} \times m_i \, \bar{V}_{IP} \tag{B-14}$$

Relating the velocity of the element of mass with respect to B as observed in the I-frame to the velocity as observed in the B-frame yields

$$\left[\frac{d\,\bar{R}_{BP}}{dt}\right]_I = \left[\frac{d\,\bar{R}_{BP}}{dt}\right]_B + \bar{\omega}_{IB} \times \bar{R}_{BP} \tag{B-15}$$

Assuming the vehicle to be a rigid body, Equation B-15 reduces to

$$\left[\frac{d\,\bar{R}_{BP}}{dt}\right]_I = \bar{\omega}_{IB} \times \bar{R}_{BP} \tag{B-16}$$

Substitution of Equations B-8 and B-16 into Equation B-14 gives

$$\bar{H} = \sum_i \bar{R}_{BP} \times m_i \left[\frac{d\,\bar{R}_{IB}}{dt}\right]_I + \sum_i \bar{R}_{BP} \times m_i \, (\bar{\omega}_{IB} \times \bar{R}_{BP}) \tag{B-17}$$

Here again, since $\left[\frac{d\bar{R}_{IB}}{dt}\right]_I$ is independent of the summation and by placing B at the mass center of the vehicle, the first term on the right side of Equation B-17 is zero and the moment of momentum reduces to

$$\bar{H} = \sum_i \bar{R}_{BP} \times m_i \, (\bar{\omega}_{IB} \times \bar{R}_{BP}) \tag{B-18}$$

which upon expansion of the vector triple product is

$$\bar{H} = \sum_i \bar{\omega}_{IB} \quad (R_{BP})^2 \; m_i \; - \sum_i \bar{R}_{BP} \; (\bar{\omega}_{IB} \cdot \bar{R}_{BP}) \, m_i \tag{B-19}$$

By defining

$$\bar{\omega}_{IB} = \begin{bmatrix} P \\ Q \\ R \end{bmatrix} \tag{B-20}$$

and

$$\bar{R}_{BP} = \begin{bmatrix} x \\ y \\ z \end{bmatrix} \tag{B-21}$$

Equation B-19 is

$$\bar{H} = \begin{bmatrix} H_x \\ H_y \\ H_z \end{bmatrix} = \begin{bmatrix} P \\ Q \\ R \end{bmatrix} \sum_i (x^2 + y^2 + z^2) \, m_i - \sum_i \begin{bmatrix} x \\ y \\ z \end{bmatrix} (Px + Qy + Rz) \, m_i \tag{B-22}$$

The terms of Equation B-22 are by definition the following inertias

$$I_{xx} = \sum_i (y^2 + z^2)\, m_i$$

$$I_{yy} = \sum_i (x^2 + z^2)\, m_i$$

$$I_{zz} = \sum_i (x^2 + y^2)\, m_i$$

$$I_{xy} = \sum_i (xy)\, m_i \qquad \text{(B-23)}$$

$$I_{xz} = \sum_i (xz)\, m_i$$

$$I_{yz} = \sum_i (yz)\, m_i$$

Substitution of Equations A-23 into B-22 yields

$$\bar{H} = \begin{bmatrix} I_{xx} & -I_{xy} & -I_{xz} \\ -I_{xy} & I_{yy} & -I_{yz} \\ -I_{xz} & -I_{yz} & I_{zz} \end{bmatrix} \begin{bmatrix} P \\ Q \\ R \end{bmatrix} \qquad \text{(B-24)}$$

The total moment (Equation B-13) in terms of the time derivative of the moment of momentum observed in the B-frame is

$$\bar{M} = \left[\frac{d\bar{H}}{dt}\right]_I = \left[\frac{d\bar{H}}{dt}\right]_B + \bar{\omega}_{IB} \times \bar{H} \qquad \text{(B-25)}$$

Taking the derivative of Equation B-22 with respect to time, where each of the elements of mass are considered to be of fixed mass and at discrete locations, and upon substitution of Equations B-23, the rate of change of the moment of momentum in the B-frame (because P, Q, R are in the B-frame) becomes

$$\left[\frac{d\bar{H}}{dt}\right]_B = \begin{bmatrix} I_{xx} & -I_{xy} & -I_{xz} \\ -I_{xy} & I_{yy} & -I_{yz} \\ -I_{xz} & -I_{yz} & I_{zz} \end{bmatrix} \frac{d}{dt} \begin{bmatrix} P \\ Q \\ R \end{bmatrix} \tag{B-26}$$

Upon completion of the cross product of Equation B-25, the expressions for the rotational dynamics of the vehicle become

$$\begin{bmatrix} I_{xx} & -I_{xy} & -I_{xz} \\ -I_{xy} & I_{yy} & -I_{yz} \\ -I_{xz} & -I_{yz} & I_{zz} \end{bmatrix} \frac{d}{dt} \begin{bmatrix} P \\ Q \\ R \end{bmatrix} = - \begin{bmatrix} (-I_{xz} Q + I_{xy} R) P + (-I_{yz} Q - I_{yy} R) Q + (I_{zz} Q + I_{yz} R) R \\ (I_{xz} P + I_{xx} R) P + (I_{yz} P - I_{xy} R) Q + (-I_{zz} P - I_{xz} R) R \\ (-I_{xy} P - I_{xx} Q) P + (I_{yy} P + I_{xy} Q) Q + (-I_{yz} P + I_{xz} Q) R \end{bmatrix} + \begin{bmatrix} M_x \\ M_y \\ M_z \end{bmatrix} \tag{B-27}$$

Since the vehicle under consideration has planes of symmetry in the x-y and x-z planes of the B-frame, the products of inertia can be dropped (assuming equally distributed density of the vehicle). This occurs since, referring to Equations B-23, there are plus and minus distances in the y and z directions for corresponding pairs of elements of mass, and in the summation of Equations 23 cancel, yielding

$$I_{xy} = I_{xz} = I_{yz} = 0 \tag{B-28}$$

With the assumption that the products of inertia are zero, the expression for the rotational dynamics of the vehicle (Equations B-27) become

$$\begin{bmatrix} I_{xx} & 0 & 0 \\ 0 & I_{yy} & 0 \\ 0 & 0 & I_{zz} \end{bmatrix} \frac{d}{dt} \begin{bmatrix} P \\ Q \\ R \end{bmatrix} = \begin{bmatrix} (I_{yy} - I_{zz})\, QR \\ (I_{zz} - I_{xx})\, PR \\ (I_{xx} - I_{yy})\, PQ \end{bmatrix} + \begin{bmatrix} M_x \\ M_y \\ M_z \end{bmatrix} \tag{B-29}$$

$$\frac{d}{dt} \begin{bmatrix} P \\ Q \\ R \end{bmatrix} = \begin{bmatrix} \dfrac{I_{yy} - I_{zz}}{I_{xx}}\, QR \\ \dfrac{I_{zz} - I_{xx}}{I_{yy}}\, PR \\ \dfrac{I_{xx} - I_{yy}}{I_{zz}}\, PQ \end{bmatrix} + \begin{bmatrix} \dfrac{M_x}{I_{xx}} \\ \dfrac{M_y}{I_{yy}} \\ \dfrac{M_z}{I_{zz}} \end{bmatrix} \tag{B-30}$$

The vehicle considered is in essence a body of revolution. If identical distribution of mass along the y and z axes is assumed, the expression for the vehicle rotational dynamics reduces to

$$\frac{d}{dt}\begin{bmatrix} P \\ \\ Q \\ \\ R \end{bmatrix} = \begin{bmatrix} 0 \\ \\ \dfrac{I_{zz} - I_{xx}}{I_{yy}} \quad PR \\ \\ \dfrac{I_{xx} - I_{yy}}{I_{zz}} \quad RQ \end{bmatrix} + \begin{bmatrix} \dfrac{M_x}{I_{xx}} \\ \\ \dfrac{M_y}{I_{yy}} \\ \\ \dfrac{M_z}{I_{zz}} \end{bmatrix} \tag{B-31}$$

APPENDIX C

VEHICLE DATA

The vehicle considered is one which is similar to the Saturn C-5. It is herein referred to as a "Saturn C-5 Type." The general physical parameters, such as sizes, inertial and dry weights, thrusts, etc., that are available in unclassified literature, correspond with those of the actual vehicle. Other parameters, however, such as weights as a function of fuel consumption, inertias, c.g. locations, and aerodynamic coefficients have been estimated using approximating expressions and general emperical data.

The selected vehicle configuration is shown in Figure C-1. A summary of the initial weights and masses, and the dry weights and masses from [8, p. 45] is given in Table C-1. Also given in Table C-1 are the stage thrusts in a vacuum and the assumed mass flow rates [1, p. 23-61 and 6, p. 40].

It is assumed that each section of the vehicle is a body of revolution with a uniform distribution of mass. Each section is considered separately except for the booster stages when they are

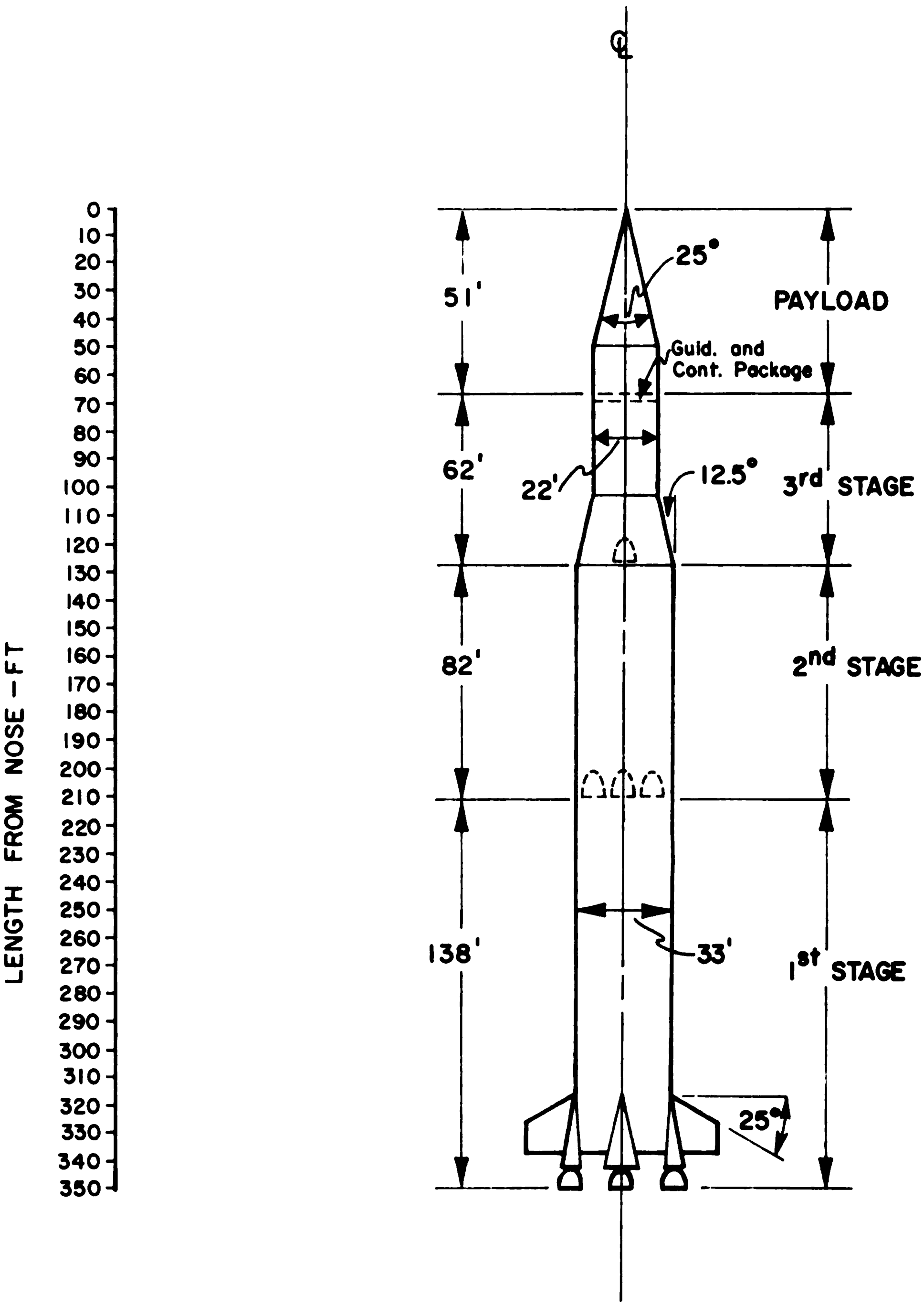

FIGURE C-1

VEHICLE CONFIGURATION

TABLE C-1

GENERAL VEHICLE PARAMETERS

SECTION	INITIAL WT/MASS	DRY WT/MASS	THRUST	MASS FLOW RATE
	LBS/SLUGS	LBS/SLUGS	LBS	SLUGS/SEC
PAYLOAD	200K/6.21K	200K/6.21K	--	--
3rd STAGE	260K/8.07K	29K/0.90K	260K	18
2nd STAGE	875K/27.20K	67K/2.08K	1300K	90
1st STAGE	4950K/153.6K	270K/8.39K	8700K	900

thrusting. The booster stages during their respective thrusting periods are divided into two cylinders -- one consisting of fuel and the other the remainder of the stage. As the fuel in each stage is used, it is assumed that the remaining mass of fuel occupies the aft end of the stage. Thus, in the computation of the c. g. 's of the vehicle over the first stage burning period, for example, the mass center of the complete vehicle except for the fuel of the first stage stays at a fixed location while the mass center of the first stage fuel moves toward the aft end of the vehicle. After burning 50% of the first stage fuel, the c. g. of the first stage fuel, as estimated from Figure C-1, is 295 feet from the nose. With this distance and with estimates of the distances to the c. g. 's of the other sections of the vehicle, the distance to the c. g. of the complete vehicle after 50% of the first stage fuel is burned using

$$\ell_g = \frac{\sum \text{MOMENTS}}{\sum \text{WEIGHTS}} \tag{C-1}$$

is

$$(\ell_{g1})_{50\%\,\text{FUEL}} = \frac{275\,(270K) + 295\,(2340K) + 164\,(875K) + 93\,(260K) + 58\,(103K) + 37.5\,(97K)}{3950K} \tag{C-2}$$

$$(\ell_{g1})_{50\%\ \text{FUEL}} = 239 \text{ ft} \tag{C-3}$$

(The third stage is assumed to be a right circular cylinder while the payload is separated into a right circular cone and a right circular cylinder.) In like manner, several c.g. locations for each stage were computed as a function of the percentage of fuel remaining and are given in Figure C-2.

The inertias were computed assuming each of the individual sections of the vehicle to be uniformly dense bodies of revolution. Referring to Figure C-3 the inertias of a right circular cylinder are

$$(I_{xx})_{CYL} = \frac{1}{12} m\,(3r^2 + 4\ell^2)$$

$$(I_{yy})_{CYL} = \frac{1}{12} m\,(3r^2 + \ell^2) \qquad \text{(C-4)}$$

$$(I_{zz})_{CYL} = \frac{1}{2} mr^2$$

and of a right circular cone are

$$(I_{xx})_{CONE} = \frac{3}{10} mr^2$$

$$(I_{yy})_{CONE} = \frac{3}{20} m\,(r^2 + 4h^2) \qquad \text{(C-5)}$$

$$(I_{zz})_{CONE} = \frac{3}{20} m\,(r^2 + \frac{1}{4}h^2)$$

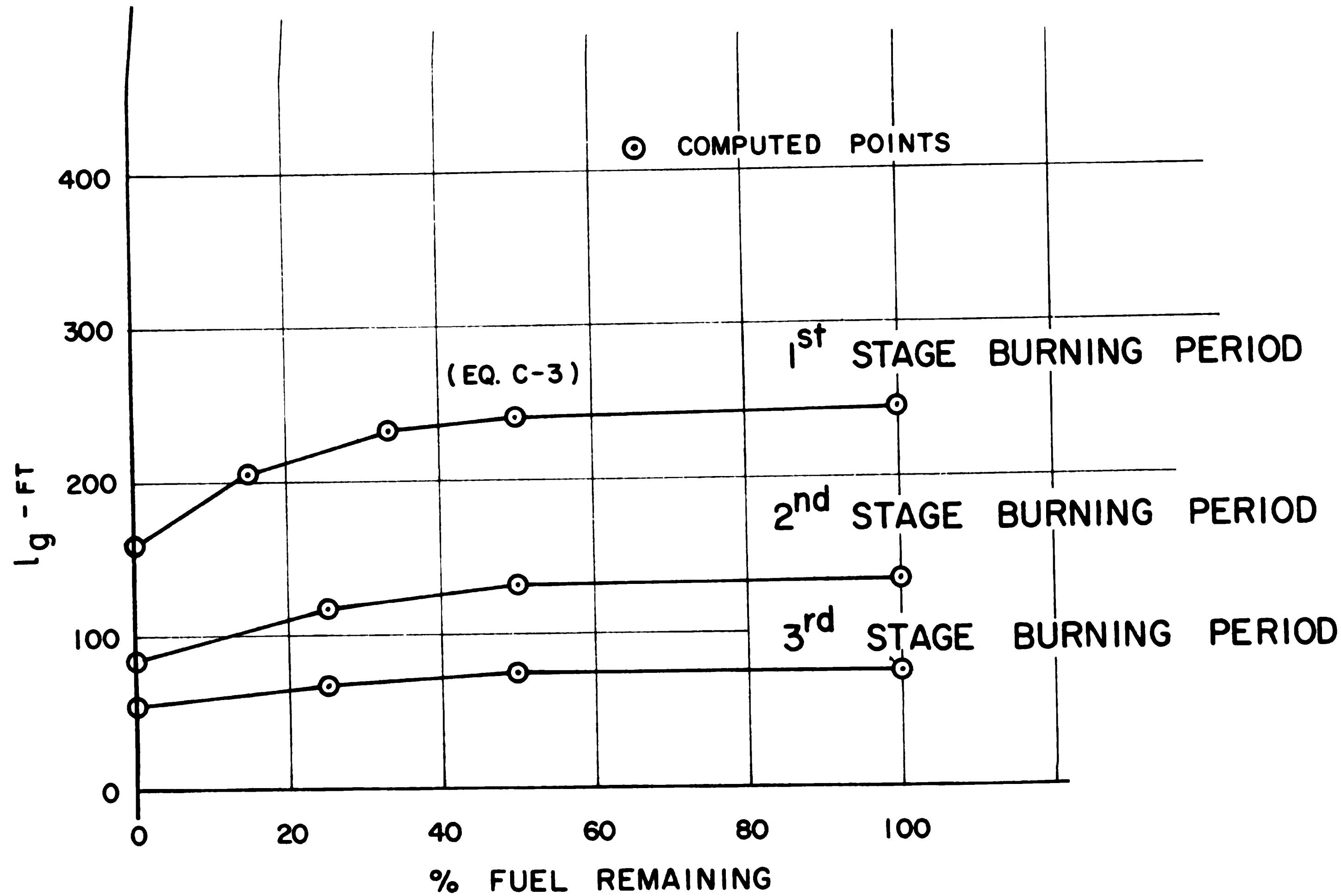

FIGURE C-2

VEHICLE CENTER OF GRAVITY LOCATION
(MEASURED FROM NOSE)

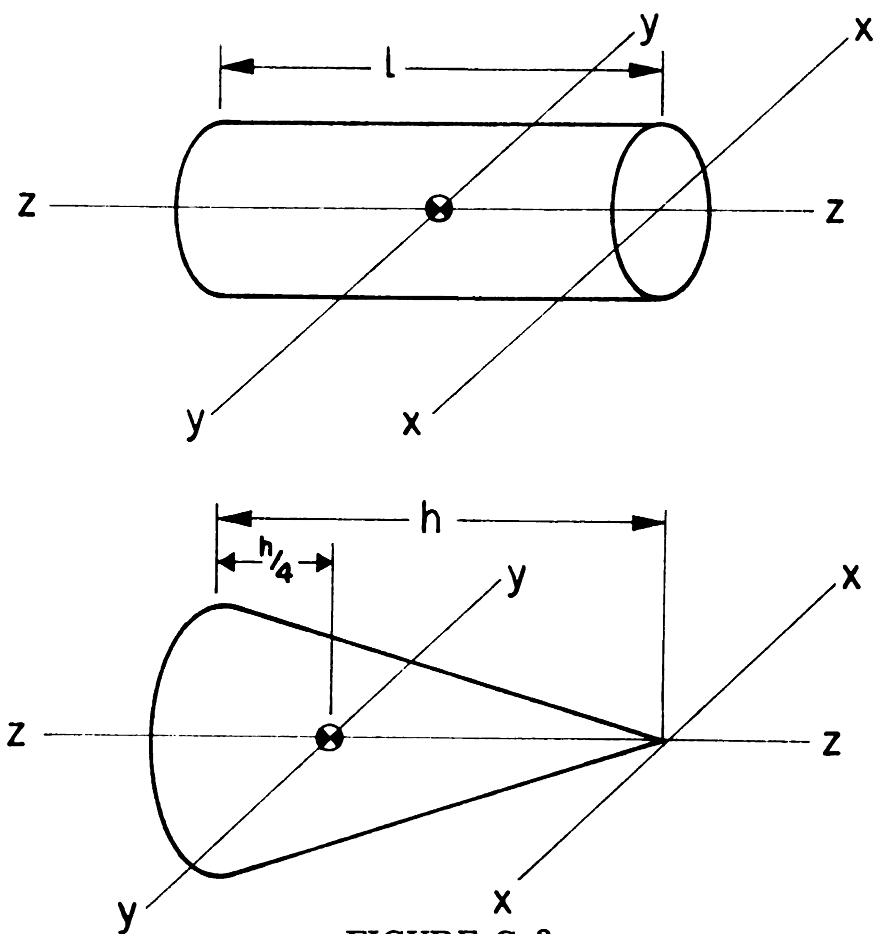

FIGURE C-3

VEHICLE BODIES OF REVOLUTION

The X_B axis inertias of each section of the vehicle were computed using Equations C-4 and C-5 and summed to give the total X_B inertia. These inertias were computed as functions of the fuel and stages remaining. The resultant X_B axis inertias are given in Figure C-4.

The Y_B and Z_B axis inertias of each section about their respective c. g.'s (they are equal) were computed and transfered to the base of the vehicle using the parallel-axis theorem,

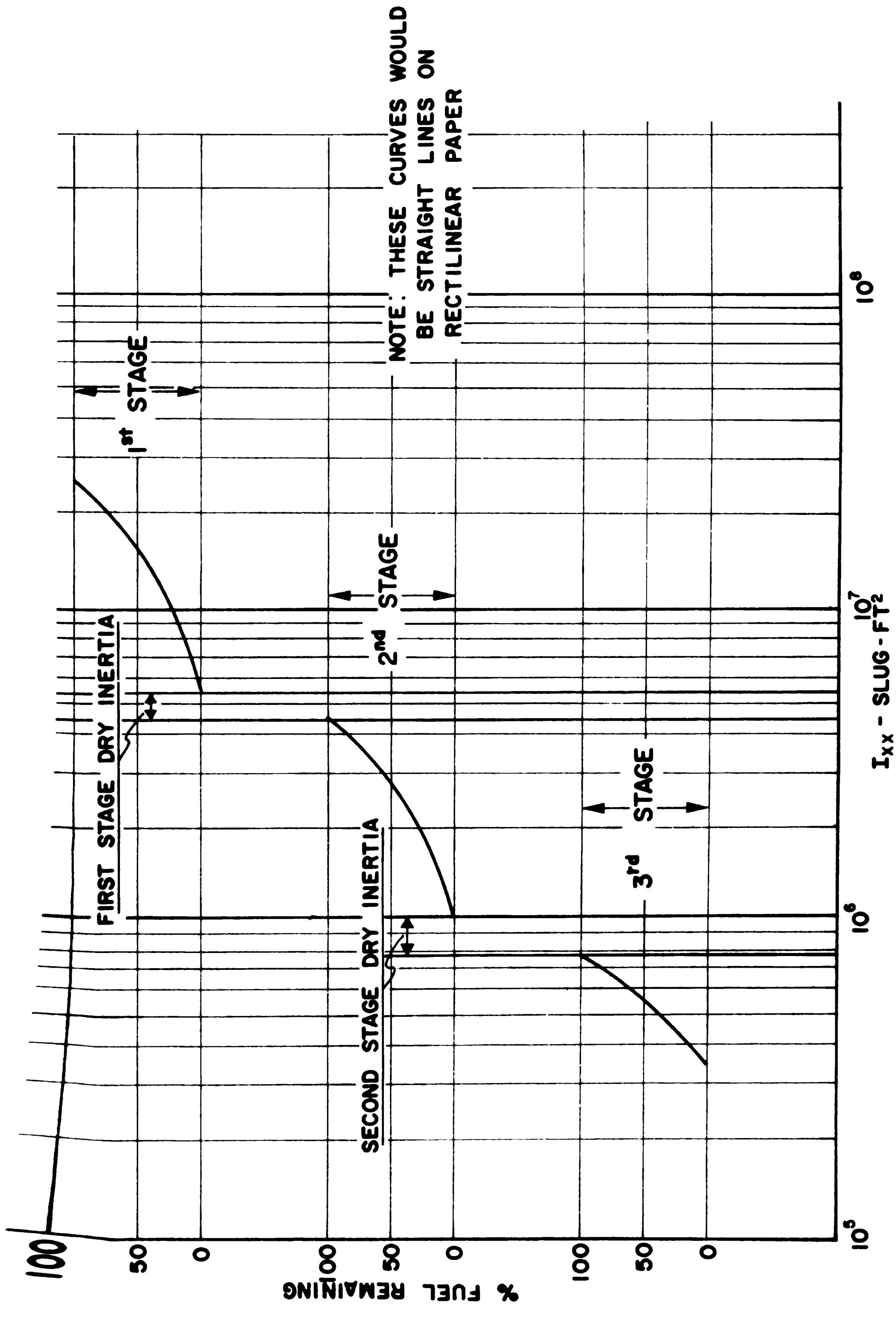

FIGURE C-4

X_B AXIS INERTIAS

$$I = \bar{I} + md^2 \tag{C-6}$$

The distance, d, is measured between the section c. g. and the vehicle base, I is the section inertia at the base around an axis which is parallel to Y_B (or Z_B), and $\bar{I}$ is the section inertia around an axis parallel to Y_B (or Z_B) which passes through the c. g. of the section. The inertias at the base were then summed and transferred back to the c. g. of the complete vehicle by a second use of Equation C-7 (solving for $\bar{I}$). Several sets of Y_B (or Z_B) axis inertias were computed as functions of the percentage of fuel remaining and the stages remaining. The Y_B and Z_B axis inertias are given in Figures C-5, C-6, and C-7.

To obtain accurate aerodynamic characteristics of a given vehicle, it is usually necessary to determine this data experimentally by using a wind tunnel and a scale model of the vehicle. Since this data is not available for the Saturn C-5, the aerodynamics were estimated using [1, pp. 5-9 to 5-26]. Slight alterations in the general data given in [1] were made to compensate for the differences of the selected vehicle.

The center of pressure (c. p.) distances were determined by first finding the location of the c. p. with the nose cone moved back and attached to the conical frustrum at the base of the 3rd stage and

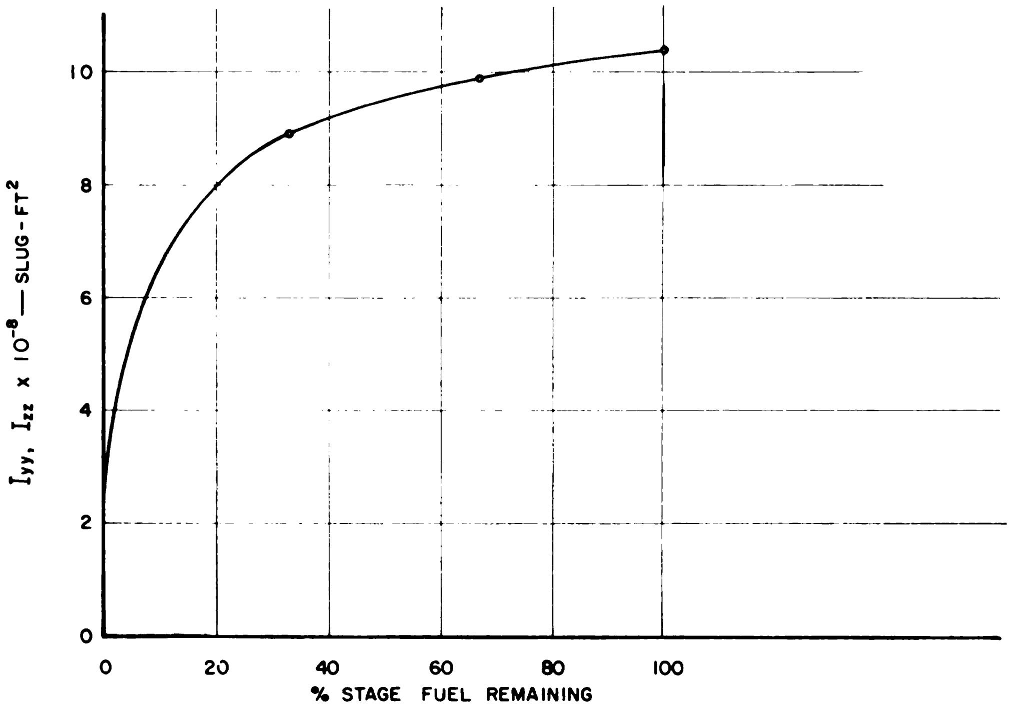

FIGURE C-5

Y_B AND Z_B AXIS INERTIAS - 1ST STAGE

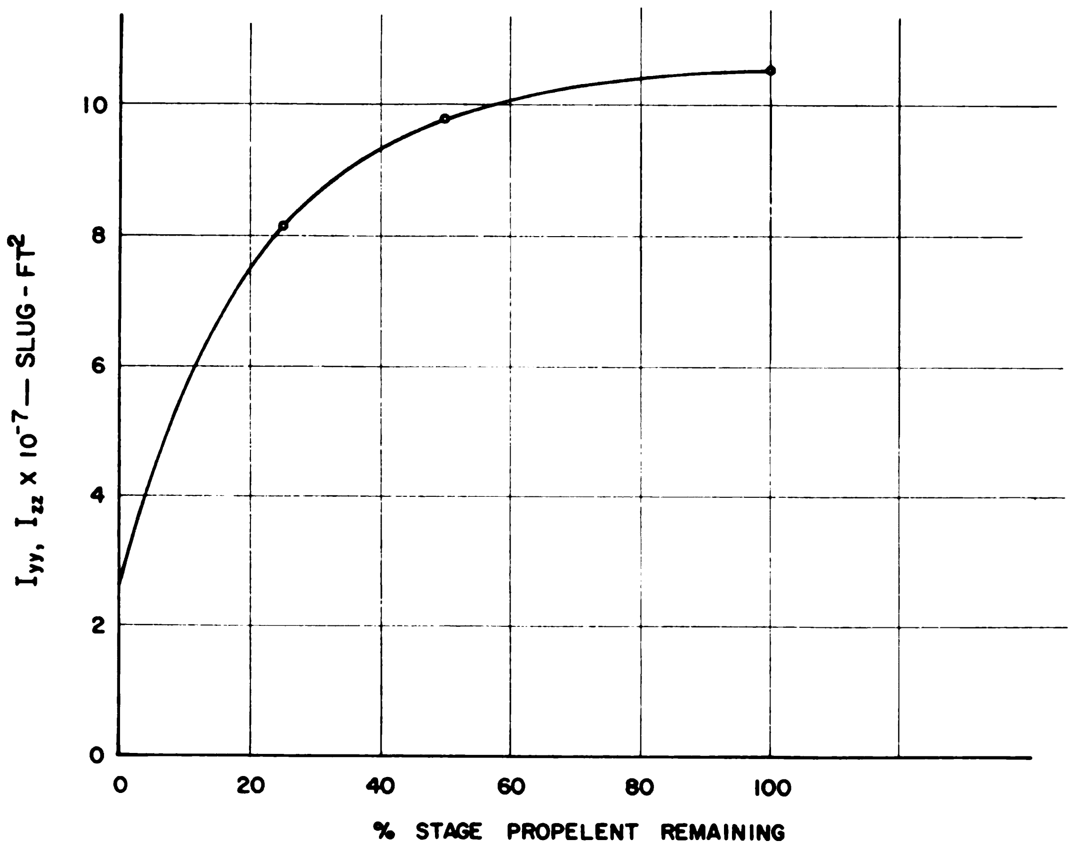

FIGURE C-6

Y_B AND Z_B AXIS INERTIAS - 2ND STAGE

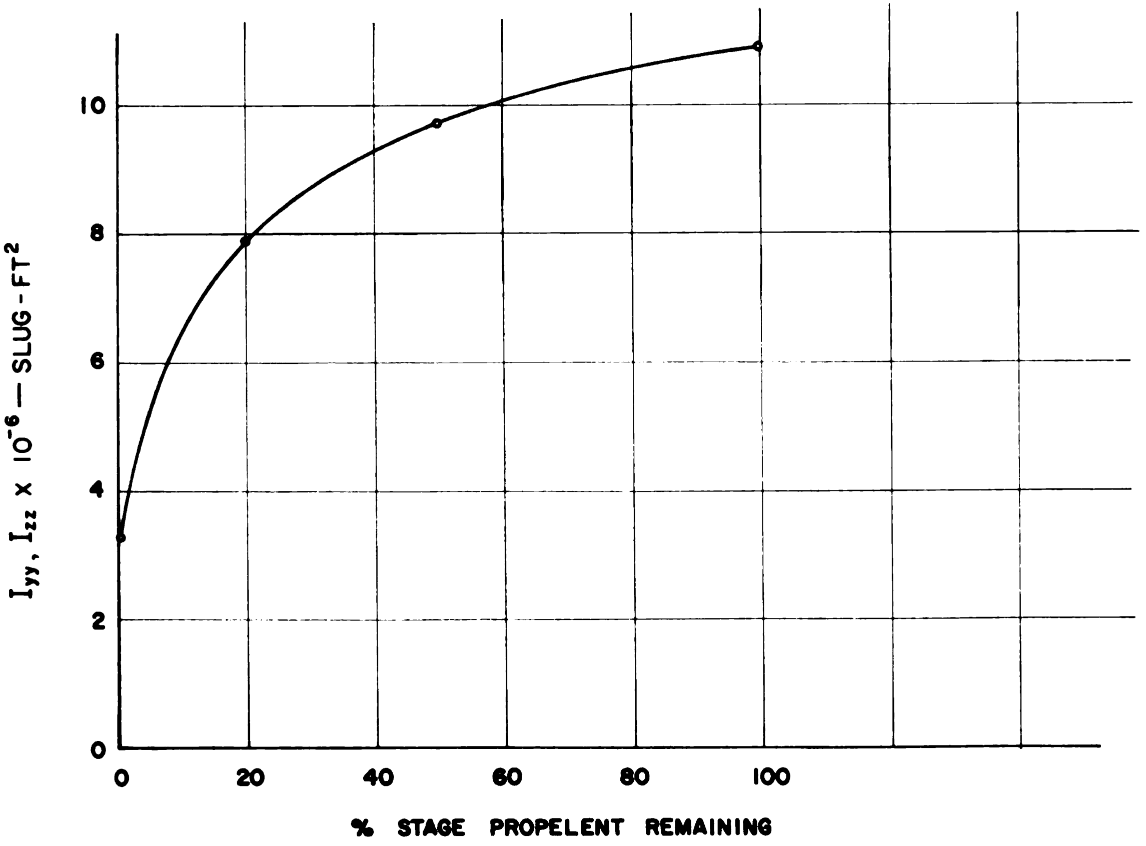

FIGURE C-7

Y_B AND Z_B AXIS INERTIAS - 3RD STAGE then by making a correction for the cylindrical section which was left out. The distance to the c. p. with the nose cone moved back was obtained from [1, Fig. 5. 10] using a body length-to-diameter ratio of 7 and a nose length-to-diameter ratio of 3. After correction for the cylindrical section which was left out, the c. p. distances become as shown in Figure C-8.

In like manner, the body lift coefficient, $C_{L_\eta} = \dfrac{\partial c_L}{\partial \eta}$, was obtained from [1, Fig. 5. 10] using a body length-to-diameter ratio of 7 and a nose length-to-diameter ratio of 3. The body lift coefficient is given in Figure C-9.

The zero-lift drag coefficient, C_{D_0}, was obtained using [1, Fig. 5. 18 and 5. 21]. The drag given in [1, Fig. 5. 18] for the nose section is based on the cross-sectional area of the forward sections of the vehicle. Upon multiplication of this coefficient by the ratio of the forward area $\left(\frac{\pi}{4} 22^2\right)$ to the desired reference area $\left(\frac{\pi}{4} 33^2\right)$ and summing with drag data from Figure 5. 21 for the conical frustrum, the total drag coefficient becomes as shown in Figure C-10.

The body drag due to lift coefficient, $\dfrac{\partial c_D}{\partial c_L^2}$, at supersonic speed was assumed to be the inverse of the lift coefficient. At subsonic speeds using [1, Eqs. 5. 28 and 5. 29] considering only the

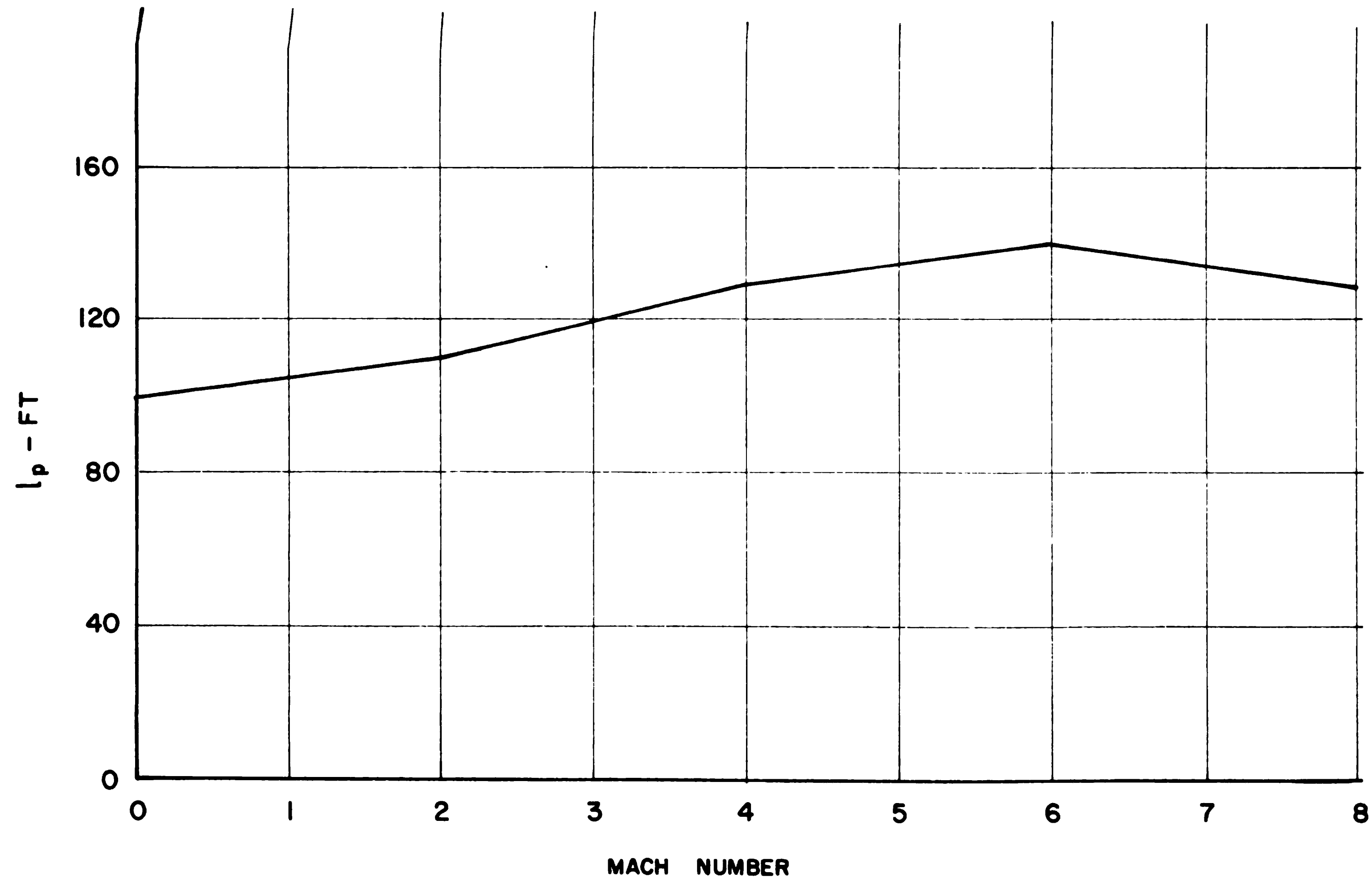

FIGURE C-8

DISTANCE FROM NOSE TO BODY CENTER OF PRESSURE

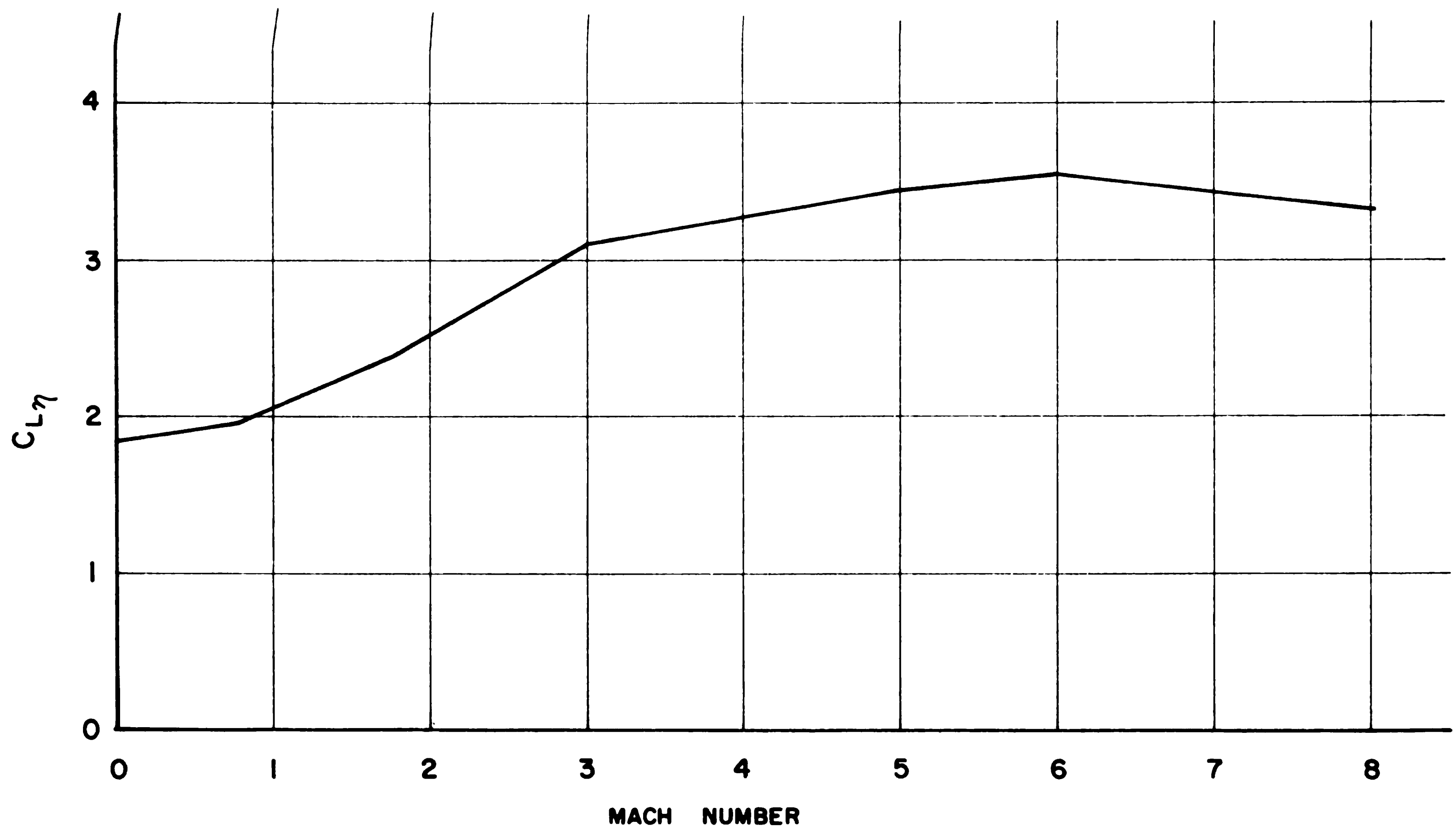

FIGURE C-9

BODY LIFT COEFFICIENT

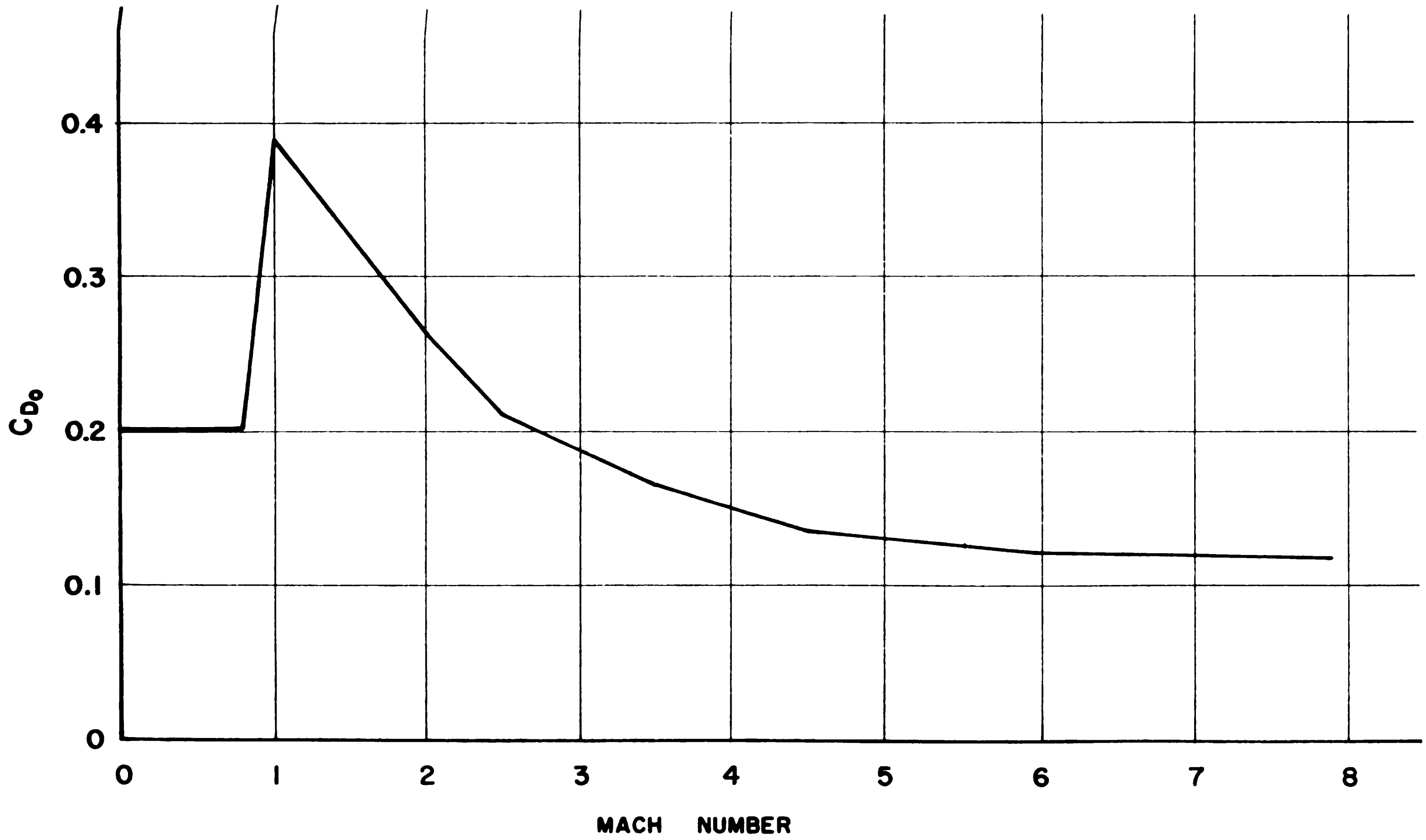

FIGURE C-10

BODY DRAG COEFFICIENT WITH $\alpha = \beta = 0$

first terms, the ratio of C_D to C_L^2 with $(k_2 - k_1) = 0.94$ is 0.266. The total body drag due to lift is given in Figure C-11.

The tail lift coefficient, $C_{Lt_\alpha} = \frac{\partial c_{Lt}}{\partial \alpha}$, at supersonic speeds was determined using [1, Fig. 5-11]. The ratio of the body diameter to the wind span is 0.5 which by extrapolation of the curves of [1, Fig. 5-11] yields a subsonic lift coefficient that is independent of Mach number. This is due to the large interference effects between the body and the tail. At subsonic speeds the interference effects are probably not as great but for the sake of simplicity and the lack of data it is assumed that this coefficient is the same as that for the supersonic case. The total tail lift coefficient referred to the body reference area is given in Figure C-12.

The tail zero-lift drag coefficient, C_{Dt_0}, was determined using [1, Eqs. 5.76 and 5.78, and Fig. 5.19]. The tail consists of a partial diamond cross-section wing (Figure C-13) and skirts. A wing thickness ratio of 6% and a sweep angle of 25° were chosen. The friction drag is assumed to be as given in [1, Fig. 5.19]. The transonic wave drag rise was calculated using [1, Eq. 5.76] and then partially reduced to account for the skirts since the transonic drag rise of the skirts is small. The supersonic wave drag of the tail was calculated using [1, Eq. 5.78] with $K = 3$ and then increased slightly in the low supersonic region to account for the

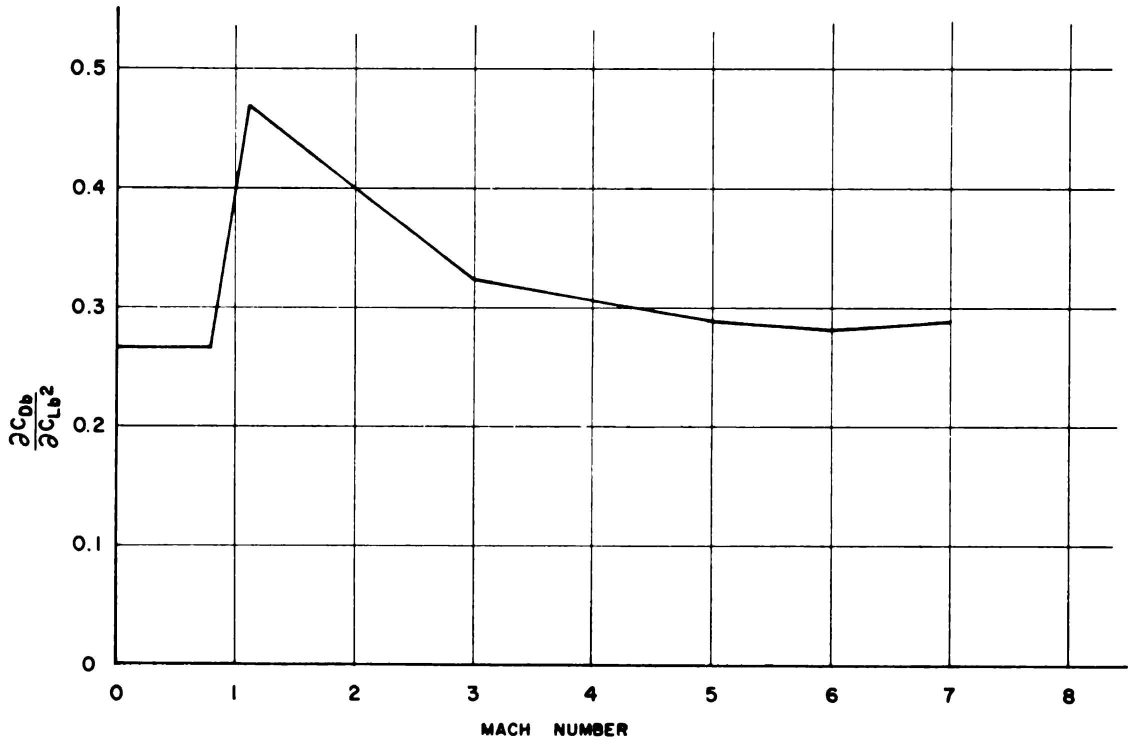

FIGURE C-11

BODY DRAG COEFFICIENT DUE TO LIFT

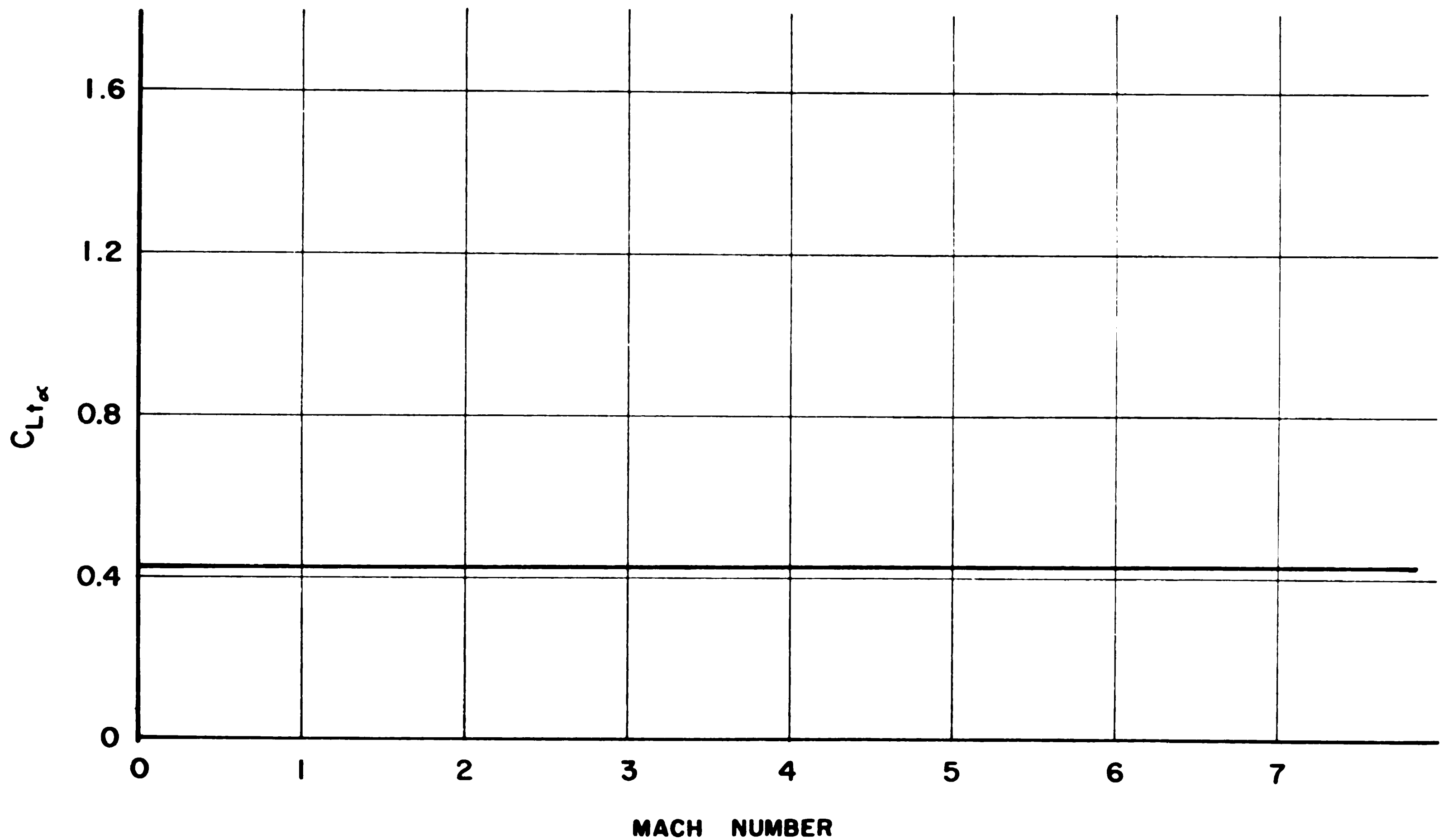

FIGURE C-12

TAIL LIFT COEFFICIENT

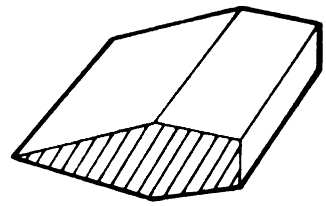

FIGURE C-13

WING CROSS-SECTION

effect of the skirts. The coefficient was then referred to the desired reference area by reducing the coefficient by the ratio of the tail area to the vehicle reference area. The results are given in Figure C-14.

The drag due to lift coefficient of the tail, $\frac{\partial_{Dt}}{\partial_{Lt}{}^{2}}$, was determined, as was the lift coefficient, using [1, Fig. 5.11]. At supersonic speeds the drag due to lift is very nearly $1/C_{Lt_{\alpha}}$. At subsonic speeds this is not true but for simplicity and for lack of data it is assumed that the drag due to lift is a constant as shown in Figure C-15.

The c.p. of the wing is at approximately 25% of the distance from the leading edge to the trailing edge subsonically and at approximately 50% of the chord length supersonically. Since the distance to the tail c.p. from the vehicle c.g. changes very little

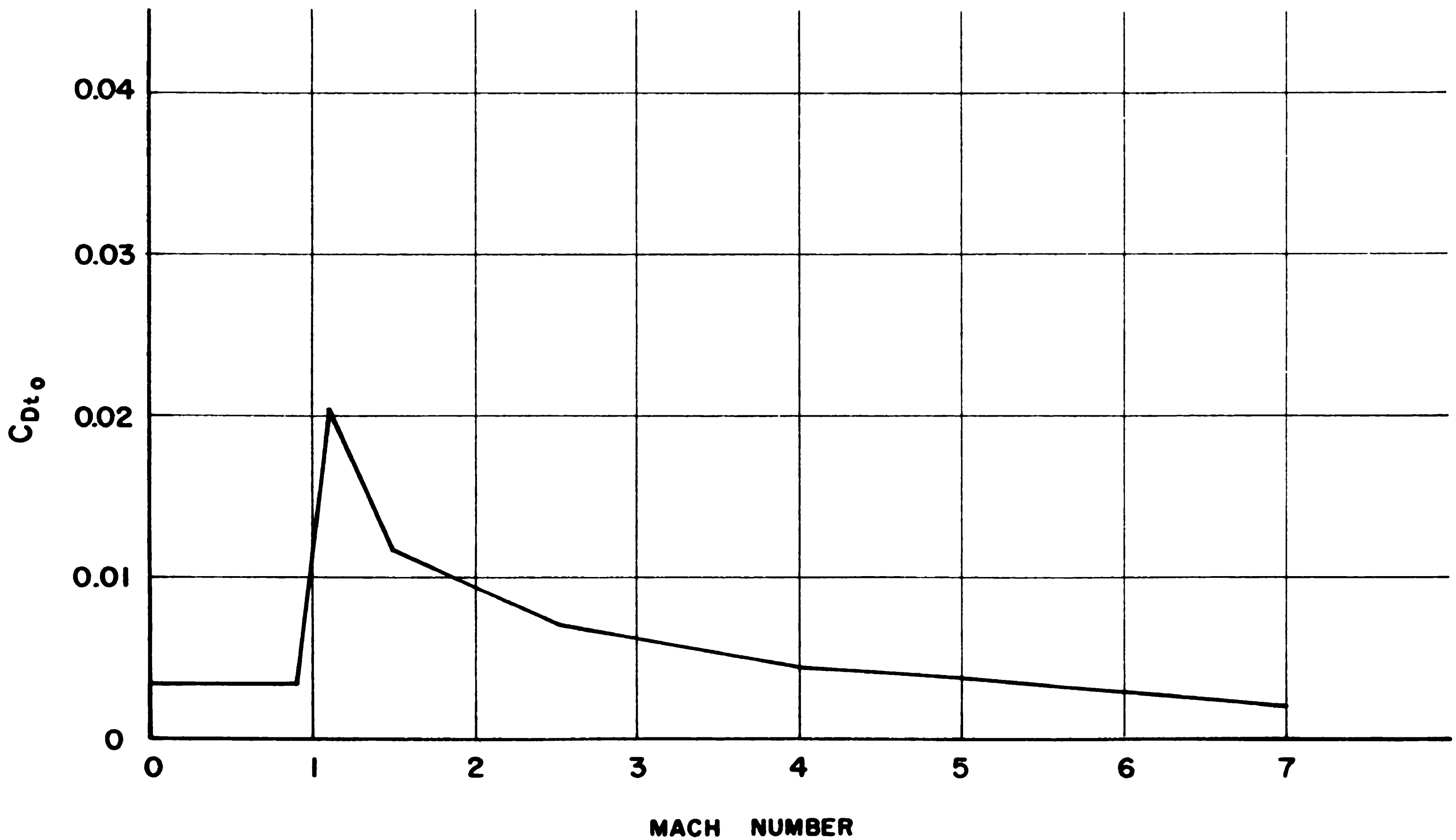

FIGURE C-14

TAIL DRAG COEFFICIENT

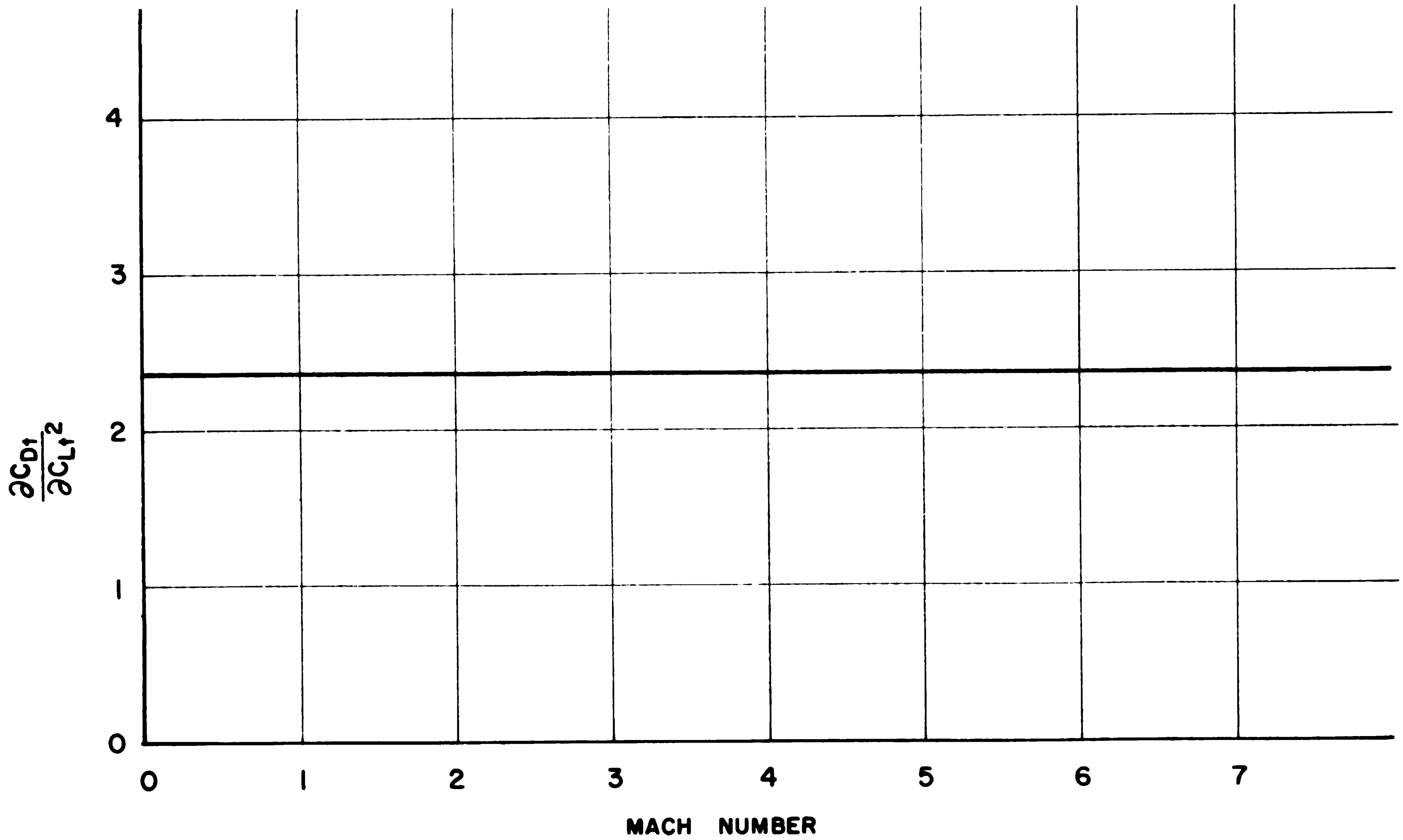

FIGURE C-15

TAIL DRAG COEFFICIENT DUE TO LIFT

with Mach number, it is assumed that the distance from the nose to the tail c.p. is constant at

$$\ell_t = 330 \text{ ft} \tag{C-7}$$

The spanwise location of the wing c.p. is at approximately 42% of the semispan for all Mach numbers yielding

$$r_t = 27 \text{ ft} \tag{C-8}$$

The aerodynamic damping is assumed to be contributed by the tail only (viscous effects on the vehicle body are ignored). Referring to Figure C-16 the angle of attack of the tail due to an

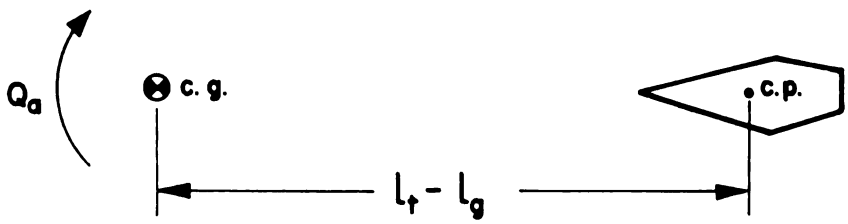

FIGURE C-16

TAIL DAMPING

angular rate of the vehicle is

$$\alpha_t = \frac{(\ell_t - \ell_g)\, Q_a}{V_a} \tag{C-9}$$

The moment due to this angle of attack is

$$M_q = -C_{L_{t\alpha}} \frac{(\ell_t - \ell_g)\, Q_a}{V_a} (\ell_t - \ell_g)\, qA \qquad \text{(C-10)}$$

In the standard non-dimensional aerodynamic derivative form the moment is

$$M_q = \frac{d}{2V_a} C_{m_q} Q_a\, (qAd) \qquad \text{(C-11)}$$

where

$$C_{m_q} = \frac{\partial C_m}{\partial q}$$

and thus

$$C_{m_q} = -\frac{2\,(\ell_t - \ell_g)^2}{d^2} C_{L_{t\alpha}} \qquad \text{(C-12)}$$

By substitution of parameters with an average distance between the c.g. and the tail of 120 ft

$$C_{m_q} = -\frac{2\,(120)^2}{(33)^2} (.43)$$

$$\text{(C-13)}$$

$$C_{m_q} = -11.4$$

and because of symmetry

$$C_{m_r} = -11.4 \tag{C-14}$$

In like manner,

$$C_{\ell_p} = -\frac{4r_t^2}{d^2} C_{Lt_\alpha} \tag{C-15}$$

which by substitution of parameters yields

$$C_{\ell_p} = -\frac{4(27)^2}{(33)^2}(.43)$$

(C-16)

$$C_{\ell_p} = -1.15$$

The reference area as previously defined, is the cross sectional area of the first stage of the vehicle as

$$A = \frac{\pi (33)^2}{4}$$

(C-17)

$$A = 855 \text{ ft}^2$$

The reference length as defined, is the first stage diameter

$$d = 33 \text{ ft} \tag{C-18}$$

The longitudinal distances to the engines are

$$\ell_{e1} = 340 \text{ ft} \tag{C-19}$$

$$\ell_{e2} = 200 \text{ ft} \tag{C-20}$$

$$\ell_{e3} = 115 \text{ ft} \tag{C-21}$$

and the radial distances are

$$r_{e1} = 15 \text{ ft} \tag{C-22}$$

$$r_{e2} = 11 \text{ ft} \tag{C-23}$$

APPENDIX D

TORQUE COMPENSATION SYSTEM ANALYSIS

Since torques are always present around the gimbal axes due to friction, motions of the vehicle, etc., the gyros on the stable element will precess, or rotate, from their initial positions. Since this is undesirable because of angular freedom restrictions, decoupling of the gyros, and cross-coupling effects between axes, it is necessary to have some kind of compensation for these torques to cause the gyros to remain in their respective orthogonal positions. For the A gyro, for example, the angle about the gyro output axis (ρ_A in Figure 4.3) could be measured and a torque could be supplied to the gimbal axis to drive the error angle back toward zero. This technique could be applied to each of the axes. The B and C gyros, however, share in the stabilization of the β and γ gimbals depending of the angle α, and thus, a coordinate transformation through α is needed. With proper resolution of the gyro error angles through the angle α, the two gyros can stabilize the two gimbals simultaneously and always be controlled (in steady-state) by the proper error signal. Figure D-1 shows a B and C gyro compensation system.

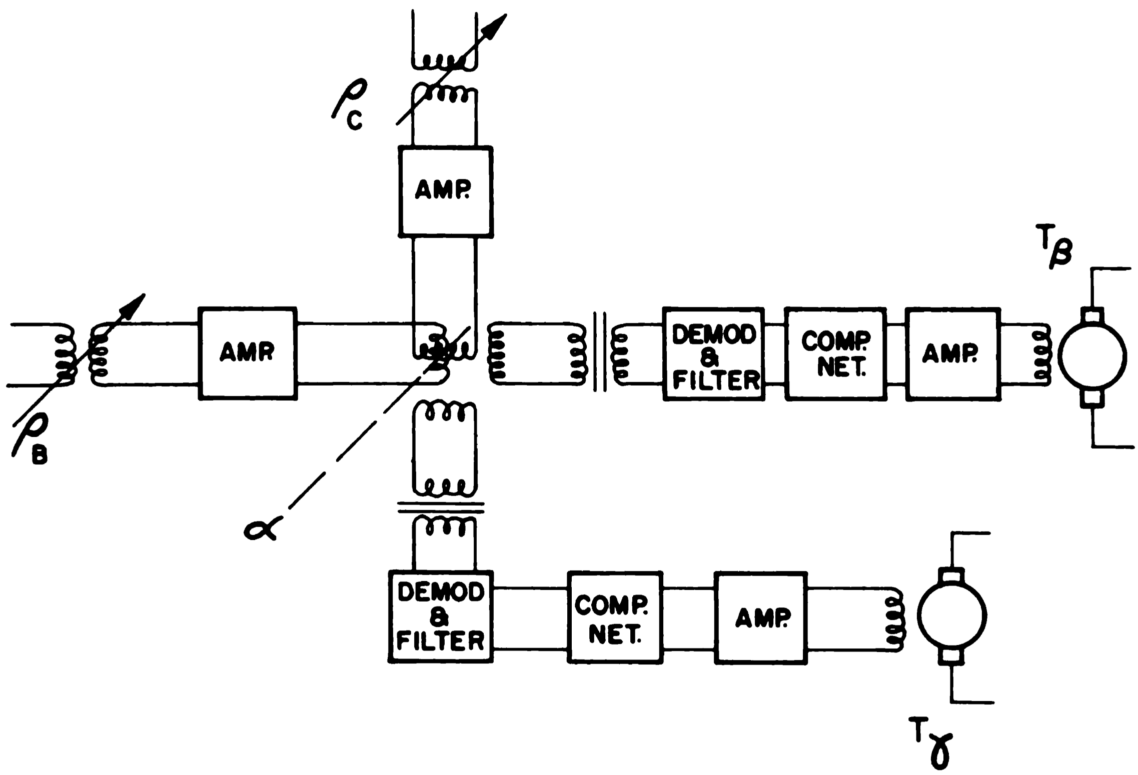

FIGURE D-1

TORQUE COMPENSATION SYSTEM WITH CODING

Upon simplification Figure D-1 reduces to Figure D-2 for the γ axis.

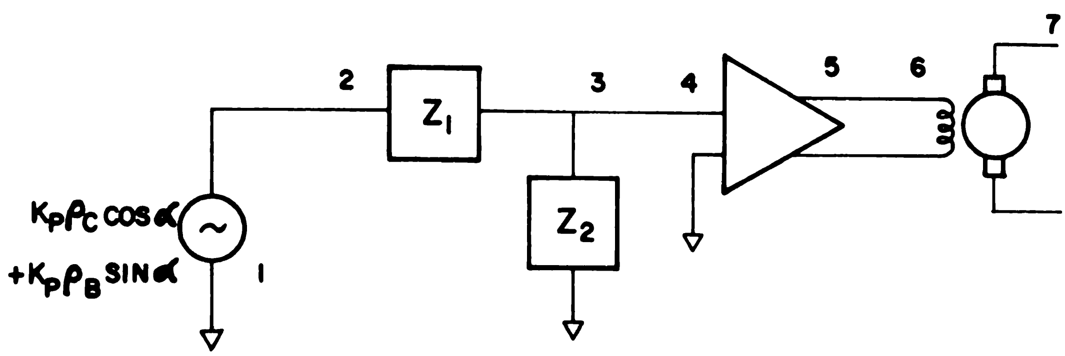

FIGURE D-2

SINGLE AXIS OF TORQUE COMPENSATION SYSTEM

The system graph including the gyro and the compensation system of the single axis is given in Figure D-3

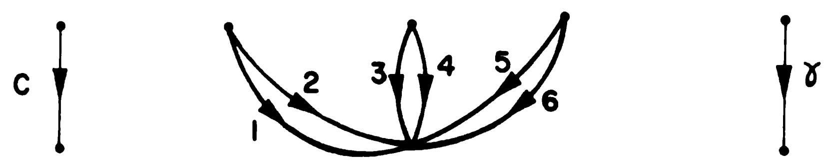

FIGURE D-3

GRAPH OF TORQUE COMPENSATION SYSTEM

where for the amplifier

$$\begin{bmatrix} v_4 \\ i_5 \end{bmatrix} = \begin{bmatrix} h_{44} & 0 \\ h_{54} & h_{55} \end{bmatrix} \begin{bmatrix} i_4 \\ v_5 \end{bmatrix} \tag{D-1}$$

and for the torquer (DC motor)

$$\begin{bmatrix} v_6 \\ T_7 \end{bmatrix} = \begin{bmatrix} R_{66} & K_{T7} \\ -K_{T7} & 0 \end{bmatrix} \begin{bmatrix} i_6 \\ \dot{\phi}_7 \end{bmatrix} \tag{D-2}$$

In cascaded form the amplifier equations are

$$\begin{bmatrix} i_4 \\ v_4 \end{bmatrix} = \begin{bmatrix} \frac{1}{h_{54}} & -\frac{h_{55}}{h_{54}} \\ \frac{h_{44}}{h_{54}} & -\frac{h_{44} h_{55}}{h_{54}} \end{bmatrix} \begin{bmatrix} i_5 \\ v_5 \end{bmatrix} \tag{D-3}$$

and the torquer equations are

$$\begin{bmatrix} i_6 \\ \\ v_6 \end{bmatrix} = \begin{bmatrix} -\dfrac{1}{K_{T7}} & 0 \\ \\ -\dfrac{R_{66}}{K_{T7}} & K_{T7} \end{bmatrix} \begin{bmatrix} T_7 \\ \\ \dot{\phi}_7 \end{bmatrix} \tag{D-4}$$

With a compensation network and terminal graph as shown

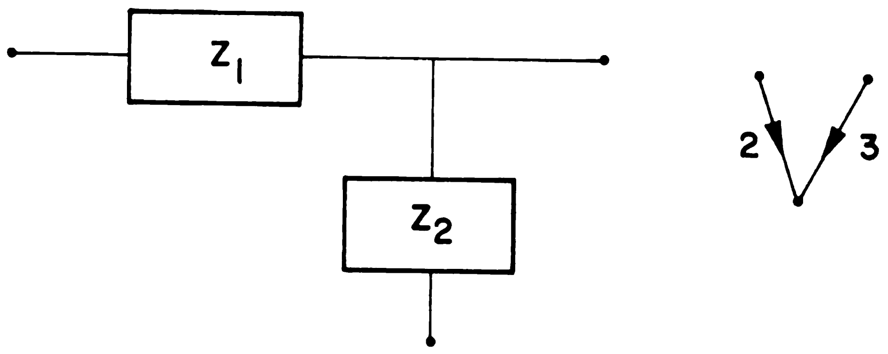

FIGURE D-4

COMPENSATION NETWORK

in Figure D-4, the network terminal equations are

$$\begin{bmatrix} i_2 \\ \\ v_2 \end{bmatrix} = \begin{bmatrix} 1 + \dfrac{1}{Z_1} + \dfrac{1}{Z_2} & -\dfrac{1}{Z_2} \\ \\ -Z_1 & 1 + \dfrac{Z_1}{Z_2} \end{bmatrix} \begin{bmatrix} i_3 \\ \\ v_3 \end{bmatrix} \tag{D-5}$$

From Figure D-3 using circuit and cutset equations

$$
\begin{aligned}
i_3 &= -i_4 \\
v_3 &= -v_4 \\
i_5 &= -i_6 \\
v_5 &= v_6 \\
v_1 &= v_2
\end{aligned}
\tag{D-6}
$$

Combining Equations D-3, D-4, D-5, and D-6 with

$$v_1 = -K_P \rho_C \tag{D-7}$$

the expressions for the compensation system become

$$\rho_C = -\frac{T_7}{Z_C K_C} + \frac{K_D \dot{\phi}_7}{Z_C K_C} \tag{D-8}$$

and

$$T_7 = -Z_C K_C \rho_C + K_D \dot{\phi}_7 \tag{D-9}$$

where

$$Z_C = \frac{1}{Z_1/h_{44} + 1 + Z_1/Z_2}$$

$$K_C = \frac{K_P h_{54} K_{T7}}{h_{44}(1 + h_{55} R_{66})} \tag{D-10}$$

$$K_D = h_{55} (K_{T7})^2$$

Application of Equations 4.24, with $K_\rho = 0$, to the C gyro and the outer gimbal yields gyro terminal equations of

$$\begin{bmatrix} T_c \\ \\ T_\gamma \end{bmatrix} = \begin{bmatrix} J_c \frac{d}{dt} + D_c & H \\ \\ -H & J_\gamma \frac{d}{dt} + D_\gamma \end{bmatrix} \begin{bmatrix} \dot{\rho}_c \\ \\ \dot{\gamma} \end{bmatrix} \qquad \text{(D-11)}$$

which when coupled with the torque compensation system has a system graph as shown in Figure D-5.

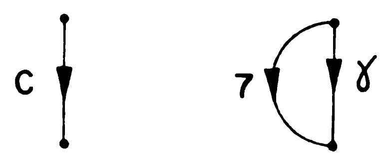

FIGURE D-5

GRAPH OF GYRO AND TORQUE COMPENSATION SYSTEM

Use of the branch formulation with drivers as shown in Figure D-6

FIGURE D-6

GRAPH OF GYRO AND TORQUE COMPENSATION SYSTEM WITH DRIVERS yields

$$\begin{bmatrix} T_{D_1}(s) \\ \\ T_{D_2}(s) \end{bmatrix} = - \begin{bmatrix} J_\gamma s + D_\gamma + K_D & -(H + K_C Z_C(s)/s) \\ \\ H & J_C s + D_C \end{bmatrix} \begin{bmatrix} \dot{\phi}_{D_1}(s) \\ \\ \dot{\phi}_{D_2}(s) \end{bmatrix}$$

(D-12)

Assuming there are no net torques acting on the C gyro output axis

$$T_{D_2}(s) = 0 \qquad \text{(D-13)}$$

and

$$\dot{\phi}_{D_1}(s) = -\frac{J_C s + D_C}{H} \dot{\phi}_{D_2}(s) \qquad \text{(D-14)}$$

Since

$$\dot{\phi}_C(s) = \dot{\phi}_{D_2}(s) \qquad \text{(D-15)}$$

and assuming K_D to be part of D_γ, the solution of Equations D-12 yields

$$\frac{\rho_C(s)}{T_{D_1}(s)} = \frac{H}{s(J_\gamma s + D_\gamma)(J_C s + D_C) + H^2 + H K_C Z_C(s)} \qquad \text{(D-16)}$$

where $Z_C(s)$ must be of the form

$$Z_c(s) = \frac{(\tau_1 s+1)(\tau_2 s+1)\cdots}{(\tau_a s+1)(\tau_b s+1)\cdots} \tag{D-17}$$

The steady-state error of the compensated gyro, from Equation D-16, is

$$\phi_{c_{ss}} = \frac{T_{D_{ss}}}{K_c} \tag{D-18}$$

Because of drift caused by geometric considerations, and mechanical limitations, etc., it is desired to have a maximum steady-state error of less than 1.0 degree. Thus, for a maximum bearing friction and geometric torque input of

$$T_{D_{1ss}} = 200,000 \text{ dyne-cm} \tag{D-19}$$

the compensation gain must be

$$K_c = \frac{200,000}{1/57.3} \tag{D-20}$$

$$K_c = 11.5 \times 10^6 \text{ dyne-cm/rad}$$

Without a compensating network where

$$Z_c(s) = 1 \tag{D-21}$$

the rearranged loop transfer function becomes

$$\frac{\rho_c(s)}{T_{D_1}(s)} = \frac{H/J_\gamma J_c}{s^3 + \left(\dfrac{D_\gamma}{J_\gamma} + \dfrac{D_c}{J_c}\right)s^2 + \left(\dfrac{D_\gamma D_c + H^2}{J_\gamma J_c}\right)s + \dfrac{HK_c}{J_\gamma J_c}} \tag{D-22}$$

Upon application of the Routh criterion (Table D-1) it turns out

TABLE D-1

ROUTH ARRAY

s^3	1	$\dfrac{D_\gamma D_c + H^2}{J_\gamma J_c}$
s^2	$\dfrac{D_\gamma}{J_\gamma} + \dfrac{D_c}{J_c}$	$\dfrac{H\ K_c}{J_\gamma J_c}$
s^1	$\left(\dfrac{D_\gamma}{J_\gamma} + \dfrac{D_c}{J_c}\right)\left(\dfrac{D_\gamma D_c + H^2}{J_\gamma J_c}\right) - \left(\dfrac{H\ K_c}{J_\gamma J_c}\right)$	
s^0	$\left[\left(\dfrac{D_\gamma}{J_\gamma} + \dfrac{D_c}{J_c}\right)\left(\dfrac{D_\gamma D_c + H^2}{J_\gamma J_c}\right) - \left(\dfrac{H\ K_c}{J_\gamma J_c}\right)\right]\dfrac{H\ K_c}{J_\gamma J_c}$	

that the single requirement for stability, since all the parameters are positive, is that

$$\left(\frac{D_\gamma}{J_\gamma} + \frac{D_c}{J_c}\right)\left(\frac{D_\gamma D_c + H^2}{J_\gamma J_c}\right) > \left(\frac{H\ K_c}{J_\gamma J_c}\right) \tag{D-23}$$

The nominal parameters for a typical platform with ball-bearing gyros are

$$\begin{aligned} H &= 6 \times 10^6 \text{ gm-cm}^2/\text{sec} \\ J_\gamma &= 340,000 \text{ gm-cm}^2 \\ D_\gamma &= 500,000 \text{ gm-cm}^2/\text{sec} \\ J_c &= 3,000 \text{ gm-cm}^2 \\ D_c &= 3,000 \text{ gm-cm}^2/\text{sec} \end{aligned} \tag{D-24}$$

By consideration of the relative magnitude of the terms in Equation D-23 using these parameters it is seen that

$$H^2 >> D_\gamma D_c \tag{D-25}$$

and therefore, the stability requirement reduces to

$$\left(\frac{D_\gamma}{J_\gamma} + \frac{D_c}{J_c}\right) H > K_c \tag{D-26}$$

By substitution of parameters

$$\begin{gathered}(1.47 + 1)\ 6 \times 10^6 > 11.5 \times 10^6 \\ 14.8 > 11.5\end{gathered} \tag{D-27}$$

and thus the system is stable.

The relative magnitudes of the terms in the loop transfer function are such that the equation can be factored in general terms. This equation is

$$\frac{\rho_c(s)}{T_{D_1}(s)} = \frac{H/J_\gamma J_c}{\left(s + \frac{K_c}{H}\right)\left[s^2 + \left(\frac{D_\gamma}{J_\gamma} + \frac{D_c}{J_c} - \frac{K_c}{H}\right) s + \frac{H^2}{J_\gamma J_c}\right]} \qquad \text{(D-28)}$$

The damping term of the second order part of the characteristic equation shows that the same requirement exists here as stated by the Routh criterion: namely, that for the system to be positively damped

$$\left(\frac{D_\gamma}{J_\gamma} + \frac{D_c}{J_c}\right) > \frac{K_c}{H} \qquad \text{(D-29)}$$

Upon substitution of parameters the closed-loop transfer function of the system without a compensation network becomes

$$\frac{\dot{\rho}_c(s)}{T_{D_1}(s)} = \frac{67,600}{(s + 1.92)(s^2 + 0.55\, s + 35,300)} \qquad \text{(D-30)}$$

Figure D-7 shows the closed-loop frequency response of the system with the value of K_c equal to that value necessary to limit the

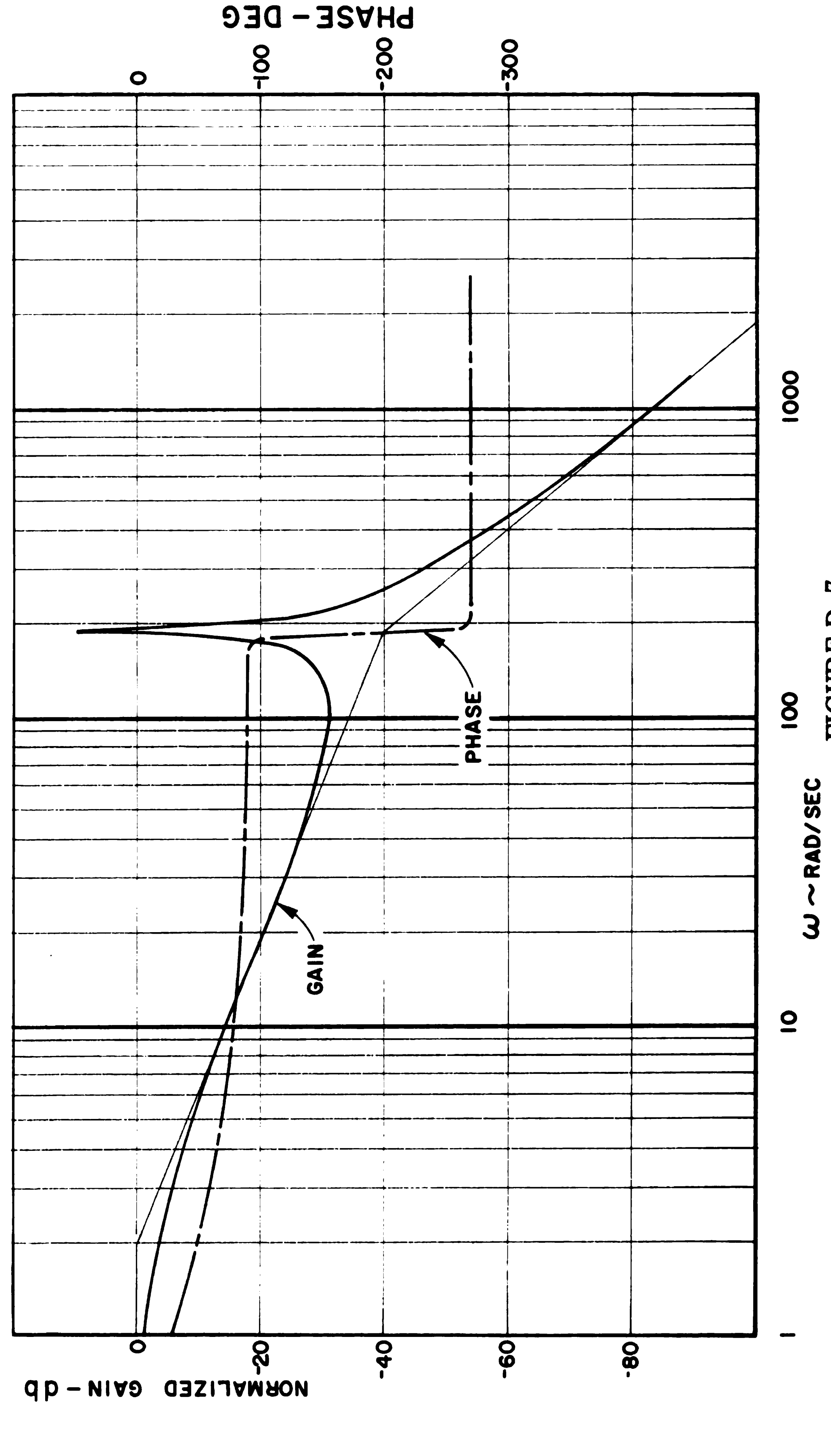

FIGURE D-7

GYRO FREQUENCY RESPONSE, K_C = 11.5 x 10^6 DYNE-CM/RAD, WITHOUT COMPENSATION NETWORK maximum steady-state gyro error angle to 1.0 degree. It shows a low bandwidth and extreme sensitivity to frequency inputs around 188 rad/sec. The low bandwidth is good but the high frequency sensitivity (to noise, for instance) is objectionable.

With a compensation network it is hoped to reduce this high frequency sensitivity. In addition, since the values of D_γ and D_c are not accurate and change depending on the platform environment, etc., it is necessary to have more damping than is provided by the axis frictions. Thus, for damping also, it is desired to have a compensation network.

The open-loop terminal equations for the system can be obtained by opening the loop at the pickoff as shown in Figure D-8.

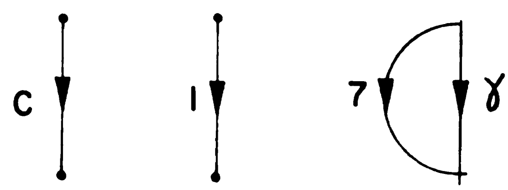

FIGURE D-8

OPEN LOOP TERMINAL GRAPH

Using the branch system of equations with drivers as shown in

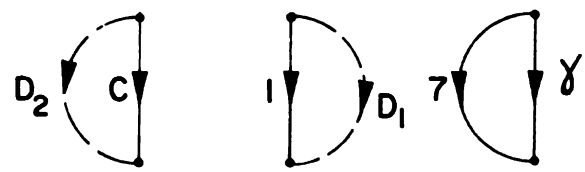

FIGURE D-9

OPEN LOOP TERMINAL GRAPH WITH DRIVERS

Figure D-9 the cutset equations are

$$\begin{array}{c} \\ D_1 \\ D_2 \\ \gamma \end{array} \begin{array}{c} \begin{array}{cccccc} D_1 & D_2 & \gamma & C & 1 & 7 \end{array} \\ \begin{bmatrix} 1 & 0 & 0 & 0 & 1 & 0 \\ 0 & 1 & 0 & 1 & 0 & 0 \\ 0 & 0 & 1 & 0 & 0 & 1 \end{bmatrix} \end{array} \begin{bmatrix} i_{D_1} \\ T_{D_2} \\ T_\gamma \\ T_C \\ i_1 \\ T_7 \end{bmatrix} = 0 \qquad \text{(D-31)}$$

the terminal equations are

$$\begin{bmatrix} T_\gamma \\ T_C \\ i_1 \\ T_7 \end{bmatrix} = \begin{bmatrix} J_\gamma s + D_\gamma & -H & 0 & 0 \\ H & J_C s + D_C & 0 & 0 \\ 0 & 0 & g_1 & 0 \\ 0 & 0 & \dfrac{Z_C K_C}{K_P} & K_D \end{bmatrix} \begin{bmatrix} \dot{\phi}_\gamma \\ \dot{\phi}_C \\ v_1 \\ \dot{\phi}_7 \end{bmatrix} \qquad \text{(D-32)}$$

and

$$\begin{bmatrix} 1 & 0 \\ 0 & 1 \\ 0 & 0 \end{bmatrix} \begin{bmatrix} i_{D_1} \\ T_{D_2} \end{bmatrix} = - \begin{bmatrix} g_1 & 0 & 0 \\ 0 & J_C s + D_C & H \\ \dfrac{Z_C K_C}{K_P} & -H & J_\gamma s + D_\gamma + K_D \end{bmatrix} \begin{bmatrix} v_{D_1} \\ \dot{\phi}_{D_2} \\ \dot{\phi}_\gamma \end{bmatrix} \qquad \text{(D-33)}$$

Using

$$v_{D_1} = K_P \ \dot{\phi}_{D_1}(s)/s \qquad \text{(D-34)}$$

and solving the last equation of Equations D-33 as

$$v_{D_1}(s) = \frac{K_P}{Z_C(s) K_C} \left[- (J_\gamma s + D_\gamma + K_D) \dot{\phi}_\gamma(s) + H \dot{\phi}_{D_2}(s) \right] \qquad \text{(D-35)}$$

and the second equation with no load ($T_{D_2} = 0$), as

$$\dot{\gamma}(s) = -\left(\frac{J_C \ s + D_C}{H} \right) \dot{\phi}_{D_2}(s) \qquad \text{(D-36)}$$

the solution of Equations D-33 becomes

$$\frac{\dot{\phi}_{D_2}(s)}{\dot{\phi}_{D_1}(s)} = \frac{(H/J_\gamma J_C) \ Z_C(s) \ K_C}{s \left[s^2 + \left(\dfrac{D_\gamma}{J_\gamma} + \dfrac{D_C}{J_C} \right) s + \dfrac{H^2}{J_\gamma J_C} \right]} \qquad \text{(D-37)}$$

Using parameters as given in Equations D-20 and D-24

$$\frac{\dot{\phi}_{D_2}(s)}{\dot{\phi}_{D_1}(s)} = \frac{67,600\ Z_C(s)}{s\,(s^2 + 2.47\ s + 35,300)} \tag{D-38}$$

With a compensation network of

$$Z_C(s) = \frac{(5.3)^2}{(s + 5.3)^2} \tag{D-39}$$

adequate stability as shown in Figure D-10 is obtained. The phase margin is more than 50 degrees and the gain margin is 13 db.

The normalized closed-loop transfer function is

$$\frac{K_C\ \phi_{C_1}(s)}{T_{D_1}(s)} = \frac{(s+5.3)^2\ 67,600}{s\,(s^2 + 2.47\ s + 35,300)(s + 5.3)^2 + 1,900,000} \tag{D-40}$$

$$= \frac{(s+5.3)^2\ 67,600}{(s+7.9)(s^2 + 1.35\ s + 6.82)(s^2 + 1.24\ s + 35,200)} \tag{D-41}$$

A frequency response plot of this equation is shown in Figure D-11. The high frequency sensitivity is down 8 db from that of the system without compensation. This is within acceptable limits and the system preliminary design is completed.

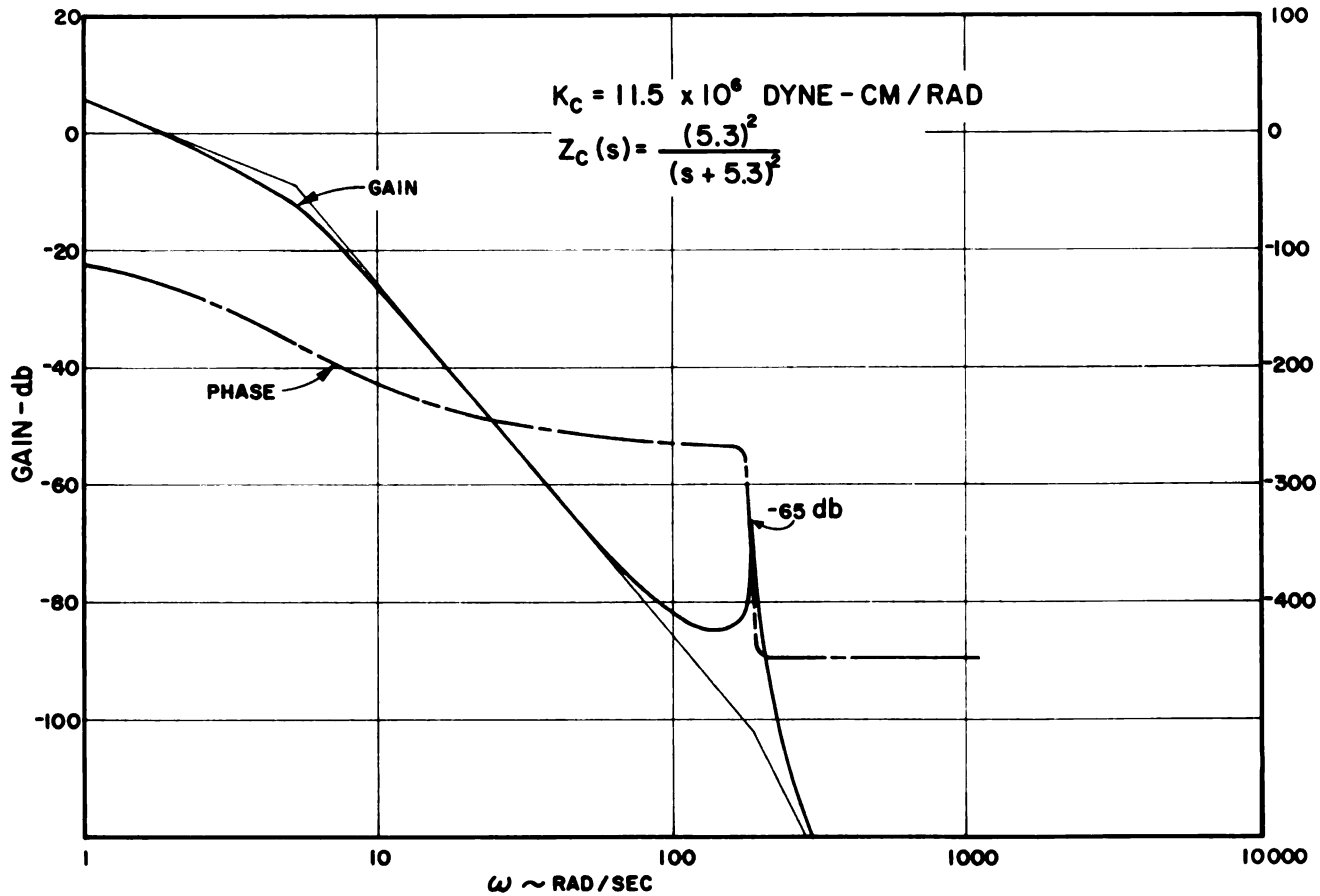

FIGURE D-10

GYRO OPEN LOOP FREQUENCY RESPONSE, $K_C = 11.5 \times 10^6$ DYNE-CM/RAD, $Z_C(s) = (5.3)^2/(s+5.3)^2$

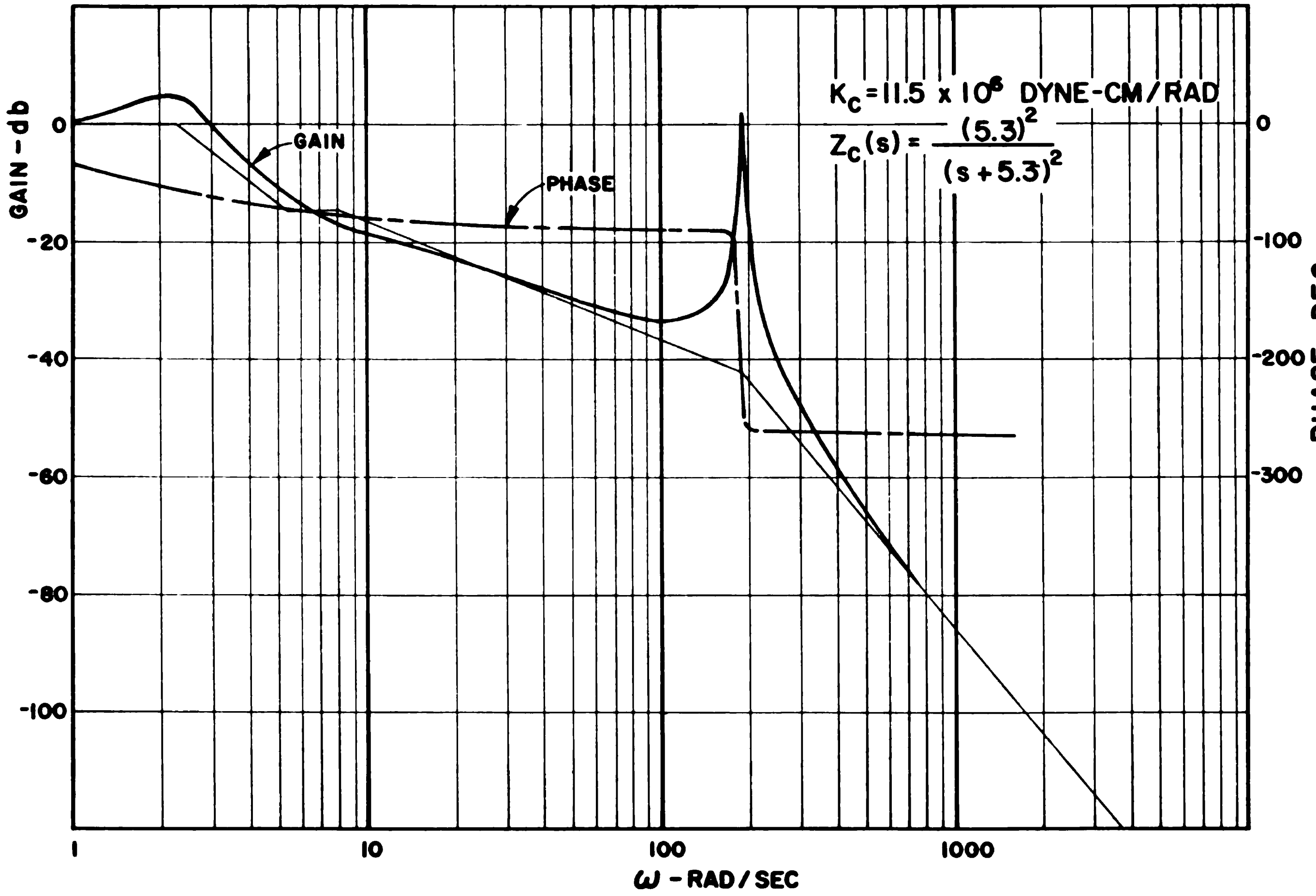

FIGURE D-11

GYRO FREQUENCY RESPONSE, K_C = 11.5 x 10^6 DYNE-CM/RAD, Z_C (s) = 5.3^2 /(s + 5.3$)^2$

LIST OF REFERENCES

1. Koelle, H. H.: Handbook of Astronautical Engineering. McGraw-Hill Book Company, Inc., 1961.

2. Allen, C. W.: Astrophysical Quantities. The Athlone Press, University of London, 1963.

3. Arnold, R. N., Maunder, L.: Gyrodynamics and Its Engineering Application. Academic Press, 1961.

4. Minzer, R. A., Champion, Pond, The ARDC Model Atmosphere. AFCRC TR-59-267, 1959.

5. Pitman, G. R.: Inertial Guidance. John Wiley and Sons, Inc., 1962.

6. Astronautics, February, 1962 issue, "The Saturn Program." ARS publication.

7. Page, L.: Introduction to Theoretical Physics. D. Van Nostrand Company, 1952.

8. Astronautics, March, 1963 issue, AIAA Publication.

LIST OF SYMBOLS

SYMBOL	DEFINITION	UNITS
A	Vehicle reference area	ft^2
A	Center of A-frame	---
A	Acceleration indicated by accelerometer	ft/sec
A	Area	ft^2
a, b	Coefficient matrix elements as defined by subscript	as used
a	Speed of sound	ft/sec
B	Center of B-frame	---
C	Non-dimensional coefficient as defined by subscript	---
C_F	Non-dimensional force coefficient	---
C_M	Non-dimensional moment coefficient	---
D	Driver	as used
D	Coefficient of viscous friction	dyne-cm-sec
d	Vehicle reference length (maximum diameter)	ft
d	Day of the year	Days
E	Center of E-frame	---
e	Earth's ellipticity	---

SYMBOL	DEFINITION	UNITS
F	Force	lbs
G	Acceleration due to gravitation	ft/sec^2
H	Angular momentum	slug-ft^2/sec, gm cm^2/sec
h	Hybrid parameters	as used
h	Altitude ($Z - Z_o$)	ft
$\bar{I}$	Inertia about c. g.	slug-ft^2, gm-cm^2
I	Inertia	slug-ft^2, gm-cm^2
I	Center of I-frame	---
i, j, k	Unit vectors in the x, y, z direction respectively or as defined by subscripts	as used
i	Current	amps
J	Inertia	gm-cm^2
J	Gravitational constant	---
K	Gain constant	as used
ℓ, m, n	Direction cosines as defined by subscript	---
ℓ	Longitudinal vehicle length as defined by subscript measured from the nose	ft
M	Mach number	---
M	Moment	lb-ft
m	Mass	slugs, gms

SYMBOL	DEFINITION	UNITS
$\dot{m}$	Engine mass flow rate as defined by subscript	slugs/sec
N	North	---
O	Center of O-frame	---
P, Q, R	Angular rates in B-frame coordinates or as defined by subscripts	rad/sec
R	Resistance	ohms
P	Pressure - atmospheric or as defined by subscript	lbs/ft^2
q	Free stream dynamic pressure	lbs/ft^2
R	Length as defined by subscript	ft
R	Gas constant	ft-lbs/slug°R
r	Vehicle radial length as defined by subscript measured perpendicular to the X_B axis	ft
s	Laplace operator	1/sec
T	Julian century	centuries
T	Center of the T coordinate system	---
T	Torque	dyne-cm, gm-cm, lb-ft
T	Atmospheric temperature	°R
T	Thrust	lbs
T	Seasonal variation of earth rate	msec
t	Time	sec
t_b	Engine burning period time	sec

SYMBOL	DEFINITION	UNITS
U, V, W	Components of V_a along X_B, Y_B, Z_B, respectively	ft/sec
V	Total speed as defined by subscript	ft/sec
v	Voltage as defined by subscript	volts
X, Y, Z	Coordinates as defined by subscripts	as used
X, Y, Z	Distances along O-frame axes from a specified origin	ft
x, y, z	General axis designations	---
x, y, z	Components of length in the B-frame	cm, ft
Z	Impedance	ohms
α	Angle of Attack	rad, deg
α	Gyro Gimbal Angle	rad, deg
α, β, γ	Platform gimbal angles corresponding with pitch, yaw, and roll, respectively	rad, deg
β	Sideslip angle	rad, deg
γ	Flight path angle	rad, deg
γ	Ratio of specific heat at a constant pressure to specific heat at a constant volume	---
δ	Angle as defined	rad, deg
ζ	Damping ratio	---
η	Flow incidence angle	rad/sec
θ, ψ, ϕ	Euler angles	rad, deg
λ	Cross-range angle	rad, deg

SYMBOL	DEFINITION	UNITS
μ	Specific gravitational constant of the earth	ft^3/sec^2
ξ	Azimuth angle	rad, deg
ρ	Air density	$slugs/ft^3$
ρ	Gyro output axis angle	rad, deg
σ	Range angle	rad, deg
λ	Characteristic root	1/sec
τ	Time constant	sec
Φ	Vehicle latitude angle	rad, deg
ϕ	Gyro angle as defined by subscript	rad, deg
ϕ	Aerodynamic parameter as defined by subscript	---
ϕ	Angle	rad, deg
Ψ	Vehicle longitude angle	rad, deg
ω	Angular rate	rad/sec

Subscripts

SYMBOL	DEFINITION
A	Refers to amplifier
A	Refers to accelerometer coordinates
A	Refers to total applied
A, B, C	Refers to platform pitch, yaw, and roll gyros, respectively
a	Aerodynamic
a	With respect to air mass
a	Refers to accelerometer
B	Refers to body axes
b	Refers to body or body center of pressure
b, c, d	Refers to auxillary coordinate frames
c	Refers to command parameter
c	Refers to gyro case coordinates
c. g.	Refers to center of gravity
c. p.	Refers to center of pressure
D	Refers to drag
D	Refers to drift torques
D	Refers to damping term
d	Refers to stage mass without fuel (dry mass)
E	Refers to earth axes
EX	Refers to external forces
e	Refers to engine exist conditions

SYMBOL	DEFINITION
e	Refers to length to engine
eq.	Refers to earth's equator
f	Refers to gyro float
g	Refers to gyro gimbal
I	Refers to inertial axes
i	Refers to arbitrary element of mass or the force on this element of mass
i, o, r	Refers to gyro float axes
L	Refers to lift
ℓ, m, n	Refers to angular effects around the X_B, Y_B, Z_B axes, respectively
m	Measured parameter
n	Refers to natural frequency
O	Refers to O-frame axes
o	Refers to zero-lift drag coefficient
P	Arbitrary point in the vehicle
S	Spring
S	Target satellite
ss	Steady-state
T	Total
T	Refers to torquer
t	Refers to tail or tail center of pressure

SYMBOL	DEFINITION
U	Universe
V	Vacuum
w	Refers to wind or air mass
X, Y, Z	Refers to O-frame axes
x, y, z	Refers to B-frame axes
ϵ	Error
1, 2, 3	Refers to vehicle stages
1, 2, 3, 4, 5	Refers to stage engines
1, 2, 3	Components of direction cosines
1, 2, 3· · · · ·	Refers to elements of coefficient matrix